TU
WIEN
TECHNISCHE
UNIVERSITÄT
WIEN
Vienna University of Technology

ESEA
Institut für Energiesysteme
und Elektrische Antriebe

Master Thesis

Influence of the Modified Static Load Characteristic on the Voltage Stability

In partial fulfillment of the requirements for the degree

Diplom-Ingenieur (Dipl.-Ing.)

committed by

Univ.-Prof. Dr.-Ing. Wolfgang Gawlik
Univ.Ass. Dipl.Ing. Dr.techn Albana Ilo

of the

Vienna University of Technology

Faculty of Electrical Engineering and Information Technology
Institute of Energy Systems and Electrical Drives

by
Christian Schirmer
Leonard-Bernsteinstraße 4-6/10/43
1220 Wien

Wien, im Oktober 2015

Department: Energy Systems
A-1040 Wien, Gusshausstr. 25/370-1, Internet: http://www.ea.tuwien.ac.at

"I'd put my money on the sun and solar energy. What a source of power! I hope we don't have to wait till oil and coal run out before we tackle that."

Thomas Alva Edison, approximately 1870

Vienna, October 2015

Acknowledgement

This thesis is the final step to finish my studies in electrical engineering, therefore I would like to express my thanks. I would like to express my sincere thanks to Professor Wolfgang Gawlik and Dr Albana Ilo for giving me the opportunity to study this phenomenon and for their help and valuable advice. Without Professor Wolfgang Gawlik I would not have been writing this thesis at all. He inspired me to start a Energy Systems and Automation Technology study a long time ago. Thank you very much Albana for joining me in a project on Voltage Stability and for all interesting debates on power system issues. You have been a good manager, inspiring supervisor and persistent proof reader.

I would like to gratefully acknowledge the Salzburg Netz GmbH for providing the data for the real grid as well as the Siemens AG for their PSS Netomac support.

Last, but not least, I would like to thank my family and friends for their continuous support and encouragement.

Kurzzusammenfassung

Die steigende Anzahl an dezentraler Stromerzeugung erzwingt die Benutzung von Blind-
leistung zur lokalen Spannungsregulierung, was wiederum zu einem ungewollten und
unkontrollierten Blindleistungsfluss führen kann. Dieser unkontrollierte Blindleistungs-
fluss hat Auswirkungen auf das überlagerte Hochspannungsnetz und modifiziert das
Verhalten des Mittelspannungsnetzwerks. Im Rahmen dieser Diplomarbeit wird die Span-
nungsstabilität im Hochspannungsnetz bei einer Erhöhung der Anteile der dezentralen
Erzeugung untersucht. In den letzten Jahren ist die Tendenz festzustellen dezentrale
Erzeuger mit lokalen Reglern aufzurüsten, um die Spannung innerhalb der erlaubten
Grenzen zu halten. Die Einführung von zahlreichen lokalen $Q(U)$ Reglern in das Verteil-
netz (sei es Mittel- oder Niederspannungsnetz) modifiziert das Verhalten des Verteilnetzes
oder vielmehr die Charakteristik der Last vom darüberliegenden Hochspannungsnetz aus
betrachtet. Dadurch kann die Spannungsstabilität nicht mehr so angenommen werden
wie dies bisher der Fall war.

Zuerst wurde ein vereinfachten Zwei-Bus Stromnetz untersucht. Desweiteren wurden die
Auswirkungen der dezentralen Stromerzeugung auf die Lastkennlinie und Spannungsstabi-
lität in einem komplexen IEEE Testnetz gezeigt. Zuletzt wurde ein reales Stromnetz, das
Netz des Landes Salzburg, analysiert. Die Spannungsstabilität, die Spannungssensitivität
und die modifizierte Charakteristik der Last wurden mit Hilfe von Lastflussberechnungen
untersucht. Alle Simulationen wurden mit dem Lastflussprogramm PSS Sincal und PSS
Netomac durchgeführt.

Die Nachforschungen haben gezeigt, dass das Lastverhalten am Netztransformator nicht-
linear wird wenn die Anzahl an dezentraler Stromproduktion steigt. Dadurch kann
die Lastcharakteristik nicht mehr als starr bezeichnet werden. Die statische Lastcha-
rakteristik hängt stark von der dezentralen Stromproduktion ab und ist deshalb eine
Funktion des Wetters. Die Spannungsstabilität sinkt für den Fall dass Wirkleistung vom
Mittelspannungsnetz in das darüberliegende Hochspannungsnetz gespeist wird.

Abstract

The increased share of the distributed generators has forced the use of the reactive power for the local voltage control, which causes an unwanted and uncontrolled reactive power flow. The last one has an impact on the superimposed high-voltage network and modifies the distribution network behaviour. This thesis investigates the voltage stability on high voltage grid by an increased share of distributed generation. Distributed generators, except run of river power plants, are usually connected on the grid through inverters, which are normally upgraded with local voltage controller to keep the voltage within the limits. The introduction of the numerous $Q(U)$ local controllers in distribution grid (be medium or low voltage grid) modifies the distribution network behaviour or rather the load characteristic seen from superimposed high voltage grid. Therefore voltage stability behaviour is no longer as it was previously known.

Firstly, the voltage behaviour its stability of a simplified two bus power network has been studied. Secondly, the impact of the distributed generation on the characteristic of the load and the voltage stability has been analysed in the IEEE 30 Bus Test case network. Thirdly, a real power network, the Salzburg power grid, has been investigated. The voltage stability, voltage sensitivity and the modified characteristic of the load has been studied by performing load flow analysis. All simulations have been performed by using the PSS Sincal and PSS Netomac.

Investigations have shown that the load behaviour on supply transformer level is becoming non-linear by increasing the amount of distributed generation production and can't be considered as stiff any more. The static load characteristic depends strongly on the distributed generation production and therefore is a function of weather conditions. The voltage stability margin decreases if active power is injected from medium voltage grid into the high voltage grid.

Contents

1 Introduction

1.1 Background

The Earth's climate change and its negative effects are a common concern of the humankind. On 12th of June 1992, 154 countries signed an international treaty, the Framework Convention of the United Nations Convention on Climate Change (UNFCCC), with the purpose to reduce the Greenhouse Gas emissions which are emitted worldwide [1]. Last Obamas Speech concerning climate change presented a plan ("The Clean Power Plan") which shall lead to 30 percent more renewable energy generation until the year 2030 [2]. The EU commission signed treaties about climate change and energy autarchy which focuses on energy from renewable energy resources. The European 2020 targets involve a 20% increase in energy efficiency, 20% of energy from renewable energy resources and a reduction of greenhouse gas emissions of 20% lower than 1990 [3]. These political targets are driving the further integration of renewable resources in Europe and worldwide. The integration of energy produced from renewable energy resources into the electrical power network is a major technical challenge. This thesis is focused on the effects of the distributed generators on the voltage stability in the high voltage grid.

1.2 Motivation

Due to the political decisions and the advances in technology the electric power system is facing an increasing amount of distributed generation in all voltage levels of distributed networks. An uncontrolled reactive power flow from the distribution network (medium voltage grid) into the transmission network (high voltage grid) has been observed when the distributed generation production capacity reaches a critical mass. [4, 5, 6]

In this Master Thesis the effects of the reactive power and voltage interdependencies between the high and medium voltage grid is analysed as well as the impact of the distributed generation on the static load characteristic and voltage stability. The large scale penetration of distributed generation causes a notable uncontrolled reactive flow on the high voltage grid, which affects the voltage stability. These issues are not apparent and have been hardly investigated for the following reasons:

- Nowadays the distributed generation penetration is still often limited. The high voltage grid is well sized and their impact on voltage stability in high voltage grid

is not clearly perceptible. A large scale penetration of distributed generation may highlight the voltage stability issue.

- Normally research projects are limited to one model region. The effects of distributed generation are analysed focusing either on the high voltage grid or the medium voltage grid. The dependencies of the high voltage grid and the medium voltage grid have not been in focus.

In this Master Thesis both factors are considered:

- A large scale penetration of distributed generation.

- The interdependencies between high and medium voltage grids.

1.3 Objectives

The object of this thesis is the analysis of transmission grid operation due to the large share integration of distributed generation and how this issue affects the voltage stability. The main objective is the adequate modelling of the distribution grid with a large share of distributed generation for the voltage stability investigations.

The static load characteristic, as well as on the behaviour of the load, seen from different voltage levels (bus bars) is investigated. The lumped load behaviour is being changed due to the presence of distributed generation and their local controller effect. The influences of these $Q(U)$ controller on the voltage stability of the high- and medium voltage grid are investigated carefully. The voltage stability has been analysed using Q-U curves in each high voltage bus bar. The investigation is performed by using the software PSS Sincal version 11.0 and PSS Netomac version 11.0 developed by Siemens PTI. Even though power system stability is a multifaceted phenomena [7], this thesis is limited to the study of small disturbance voltage stability.

1.4 Scope

This thesis focuses on the high and medium voltage grid but the effect of the distributed generation penetration on the low voltage grid including the distributed transformers is taken into account as well. The low voltage grids are represented as a lumped load and/or an injection. The high voltage grid and the medium voltage grids are connected via on-load tap changer transformers which have an impact on the voltage level on medium voltage grid and on the reactive power flow to the high voltage grid.

Firstly the voltage sensitivity and voltage stability study is performed in a very basic power network, which consists of a generator, a transmission line, an on-load tap changer

transformer, a native load and a distributed generator. Secondly, the IEEE 30 bus test network case which includes a transmission grid and several distribution grids with distributed generation penetration is simulated and analysed. Thirdly a real power network, the Salzburg grid is simulated and analysed. The Salzburg grid consists of a sub-transmission grid (110 kV) and several medium voltage grids (30 kV, 20 kV, 10 kV). Additionally the transmission grid, controlled by the Austrian Power Grid, which consists of different voltage levels (380 kV, 220 kV) is simulated. The investigation focus is put on one specific medium voltage grid region. The complete distribution grid of the test region is simulated as well as the complete sub-transmission grid. The other medium voltage grids connected to the high voltage grid are simulated by reducing it to a lumped medium voltage load and /or injection. The low voltage grid connected to the analysed distribution grid is simulated as a low voltage lumped load (see 2.2.3).

1.5 Thesis Structure

The thesis consists of 5 chapters as follows:

In chapter 1, Introduction, the background and the motivation of this work are presented. An overview of the state of the art, the objectives as well as the scope of the work is given.

In chapter 2, Theory - Power System Stability, a definition of Power System Stability is presented. An overview of the different power system stability criteria like voltage stability, frequency stability and rotor angle stability is given. The background theory of voltage stability, focussing on small disturbance voltage stability is presented in detail. A description of how these terms have been defined and used in practice is also provided.

In chapter 3, Voltage Stability and Sensitivity, the different test scenarios as well as the test results of all three analysed power networks are presented. The voltage stability, the $Q(U)$ behaviour of the load and the $Q(U)$ sensitivity of the load, the static load characteristic, is being analysed.

In chapter 4, Conclusion, the conclusion and an outlook on further work is given.

Finally, chapter 5 presents the literature which has been used creating this work.

2 Theory - Power System Stability

This chapter gives a detailed illustration of the theory which is needed and used in this thesis. A general overview of the structure of an European power system is given as well as an explanation and definition of power system stability (Frequency, Rotor Angle and Voltage Stability) and sensitivity. Finally the theory of system loadability, $Q(U)$ curves, load characteristics and the $Q(U)$ controller of distributed generators are presented. A general overview of the power grid can be seen in Figure 2.1 which shows the different voltage levels of an European power grid.
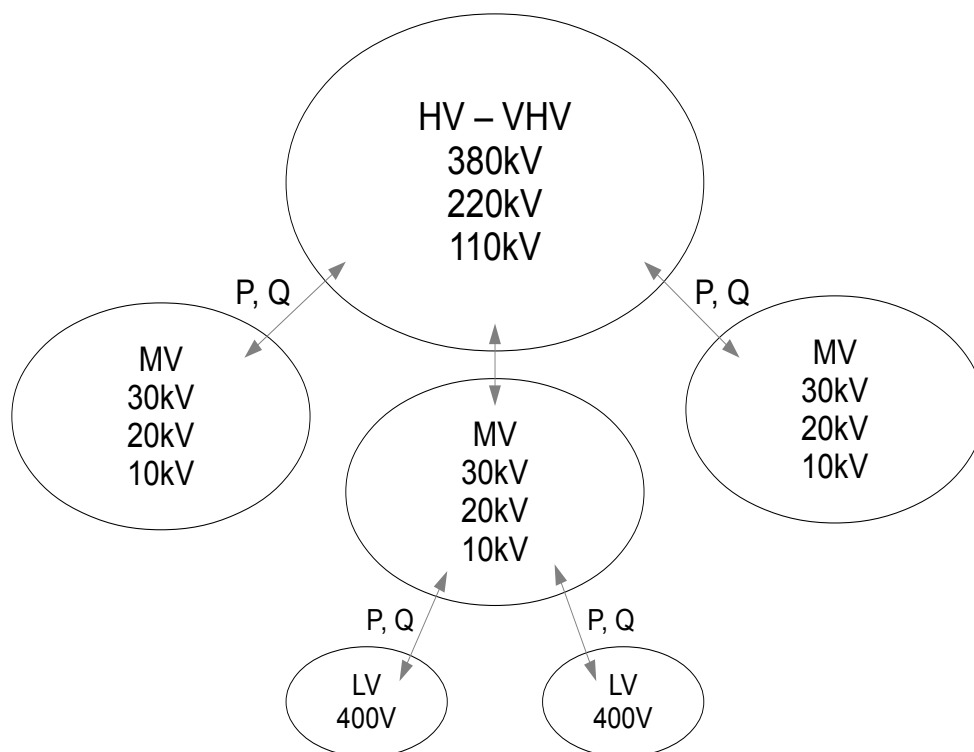

Figure 2.1: General schematic overview of the power grid

2.1 Power System Overview

High voltage AC transmission is used to transport and to distribute electrical energy. Therefore different voltage levels connected via transformers have been established. Electric-power transmission is the bulk transfer of electrical energy, from generating power plants to electrical substations located near the demand. This is distinct from the local wiring between high-voltage substations and customers, which is typically referred to as electric power distribution. Transmission lines are interconnected with each other fulfilling the n-1 security, which means that the transmission network keeps functional in case of a failure of one component. The combined transmission and distribution network is known as power grid. The high voltage grid and the medium voltage grids are connected via on-load tap changer transformers which have effects on the reactive power transfer through the transformer. The low voltage grids and the medium voltage grids are connected via no-load tap changer transformers, which means the tap status must be changed manually and that's why the reactive power flow between the low voltage grid and the medium voltage grid can be assumed as independently from the transformer.

- Transmission network: 220 kV, 380 kV
    - meshed

- Distribution network: 110 kV
    - meshed

- Medium Voltage network: 10 kV, 20 kV, 30 kV
    - meshed network
    - ring structure
    - reserve feeder
    - express feeder
    - radial network

- Low Voltage network: 400 V
    - radial network
    - meshed (grid islands)

A wide area synchronous grid connects a large number of generators to a large number of consumers. The different high voltage grids are connected with each other building one large grid for most of continental Europe. The whole power system has the same relative frequency (50 Hz), but almost never the same relative phase. The power interchange is a function of the phase difference between two nodes in the network. If no power is
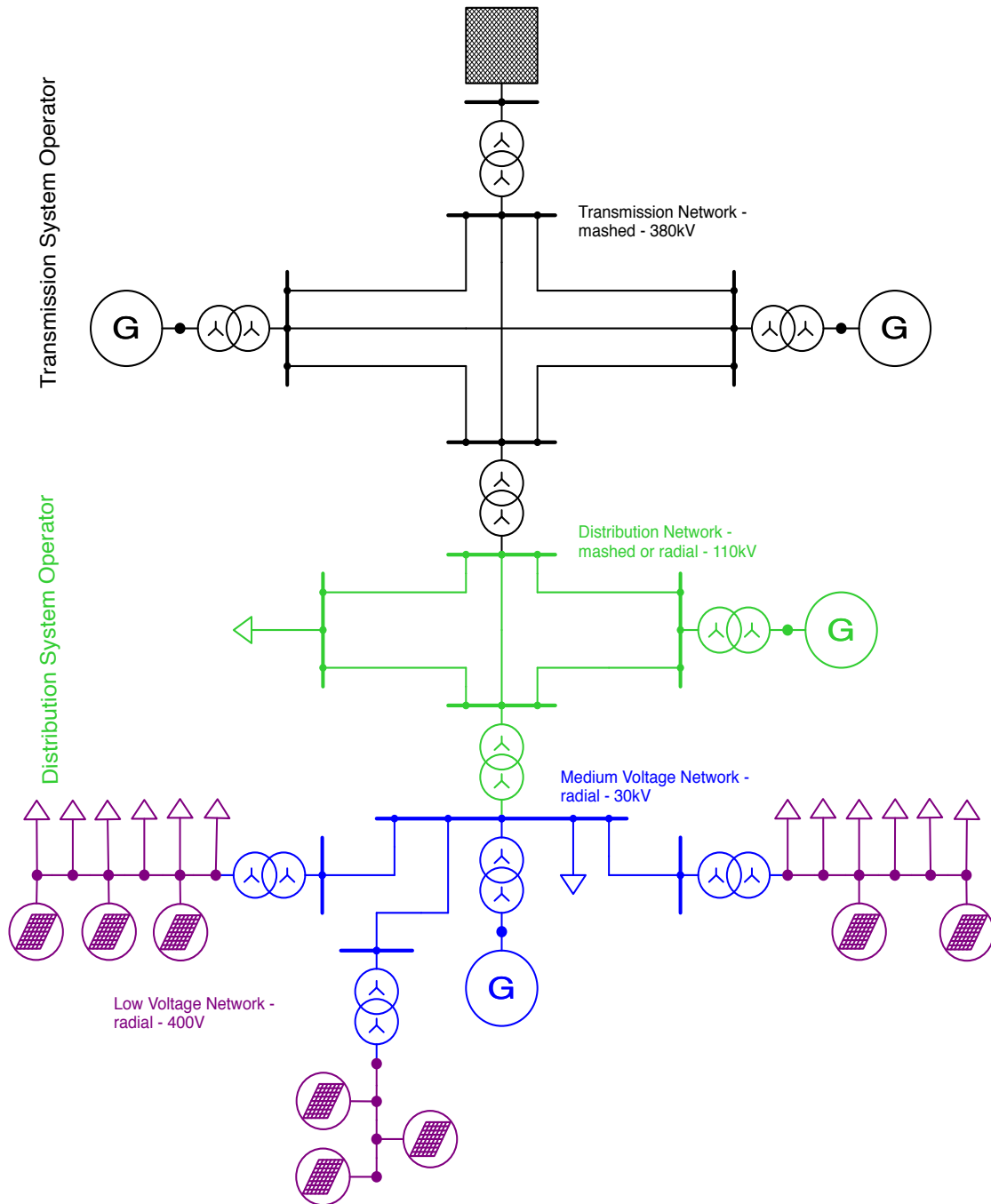
Figure 2.2: General layout of the main voltage levels of the power grid

changed between two nodes then there is no degree difference. Any phase difference up to 90 degrees is stable but above 90 degrees the system is unstable. The frequency should always be close to 50 Hz, and the phase differences between any two nodes significantly less than 90 degrees. If 90 degrees are exceeded then a system separation is executed, and the system remains separated until the failure has been corrected.

Electricity is transmitted at high voltages (mostly 380 kV) to reduce the energy losses in long-distance transmission. The electrical power is usually transmitted through overhead power lines. Underground cables have a significantly higher cost and greater operational limitations but is sometimes used in urban areas or sensitive locations. Figure 2.2 gives a graphical explanation of a European power grid as well as a general layout of the main voltage levels [8].

2.2 Power System Operation

Power System Stability is an important problem for secure system operation. Many major blackouts caused by power system instability have shown the importance of this issue [9]. Figure 2.3 gives the overall picture of the power system stability problem, showing its categories and subcategories. The focus in this master thesis is on Small Disturbance Voltage Stability, but nevertheless a short theoretical overview about Rotor Angle Stability and Frequency Stability is given in 2.2.1 and 2.2.2. A definition about the power system stability proposed by Leonard L. Grigsby [10]

Definition Power System Stability:

- *"Power System Stability denotes the ability of an electric power system, for a given initial operating condition, to regain a state of operating equilibrium after being subjected to a physical disturbance, with all system variables bounded so that the system integrity is preserved."*

- *"Integrity of the system is preserved when practically the entire power system remains intact with no tripping of generators or loads, except for those disconnected by isolation of the faulted elements or intentionally tripped to preserve the continuity of operation of the rest of the system."*

- *"Instability is a run-away or run-down situation."*

Another definition of Power System Stability proposed by IEEE, CIGRE Joint Task Force on Stability Terms and Definitions [11]

- *"Power System Stability is the ability of an electric power system, for a given initial operating condition, to regain a state of operating equilibrium after being subjected*

to a physical disturbance, with most system variables bounded so that practically the entire system remains intact."

In other words stability is a condition of equilibrium between opposing forces. If the power system is stable it will reach a new equilibrium state, keeping the whole system functional, in case of a transient disturbance. These disturbances can be caused by faulted elements or a loss of connected loads. Automatic controls and/or operator actions will restore the system to normal state if the system is stable. In case of instability a so called run-away situation will occur. An example of this is an uncontrolled increase in angular separation of generator rotors, or an uncontrolled increase or decrease in bus voltages. An unstable system could lead to outages, a shutdown of major parts of the power system, or even a complete blackout of the power system.
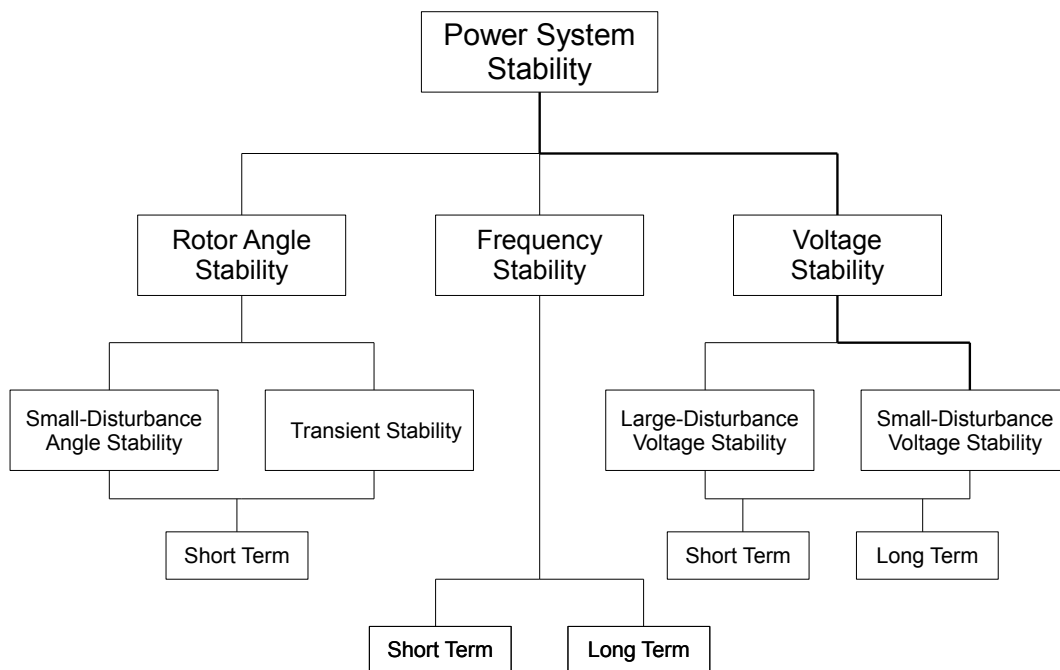

Figure 2.3: Classification of power system stability

2.2.1 Rotor Angle Stability

Rotor angle stability refers to the ability of synchronous machines of an interconnected power system to remain in synchronism after being subjected to a disturbance. A fundamental factor in this problem is the manner in which the power outputs of synchronous machines vary as their rotor angles change. In a stable situation an equilibrium between the input mechanical torque and the output electromagnetic torque of each generator, and the speed remains constant. The phenomenon of rotor angle instability is normally

separated into small-disturbance angle stability and transient stability. Rotor angle stability is the ability to restore equilibrium between electromagnetic torque and mechanical torque of each synchronous machine in the system in case of a disturbance. In case of instability some generators loose synchronism with the other generators when perturbed and results in a run-away situation due to torque imbalance. Instability occurs in the form of increasing angular swings of some generators leading to their loss of synchronism with other generators. If one generator temporarily runs faster than another, the angular position of its rotor relative to that of the slower machine will advance. An angular difference is the result which transfers part of the load from the slow machine to the fast machine, depending on the power-angle relationship. This tends to reduce the speed difference and hence the angular separation. The power-angle relationship is highly non-linear. Instability results if the system cannot absorb the kinetic energy corresponding to these rotor speed differences [11].

Some past studies have shown that a moderate integration (e.g. 30%) of power generated out of renewable energy resources do not significantly affect the rotor angle stability, but depending on the grid characteristic, it may be necessary to limit the penetration of renewable energy sources [12].

Small Disturbance Rotor Angle Stability

Is concerned with the ability of the power system to maintain synchronism under small disturbances, which means the disturbance must be sufficiently small that a linearization of the system equations is permissible. The stability depends on the initial state of the power system. Small disturbance rotor angle stability is usually associated with insufficient damping of oscillations. It is either local or global in nature. Local issues include a small part of the power system and are associated with rotor angle oscillations of a single power plant against the rest of the power system. Global problems include a group of generators in one area oscillating against a group of generators in another area. Such oscillations are called interarea mode oscillations. The interesting time frame is on the order of 10 to 20 seconds following a disturbance [12].

Transient Stability (Large Disturbance Rotor Angle Stability)

Transient stability traditionally is concerned with the ability of the power system to maintain synchronism when a severe disturbance occurs, such as a short circuit on a transmission line. The power system responds to large disturbance with large excursions of generator rotor angles. Transient stability depends on the initial operating condition, the severity of the disturbance and the strength of post-fault transmission network. Instability is usually in the form of aperiodic angular separation due to insufficient synchronizing torque [11].

2.2.2 Frequency Stability

Frequency Stability refers to the ability of a power system to maintain steady frequency (within a nominal range) following a disturbance resulting in a significant imbalance between system generation and load. In other words, Frequency stability is the ability of a power system to compensate for a power deficit. Frequency instability that may result occurs in the form of sustained frequency swings leading to tripping of generating units and/or loads. The frequency stability in large interconnected systems can result in the system splitting into one or more island. In smaller networks (island system), disturbances could generate frequency stability problems, which could cause a significant loss of load and/or generation. In small island grids are large frequency deviations after a disturbance as there is a small reserve of rotating mass. In large interconnected power systems is the frequency a controlled global parameter, including a inertial reserve (energy stored in rotating masses of all generators), the primary control (lost power is compensated by an increase in production of primary controlled units), the secondary control (frequency and are exchange flows re-established) and a re-dispatch of generation. The integration of power generated out of renewable energy resources have effects on the frequency stability. An important factor is that renewable energy sources are often connected via a converter interface and have no inertia (transient energy storage). That means by replacing synchronous generators with sources using a converter interface, e.g. Photovoltaic, reduces the total system inertia and the whole system is more sensitive to frequency deviations [10, 12].

2.2.3 Voltage Stability

Voltage stability is normally described as the ability of a power system to maintain steady voltages at all buses in the power system after a disturbance. Or in other words, the voltage stability studies how changes of the reactive power Q affects the voltages U in the system. A disturbance could be an increase or decrease in load demand or a change in the power system topology (Circuit Breaker disconnects or connects a line, failure of a line). This could cause a progressive and uncontrollable fall or rise in voltage of some buses. A key factor to analyse voltage stability is the reactive power of the power system as the reactive power is closely connected to the voltage. That's the reason why a main factor causing voltage instability is the inability of power system to keep a balance between reactive power control actions and voltage control actions. A driving factor for voltage instability is the load and especially the characteristic of the load, hence, voltage stability is sometimes also called load stability. There are many voltage regulation units available, like on load tap changer transformers or FACTS. It is hardly possible to analyse a complete power system completely because of the immense size of it. Normally the power system is divided into sensible parts which are modelled in detail and others which are replaced and represented by a lumped load and/or injection. Normally if the study

focus shall be the distribution network, the transmission network is treated as a source and/or load at a given voltage. On the other hand, when the transmission network should be analysed, the distribution networks are replaced by a load and/or an injection, which is called a composite load [11].

Definition of Voltage Stability

There are several definitions of voltage stability. A definition given by *IEEE/CIGRE Joint Task Force on Stability Terms and Definitions* [7] reads as follows:

- *"Voltage stability refers to the ability of a power system to maintain steady voltages at all buses in the system after being subjected to a disturbance from a given initial operating condition."*

Another proposed definition from Van Cutsem and Vournas [7] describes the voltage instability as:

- *"Voltage instability stems from the attempt of load dynamics to restore power consumption beyond the capability of the combined transmission and generation system."*

A system is in voltage stable state if at a given operating condition, for every bus in the system, the bus voltage magnitude increases as the reactive power injection at the same bus is increased. On the other hand the system is said to be unstable if for at least on bus in the system, the bus voltage magnitude decreases as the reactive power injection at the same bus is increased. In other words the $Q(U)$ sensitivity for every bus bar must be positive in a stable power network. If the voltage sensitivity for at least one bus is negative, the power system is declared as unstable. A related term for voltage instability is voltage collapse. It is the sequence of events following voltage instability which leads to abnormally low voltages or even a black out of the power system.

According to figure 2.3 voltage stability can be divided into two subcategories; *Large Disturbance Voltage Stability* and *Small Disturbance Voltage Stability* [11].

Large Disturbance Voltage Stability

Large disturbance voltage stability refers to the ability of a power network to keep the voltage stable after a large disturbance, such as a loss of generation, system faults or a loss of lines. This ability is depending on the characteristic of the load and discrete controls and protections. The study period of this phenomenon extend from a few seconds up to tens of minutes. It requires the examination of the non-linear response of the power system over a period of time. The performance and interactions of devices as motors, on-load tap changer transformers and generators must be considered [11].

Small Disturbance Voltage Stability

Small disturbance voltage stability is the ability to maintain a stable power system when small perturbations, such as incremental changes in the system loads, occur. The small disturbance voltage stability is depending on the load characteristic as well as discrete and continuous controls at a given time. To analyse this phenomenon the system equations can be linearized. Non-linear effects, such as tap changer control (time delays, deadbands, discrete tap steps), don't fall into account. In this thesis the Q-U curves are used to analyse the effects of small disturbance voltage stability in power system networks. A detailed explanation of the Q-U curves is given in chapter 2.2.7 [11].

A distribution network is connected to the transmission network at the grid supply point where a change in voltage may cause complicated dynamic interactions inside the distribution network itself due to:

- voltage control action arising from transformer tap changer

- control action associated with reactive power compensation and/or small embedded generators

- a low supply voltage causing changes in the power demand as a result of induction motors stalling and/or the extinguishing of discharge lighting

- operation of protective equipment by overcurrent or undervoltage relays, electromechanically held contactors and so on

- reignition of discharge lighting and self-start induction motors when the supply voltage recovers

The effect that actions such as these can have on voltage stability is examined using the static characteristics of the composite loads. This analysis will help to give an understanding of both the different mechanisms that may ultimately lead to voltage collapse and the techniques that may be used to assess the voltage stability of a particular system. These techniques can then be extended to the analysis of large systems using computer simulation methods [12].

2.2.4 System Loadability Limit

A general explanation of how the generation and the load are connected in a power system is given in this chapter. Figure 2.4 shows the most simple equivalent circuit, which consists of a generator, an ideal transmission line and a composite load. Normally there are limits on the power that can be supplied, which is an important factor on the stability of the system [12]. The load is represented by his voltage characteristic, another

term is load characteristic. It describes the dependence of the reactive power of the load and the voltage, as well as the dependence of the active power of the load and the voltage. A short theoretical overview of how to get the power network equations and where the limits of the power network are is given in this chapter.

Voltage instability normally occurs when the power system is operated close to the maximum power transfer level and then a disturbance causes this limit to be exceeded. In the network shown in Figure 2.4 the load is assumed as independent of the voltage. The resistance of the generator and the losses of the transmission line are ignored and it is assumed that the generator can keep the voltage on the generator bus E constant.
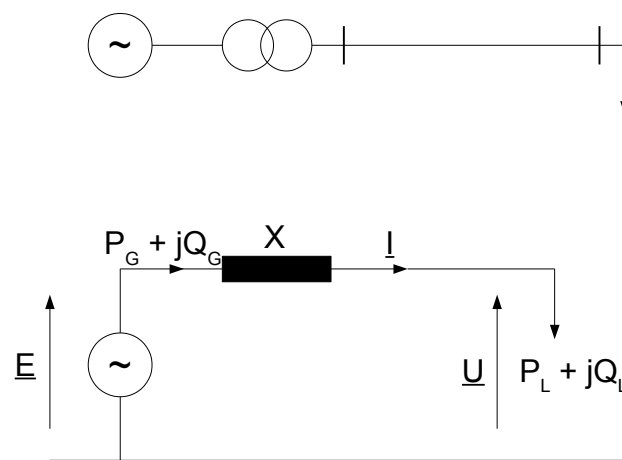

Figure 2.4: Equivalent circuit of a simplified power network

The real and reactive power absorbed by the load $P_L(U)$ and $Q_L(U)$ is determined by the power flow equations of the system (Equation: 2.1 and 2.2) which gives:

$$P_L(U) = \frac{E \cdot U}{X} \sin \delta \tag{2.1}$$

$$Q_L(U) = \frac{E \cdot U}{X} cos\delta - \frac{U^2}{X} \tag{2.2}$$

The angle δ between the generator voltage $\underline{E}$ and the voltage of the load bus $\underline{U}$ phasors can be eliminated using the identity $\sin^2 \delta + \cos^2 \delta = 1$.

$$(\frac{E \cdot U}{X})^2 = [P_L(U)]^2 + [Q_L(U) + \frac{U^2}{X}]^2 \tag{2.3}$$

Solving equation 2.3 and eliminating $Q_L(U)$ by $Q_L(U) = P_L(U) \cdot \tan\phi$ gives the opportunity to express the load voltage as a function of the active power of the load and the power factor of the load.

$$U = \sqrt{\frac{E^2}{2} - X \cdot P_L \cdot \tan\phi \pm \sqrt{\frac{E^4}{4} - X^2 \cdot P_L^2 - X \cdot E^2 \cdot P_L \cdot \tan\phi}} \quad (2.4)$$

By norming the load voltage and the active power of the load in Equation 2.4 using $u = \frac{U}{E}$ and $p = P_L / \frac{E^2}{X}$:

$$u = \sqrt{\frac{1}{2} - p \cdot \tan\phi \pm \sqrt{\frac{1}{4} - p^2 - p \cdot \tan\phi}} \quad (2.5)$$

By replacing P_L with $P_L = \frac{Q_L}{\tan\phi}$ in equation 2.4 the load voltage can be expressed as a function of the reactive load power and the power factor of the load very similar to Equation 2.4.

$$U = \sqrt{\frac{E^2}{2} - X \cdot Q_L \pm \sqrt{\frac{E^4}{4} - X^2 \cdot (\frac{Q_L}{\tan\phi})^2 - X \cdot E^2 \cdot Q_L}} \quad (2.6)$$

By norming the load voltage and the reactive power of the load in Equation 2.6 using $u = \frac{U}{E}$ and $q = Q_L / \frac{E^2}{X}$:

$$u = \sqrt{\frac{1}{2} - q \pm \sqrt{\frac{1}{4} - \frac{q^2}{(\tan\phi)^2} - q}} \quad (2.7)$$

If the equation for the Q-U curve should be independent from the power factor, then Equations 2.1 and 2.2 are normalized using $u = \frac{U}{E}$, $q = Q_L / \frac{E^2}{X}$ and $p = P_L / \frac{E^2}{X}$. One obtains:

$$p = u \cdot \sin\delta \quad (2.8)$$

$$q = u \cdot \cos\delta - u^2 \quad (2.9)$$

Squaring and rearranging gives:

$$u^2 \cdot ((\sin\delta)^2 + (\cos\delta)^2) = p^2 + (q + u^2)^2 \quad (2.10)$$

And the positive real solutions of u from 2.10 leads to the well known equation of the Q-U curve:

$$u = \sqrt{\frac{1}{2} - q \pm \sqrt{\frac{1}{4} - p^2 - q}} \tag{2.11}$$

Equations 2.4 and 2.5 are the basis of the P-V curves and equations 2.6, 2.7 and 2.11 are the basis of the Q-U curves [7, 12].

2.2.5 Voltage Sensitivity and Static Load Characteristic

Voltage sensitivity is referred to as the slope of the voltage by varying reactive power. The voltage sensitivities are expressed in per units and are normalized to the operating point [12].

$$k_{PU} = \frac{\frac{\delta P}{P_0}}{\frac{\delta U}{U_0}} \tag{2.12}$$

$$k_{QU} = \frac{\frac{\delta Q}{Q_0}}{\frac{\delta U}{U_0}} \tag{2.13}$$

The voltage sensitivity is separated in two different terms in this thesis. The voltage sensitivity seen from the system is given in equation 2.14 and the voltage sensitivity of the load is given in 2.15 and referred as the static load characteristic. The static load characteristic refers to the slope of the voltage by varying reactive power seen from the load.
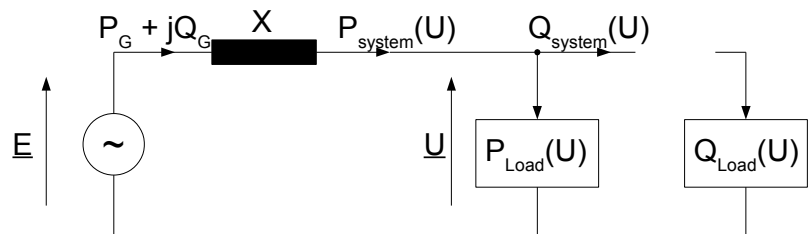

Figure 2.5: Equivalent circuit for determining the reactive power characteristic of the system

To distinguish between the power supplied by the system (source) at the load node and the power demand of the load itself, the reactive power demand of the load has been separated from the power supplied by the system. Figure 2.5 shows this separation. The real power is always connected to the transmission grid, which holds $P_{Load} = P_{System}$. To analyse the voltage stability the link between Q_{Load} and Q_{System} is opened using a fictitious synchronous condenser (see chapter 3.1.2) [12].

$$k_{SC} = \frac{\frac{\delta Q_{System}}{Q_0}}{\frac{\delta U}{U_0}} \tag{2.14}$$

$$k_{SLC} = \frac{\frac{\delta Q_{Load}}{Q_0}}{\frac{\delta U}{U_0}} \tag{2.15}$$

To analyse the voltage stability of a real network the impact of the load characteristic should be considered. The load characteristic is defined as following [12]:

- *"In the steady state the demand of the composite load depends on the bus bar voltage U and the system frequency f. The functions describing the dependence of the active and reactive load demand on the voltage and frequency P(U,f) and Q(U,f) are called the static load characteristics. The characteristics P(U) and Q(U) taken at constant frequency, are called the voltage characteristics while the characteristics P(f) and Q(f), taken at a constant voltage, are called the frequency characteristics."*

The static load characteristic is in the scope of this thesis, while the frequency characteristic of the load is not being considered.

Voltage sensitivity of the system characteristic is an important factor to analyse the voltage stability of a power system. The power system is defined as stable if the voltage sensitivity of the system characteristic is positive for every bus at the operating voltage. On the other hand, the power system is unstable if the voltage sensitivity of the system characteristic is negative for at least one bus. A load is called stiff if the static load characteristic is small. The static load characteristic of an ideally stiff load is zero, which means that the power demand (reactive and active power) is independent from the voltage. Previous reports have shown that due to the $Q(U)$ controller of distributed generators, the load characteristic is becoming less stiff [4]. A high load characteristic means that small changes on the load voltage results in high changes of the reactive power demand of the load. Usually the $Q(U)$ characteristic of the reactive power demand is higher than the $Q(U)$ characteristic of the active power demand [12].

A positive value of the voltage sensitivity means that the voltage of the bus is increasing if the power system transfers more reactive power to the bus. The system is voltage unstable if the voltage of the bus is decreasing if the power system transfers more reactive power to the bus. All control systems, like on-load tap changer transformers, generators and FACTS assume that increasing reactive power will increase the voltage of the bus. If this assumption is wrong, the control systems will behave incorrectly and cause a voltage collapse.

The classic voltage stability criterion $\delta \Delta Q / \delta U$ is based on the derivative of the surplus of reactive power (see equation 2.16). Generally, for a multi-machine system, it is not possible to give an analytical formula for the $\delta \Delta Q / \delta U$ stability criterion, but using a fictitious synchronous generator the load node is treated as a PV node and executing a load flow program several times for different voltage values of the node gives the system characteristic and the load characteristic [12].

$$\frac{\delta(Q_{System} - Q_{Load})}{\delta U} < 0 \text{ or } \frac{\delta Q_{System}}{\delta U} < \frac{\delta Q_{Load}}{\delta U} \tag{2.16}$$

2.2.6 Local Controller

Traditionally distributed generators which are connected either to the low voltage or medium voltage grid by producing only active power ($\cos \phi = 1$). Previous studies [4] have shown that the distributed generators must be upgraded with local $Q(U)$ controller to provide the needed reactive power, which is needed to control the voltage. Figure 2.6 shows the characteristic of the local controller. The reactive power of the distributed generation is controlled from the $Q(U)$ controller and functions as following. The reactive power is only depending on the voltage at the bus bar of the photovoltaic cell. If this voltage is high (about 1.05 p.u.), compared to the optimal operating voltage (which is between 1.02 p.u. and 1.05 p.u.), the $Q(U)$ controller consumes inductive reactive power. The power factor $\cos \phi$ changes continuously from 1 to -0.95. If the bus bar voltage of the distributed generation is lower than the operating voltage (about 1.02 p.u.), the $Q(U)$ controller produces capacitive reactive power. The power factor $\cos \phi$ changes continuously from 1 to 0.95. The purpose of the $Q(U)$ controller is to influence the voltage of the distributed generation bus bar and to keep the voltage near the optimal operating voltage. The needed reactive power is produced locally only if it is needed. Additionally the $Q(U)$ controller reduces the network losses, as the reactive power through the lines is reduced. The following equations show the relationship between the reactive power, active power and the power factor [5, 12].

$$S^2 = P^2 + Q^2 \tag{2.17}$$

$$S = \sqrt{3} \cdot U \cdot I \tag{2.18}$$

$$P = S \cdot \cos \phi \tag{2.19}$$

$$Q = S \cdot \sin \phi \tag{2.20}$$

$$Q = P \cdot \tan \phi \tag{2.21}$$

As presented in equation 2.17 to 2.21 the reactive power of the $Q(U)$ controller is highly dependent of the nominal active power of the photovoltaic cell. The power factor $\cos \phi$ is changing from -0.95 to 0.95 which includes a change of the reactive power from $Q = P \cdot (\pm 0.32868)$.
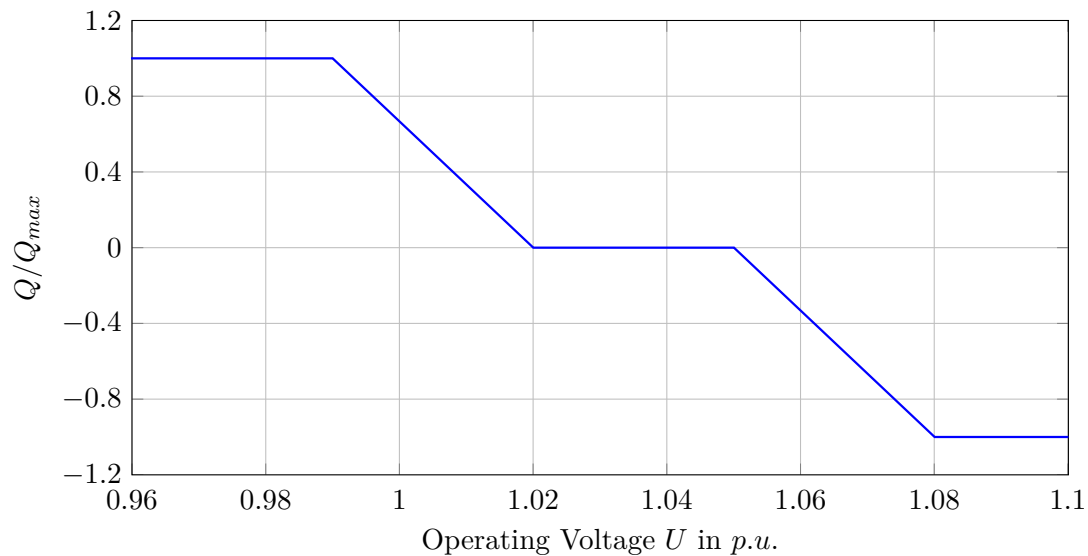

Figure 2.6: $Q(U)$ controller of the distributed generator

2.2.7 Q-U Curve

The Q-U curve can be used to analyse voltage stability in a very effective way. Equations 2.6 and 2.7 are the mathematical basis for a Q-U curve. A major advantage of the Q-U curve analysis (compared to the P-U curve method) is, that it doesn't require the power system to be represented as a two-bus equivalent, which allows stability analysis of complex power networks. The voltage at a bus bar is plotted against the reactive power at that specific bus. A normalized Q-U curve for the 2 bus power system (shown in figure 2.4) is presented in figure 2.7 and calculated by using equation 2.22 which has been calculated by rearranging equation 2.11. The relationship between the reactive

power and the voltage shows the sensitivity of the voltages of the analysed bus bars with respect to reactive power injections or absorptions [7, 14].

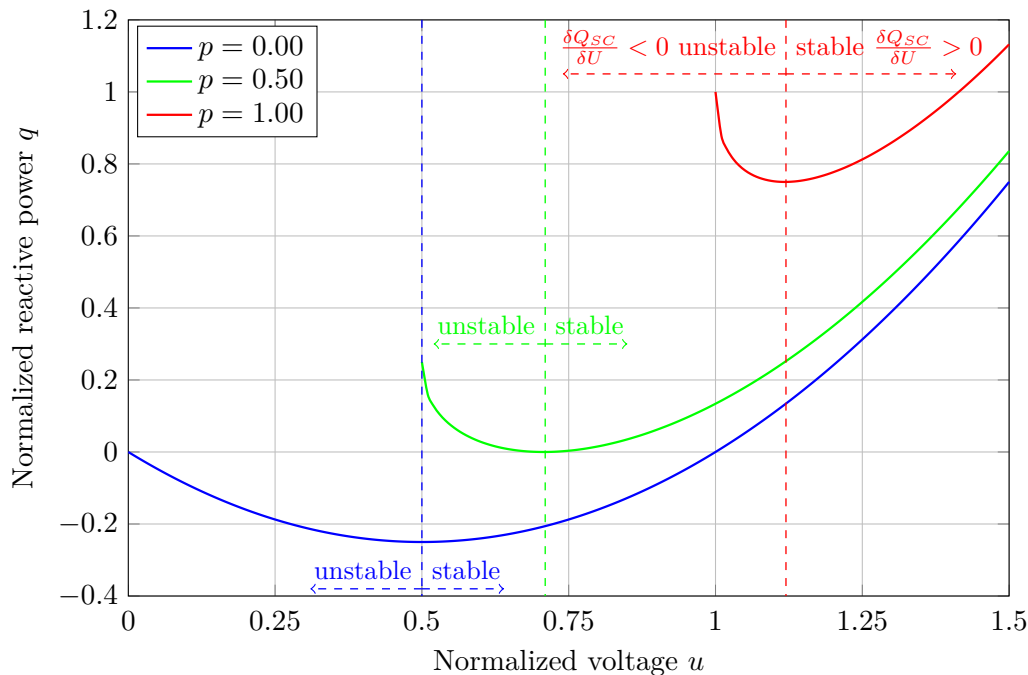$$q = -\sqrt{u^2 - p^2} + u^2 \tag{2.22}$$

Figure 2.7: Normalized Q-U curves for a 2-bus system shown in figure 2.4

The available reactive power reserve of the power system and the voltage stability of a bus are closely related to each other. This reactive power reserve of the analysed bus can easily be found in the Q-U curve. The reactive power reserve is the distance (in var) between the operating point and the load characteristics at the bus at a specific voltage. The greater the slope of the right portion of the Q-U curve is, the more susceptible to voltage collapse the power system is. The critical point of the Q-U curve in diagram 2.7 corresponds to the voltage where the voltage sensitivity $\frac{\delta Q}{\delta U}$ becomes zero. As visualised in figure 2.7 the form of the Q-U curve has a high dependency of the active power of the load. The greater the active power of the load is, the more reactive power is needed to prevent a voltage collapse. Figure 2.7 gives the Q-U curve for three different load situations. p is the normalized active power of the load ($p = P_L / \frac{E^2}{X}$). If the Q-U curve of the bus is below the horizontal axis, then this bus has a positive reactive power margin, which means the power system would be voltage unstable [7, 12, 14].

In a more complex power system as the 2 bus power system shown in figure 2.4 a fictitious synchronous generator with zero active power and no reactive power limits is connected to a specific bus. Then a power flow program, like PSS Sincal, can calculate

a range of specified voltages for this specific bus. The reactive power of synchronous condenser (Q_{SC}), the $Q(U)$ system characteristic and the $Q(U)$ behaviour from the load is noted from the power flow program and plotted against the specific bus voltage. The fictitious synchronous generator is needed to separate the reactive power supply of the system and the reactive power demand of the load, described in chapter 2.2.5 [7, 14].

2.2.8 Native Load Behaviour

According to [15] the term "load" can have several meanings in power engineering:

- *"A device, connected to a power system, that consumes power."*

- *"The total active and/or reactive power consumed by all devices of the power system."*

- *"A portion of the system that is not explicitly represented in a system model, but rather is treated as if it were a single power-consuming device connected to a bus in the system model."*

- *"The power output of a generator or generating plant."*

In this thesis the term load refers to a device connected to the power system that consumes or produces power, which is explained in chapter 2.2.9.
The $Q(U)$ load behaviour of traditionally load models has a static load characteristic. There are several static load model, which describe the relationship of a bus voltage and the active and reactive power of the load mathematically.

Load Behaviour: expresses the active and reactive powers as a function of the voltage magnitude. The function is independent from the time. There are several static load models which describe the load behaviour slightly different [11, 12, 15].

- Constant Impedance Load Model - The active and reactive power varies directly with the square of the voltage magnitude which has a stiff voltage characteristics ($k_{SLC} = 2$) [15, 16].

$$P = P_0 \cdot [a_1 \cdot (\frac{U}{U_0})^2] \qquad (2.23)$$

$$Q = Q_0 \cdot [a_4 \cdot (\frac{U}{U_0})^2] \qquad (2.24)$$

- Constant Current Load Model - The active and reactive power varies directly with the voltage magnitude. The load demand changes linearly with the voltage which

results in a voltage characteristics $k_{SLC} = 1$ [15, 16].

$$P = P_0 \cdot a_2 \cdot \frac{U}{U_0} \tag{2.25}$$

$$Q = Q_0 \cdot a_5 \cdot \frac{U}{U_0} \tag{2.26}$$

- Constant Power Load Model - The active and reactive power doesn't vary with the voltage magnitude, it is voltage invariant and has a stiff voltage characteristics $k_{SLC} = 0$ and $k_{SLC} = 0$ [15, 16].

$$P = P_0 \cdot a_3 \tag{2.27}$$

$$Q = Q_0 \cdot a_6 \tag{2.28}$$

- Polynomial Load Model - represents the relationship of the voltage magnitude and the active and reactive power of the load as a polynomial equation [15, 16].

$$P = P_0 \cdot [a_1 \cdot (\frac{U}{U_0})^2 + a_2 \cdot (\frac{U}{U_0}) + a_3] \tag{2.29}$$

$$Q = Q_0 \cdot [a_4 \cdot (\frac{U}{U_0})^2 + a_5 \cdot (\frac{U}{U_0}) + a_6] \tag{2.30}$$

This model is also known as "ZIP" model, since it consists of the sum of constant impedance (Z), constant current (I) and constant power (P) terms. U_0 is the rated voltage of the device and P_0 and Q_0 are the active and reactive power of the load, consumed at the rated voltage. Normally $a_1 + a_2 + a_3 = 1$ and $a_4 + a_5 + a_6 = 1$ [12, 15, 16].

- Exponential Load Model - represents the relationship of the voltage magnitude and the active and reactive power of the load as a exponential equation like following:

$$P = P_0 \cdot (\frac{U}{U_0})^{k_{SLC,p}} \tag{2.31}$$

$$Q = Q_0 \cdot (\frac{U}{U_0})^{k_{SLC}} \tag{2.32}$$

By setting the parameter k_{SLC} to 0, 1 or 2, the load model will be changed to constant power, constant current or constant impedance. The parameter k_{SLC} is the static load characteristic described in chapter 2.2.5 [15, 16]. The active power static load characteristic, $k_{SLC,p}$, refers to the slope of the voltage by varying active power.

2.2.9 Load Modelling

Previous studies have shown a changing reactive power flow on the medium voltage grid and even a reactive power flow into the high voltage grid. Additionally, the $Q(U)$ characteristic of the load seen from different load levels is changing massively [4]. A reason for this issue is the increasing amount of $Q(U)$ controlled distributed generation production. The integration of renewable energy sources with limited or no reactive power control (e.g. household-scale photovoltaic inverter with $\cos(\varphi)$ constant) has been analysed in other reports and has been rated as a risk for the voltage stability [12]. The effects of distributed power generation controlled by a $Q(U)$ controller on the voltage stability and load characteristic is focused in this thesis. Figure 2.8 gives an overview of the lumped loads seen from different voltage levels.
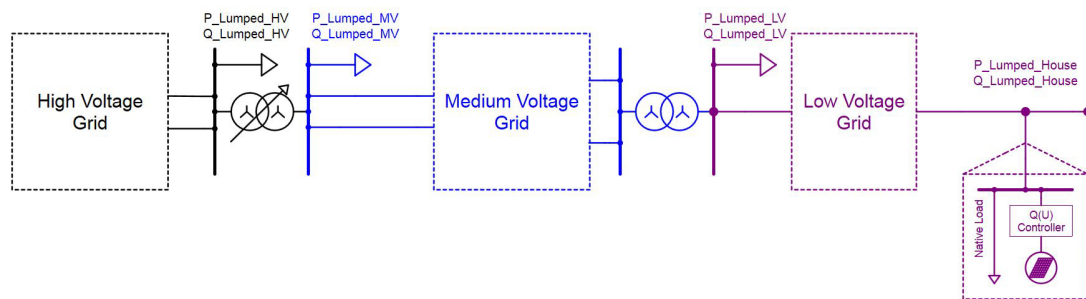
Figure 2.8: Schematic presentation of the lumped load seen from different voltage levels

Figure 2.9 gives the schematic chart of the lumped house load. The lumped house load is a superposition of the native load behaviour, which is modelled by one of the load models presented in chapter 2.2.8 and the output of the $Q(U)$ controlled distributed generator. Pending on the power demand of the native load and the power output of the distributed generator the lumped house load is either producing or consuming active and/or reactive power.
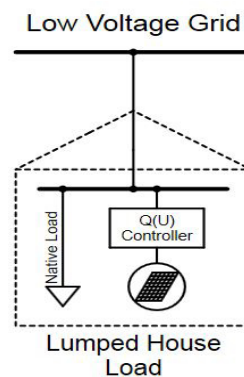

Figure 2.9: Schematic chart of the lumped house load [4]

Figure 2.10 presents the $Q(U)$ behaviour of the lumped house load. It shows that the reactive power demand/supply is pending on the bus voltage and the active power supply of the distributed generator.
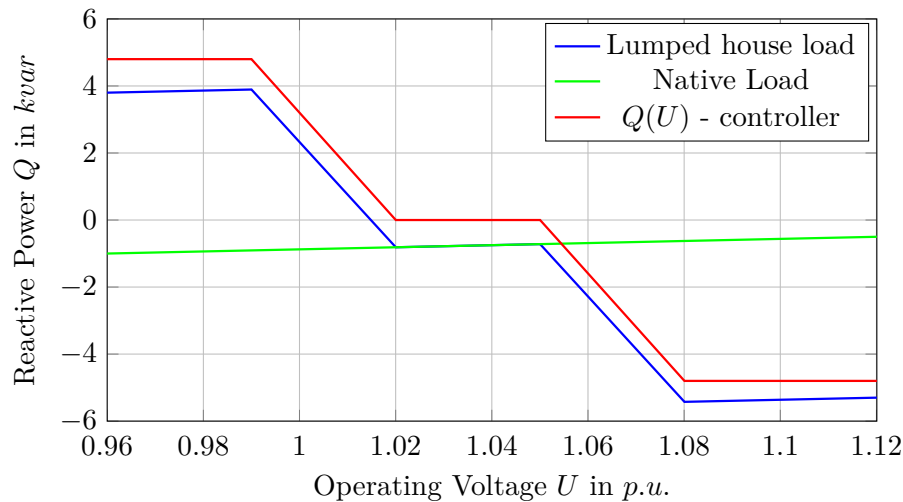

Figure 2.10: $Q(U)$ behaviour of the lumped house load [4]

The lumped load seen from the low voltage bus bar (P_{LV}^{lumped} and Q_{LV}^{lumped}) is a composition of all lumped house loads which are connected to the low voltage grid and the characteristic as well as the losses of the low voltage lines and/or cables. The medium voltage lumped load (P_{MV}^{lumped} and Q_{MV}^{lumped}) is a superposition of all connected low voltage lumped loads, the characteristic of the MV/LV transformer and the medium voltage grid behaviour. Finally, the lumped load seen from the high voltage bus bar (P_{HV}^{lumped} and Q_{HV}^{lumped}) is a composition of the HV/MV transformer behaviour and all connected medium voltage lumped loads.

The low voltage grid is not considered and simulated in this thesis as it is connected with the medium voltage grid via no-load tap changer transformers. The low voltage grid is represented with a natural load ($P_{MV}^{natural}$) and a decentralized generation (P_{MV}^{DG}). The natural load represents the composition of all low voltage native loads and is modelled according to the constant impedance load model. The medium voltage decentralized generation is a composition of all $Q(U)$ controlled generators which feed into the low voltage grid. Figure 2.11 gives a schematic overview of this issue.
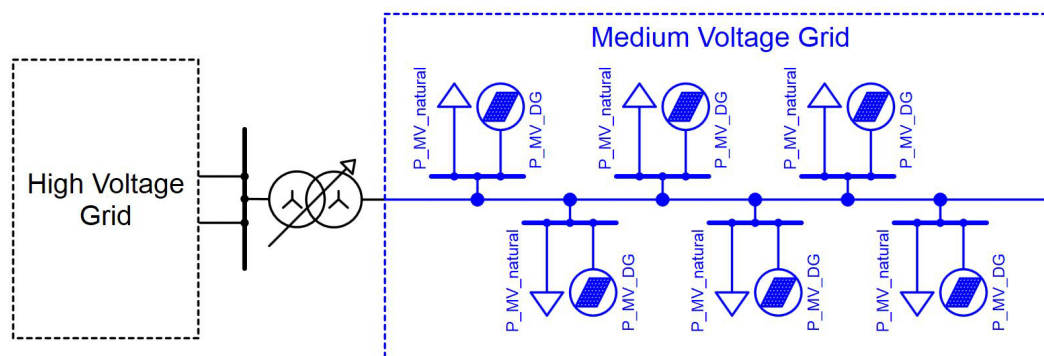

Figure 2.11: Schematic explanation of the low voltage grid reduction

3 Voltage Stability and Sensitivity

Normally voltage stability is described as the ability of a power system to maintain steady voltages at all buses in the power system after a disturbance. Or in other words, the voltage stability studies how changes of the reactive power Q affects the voltages U in the system.

Voltage sensitivity of a load, or in other words the static load characteristic, is referred to as the slope of the voltage by varying reactive power. The power system is defined as stable if the voltage sensitivity of the system characteristic is positive for every bus. On the other hand, the power system is unstable if the voltage sensitivity of the system characteristic is negative for at least one bus.

An increase of distributed power generation has effects on the voltage sensitivity and stability of the power system. In this thesis the effects of $Q(U)$ controlled distributed generation is analysed. The upgrade of the photovoltaic cells with $Q(U)$ controllers has major impacts on the characteristic of the load, seen from different load levels. A reactive power flow change on the medium voltage grid and even a reactive power flow into the high voltage grid has been detected [4]. The natural behaviour of the load seen from the medium voltage bus bar has been modified and is eclipsed by the $Q(U)$ characteristic of the photovoltaic controller. This phenomenon has been explained in chapter 2.2.9. The variation of the static load characteristic is analysed as well as the voltage stability in this chapter.

Therefore three different power networks are being examined. First a case study in a simple two bus system is presented. Secondly the more complex IEEE 30 bus test grid, including several distribution grids and distributed generation is simulated. Finally the voltage stability and static load characteristic of a real power network, the Salzburg power network, is being analysed.

3.1 Simulations Methodology

The purpose of this thesis is to analyse the static load characteristic and the voltage stability of different power networks in case of $Q(U)$ controlled distributed generation. The characteristic of the load seen from different voltage levels is changing it's behaviour as the $Q(U)$ behaviour of the load and the output of the $Q(U)$ controller of the distributed generators overlap. Also the behaviour of the on-load tap changer transformers and the characteristic of the lines are being considered, which is explained in chapter 2.2.9. With

24

distributed generation the load seen from different voltage levels can't be modelled with one of the described load models presented in chapter 2.2.8. This means the characteristic of the load is changing dramatically. A detailed illustration of the functionality of the $Q(U)$ controller is given in chapter 2.2.3. The methodology to analyse the changes of the static load characteristic, as well as the methodology to analyse the voltage stability is presented in this chapter.

3.1.1 Extraction of Static Load Characteristic

Figure 3.2 shows the flow chart to create the $Q(U)$ load behaviour seen from the medium voltage bus bar (P_{MV}^{lumped} and Q_{MV}^{lumped}) and to calculate the static load characteristic (k_{SLC}). The algorithm is performed for different simulation scenarios and all three different power networks. Either the value of the load or the distributed generation production is varied for each simulation scenario. The centralized generation is kept stable and the voltage of the medium voltage bus bar, and the voltage levels below the medium voltage bus bar, which shall be analysed, is controlled by manipulating the tap status of the on-load tap changer transformer. The on-load tap changer transformer adds a certain percentage of the nominal voltage per tap step and has a certain amount of tap steps. Varying the on-load tap changer transformer steps continuously from the maximum value to the minimum value varies the voltage on the medium voltage bus bar from minimum to maximum. Only one medium voltage grid bus bar is controlled per static load characteristic simulation scenario. The on-load tap changer transformer steps of the other distribution grids (if available) are set to be controlled automatically, calculated from the Power Flow program, to keep the voltage of the medium voltage bus bar between 1.02 p.u. and 1.06 p.u., which is the normal operation voltage range. Graph 3.1 shows how the different on-load tap changer transformers are handled. The reactive power and the active power through the HV/MV transformer, of the analysed distribution grid, is used to calculate the static load characteristic k_{SLC} according to equation 2.15.
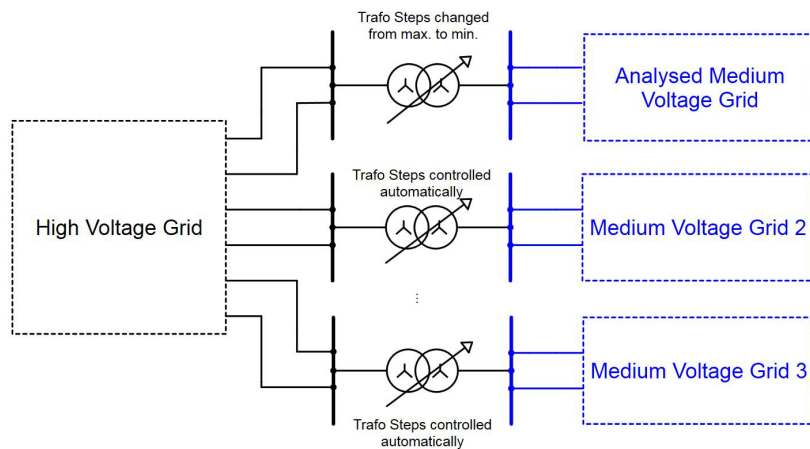

Figure 3.1: Schematic illustration of the transformer settings

The used power flow program is PSS Sincal and the Newton Raphson algorithm is used for the simulation. The results of the power flow calculations for this simulation scenario can be used to analyse the behaviour of the load seen from the medium voltage bus bar. This load behaviour can be reproduced by programming a load macro by using PSS Netomac. These macros are programmed to control the lumped load, which allows the simulation of a bigger, more complex power network. Furthermore the distribution network can be reduced by a macro controlled lumped load. The advantage of this procedure is, that the network is extremely reduced but has the same $Q(U)$ and $P(U)$ behaviour as the original network.
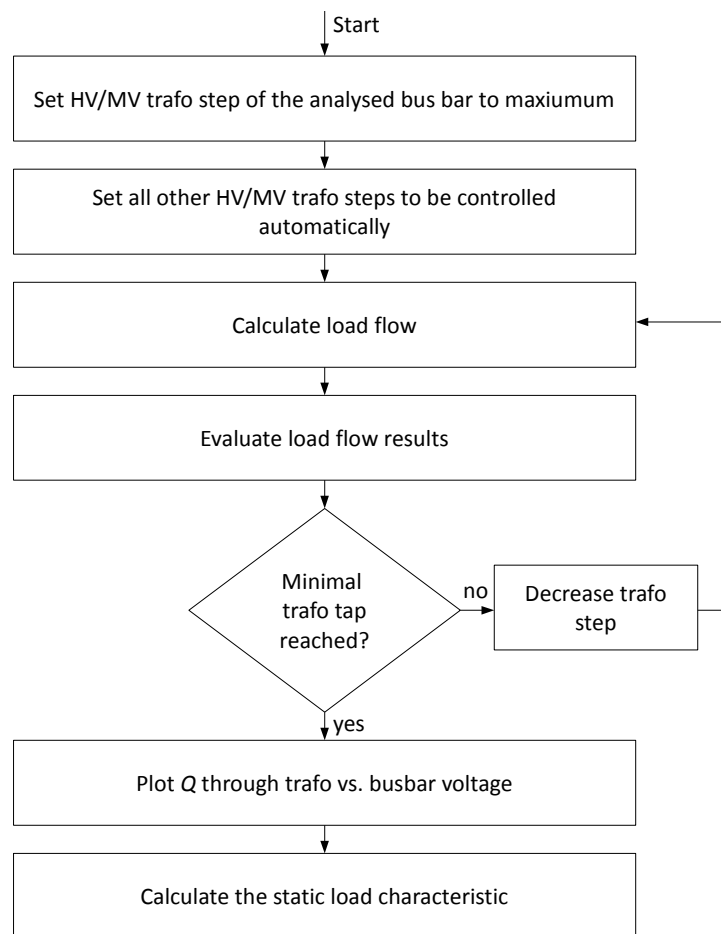
Figure 3.2: Simulation algorithm to extract the static load characteristic

3.1.2 Extraction of Power System Sensitivity and Stability

To analyse the influence of $Q(U)$ controlled distributed generation on the voltage stability, the $Q(U)$ curves are a very useful tool as it is relatively easy to create and provides a measure of absolute stability and stability margin [14]. The used power flow program is PSS Sincal / Netomac and the Newton Raphson algorithm is used for the simulation.

An individual $Q(U)$ curve for each high voltage bus bar is being created, which allows to calculate the voltage stability of the whole power system and the individual stability margin for each distribution grid. Three curves are generated for each high voltage bus bar and for each simulation scenario, using the results of the power flow program. Either the value of the load or the distributed generation production is varied for each simulation scenario. The first curve is the reactive power of the synchronous condenser versus the voltage curve. The synchronous condenser represents a fictitious and adjustable reactive power source. Figure 3.3 gives a graphical overview of the interaction between the reactive power demand or supply of the high voltage lumped load (Q_{HV}^{lumped}), the synchronous condenser (Q_{SC}) and the system (Q_{system}). The reactive power output of the synchronous condenser represents the reactive power which is needed to keep the voltage of the controlled network bus at a specific voltage. The second curve is the $Q(U)$ load behaviour, which is the reactive power through the HV/MV transformer seen from the high voltage bus bar (P_{HV}^{lumped} and Q_{HV}^{lumped}). The third curve is the system characteristic which measures the ability of the network to supply the network with reactive power in the vicinity of the bus.

$$Q_{HV}^{lumped} = Q_{SC} + Q_{system} \tag{3.1}$$
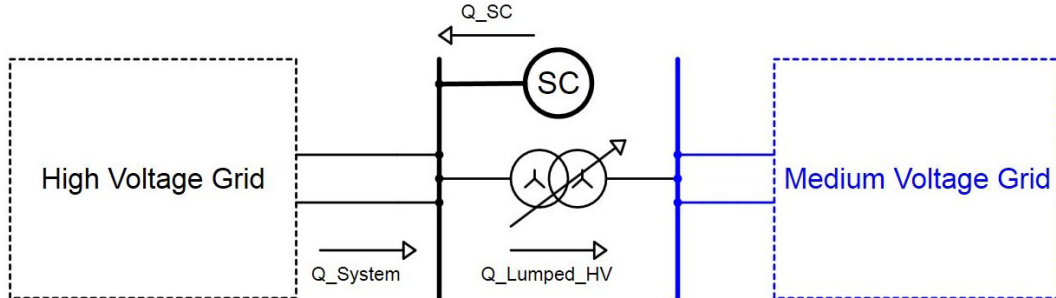
Figure 3.3: Schematic overview of the reactive power flow

The loads are modelled with the constant impedance load model. The capacity of the synchronous condenser is very large (the reactive power output is almost unlimited) but the active power output is set to zero. The reactive power output of the fictitious synchronous condenser is controlled to vary the voltage of the high voltage bus bar from about 0.5 p.u. to 1.5 p.u.. The flow chart of the algorithm to create the system characteristic and the Q-U curve is given in figure 3.1.1. The system can be considered as voltage stable if the system characteristic and the high voltage lumped load characteristic intersect in a stable operating point. If the bus voltage magnitude is increased above the minimum point then reactive power must be injected at the bus to raise the voltage. On the other hand if the bus voltage magnitude is decreased below the minimum reactive

power point then reactive power injection at the bus is required. The Q-U curve method allows also the possibility to measure the margin of stability. It is calculated as the difference of the bottom of the synchronous condenser characteristic curve and the high voltage lumped load characteristic line. A low reactive power margin of a power system means, the power system works near a voltage collapse situation. If the reactive power margin is negative, the power system is not in a operational situation. The reactive power margin is a very effective way, to compare how close the system is to a voltage collapse for different simulation scenarios. According to the algorithm given in figure 3.4 all HV/MV trafos are set to control the medium voltage bus bar voltage automatically and to keep it between $U_{MV} = 1.02$ p.u. and $U_{MV} = 1.06$ p.u.. After that the reactive power output of the fictitious synchronous condenser is being set to reach a high voltage bus bar voltage of $U_{HV} = 0.5$ p.u.. Then the reactive power output is being increased and the reactive power demand of the load, as well as the reactive power output of the synchronous condenser and the system is calculated. This procedure is being repeated until a high voltage bus bar voltage of $U_{HV} = 1.5$ p.u. is reached.
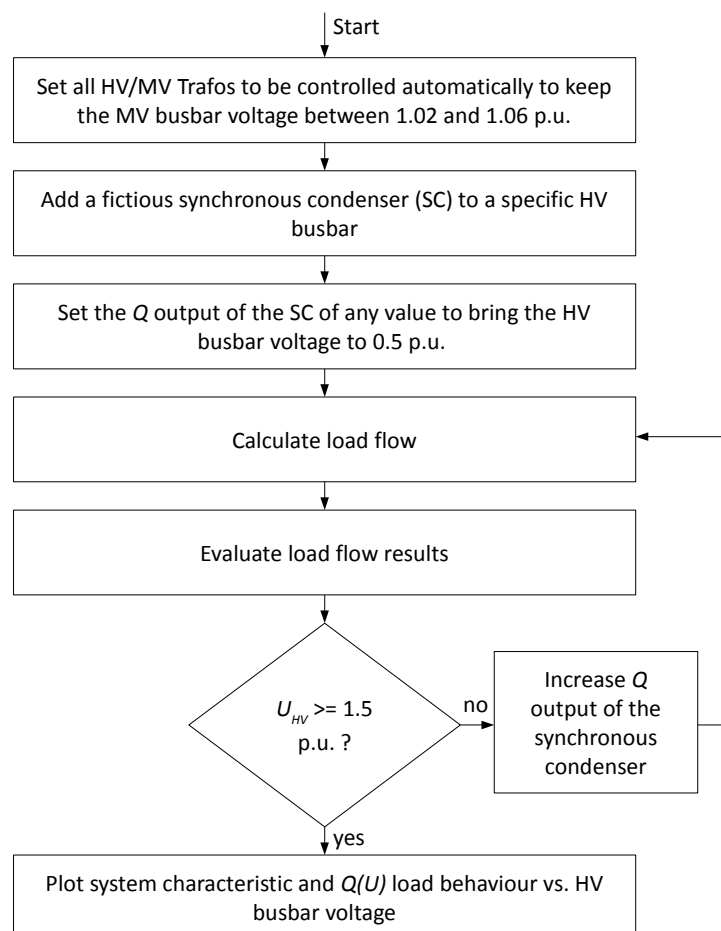
Figure 3.4: Algorithm to analyse the voltage stability as well as the HV load behaviour

3.2 Two Bus Test Network Simulations

In this chapter a case study in a two-bus system is presented. The system has been constructed to demonstrate the voltage stability and the voltage sensitivity in a very simple test network. Figure 3.5 shows the general layout of the analysed network. The network consists of the following components and elements:

- 132kV transmission grid

- 33kV distribution grid

- a generator which feeds into the transmission grid

- a on-load tap changer transformer which connects the transmission grid and the distribution grid

- a transmission line which connects the generator and a transformer

- a load which is modelled using the constant impedance load model.

- a distributed generator which feeds into the distribution grid and is controlled by a $Q(U)$ controller

- a fictitious synchronous condenser which is needed to control the bus bar voltage. Basically the synchronous condenser is an adjustable reactive power source without reactive power generation limits. The synchronous condenser is deactivated if the static load characteristic is being extracted.
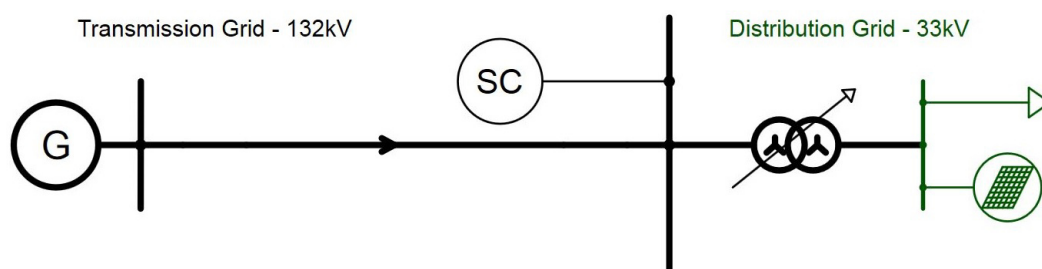
Figure 3.5: General layout of the two bus network

3.2.1 Extraction of the *Q(U)* Load Behaviour

Scenario Definition

The active power of the distributed generation and the active power of the load is being changed in the different simulation scenarios which can be seen in table 3.1. The natural load, which is described in chapter 2.2.9, is kept at the nominal value of $P_{MV}^{load} = 10$ MW and $Q_{MV}^{load} = 10$ Mvar in simulation scenario 2 to 5, while the active power output of the distributed generation is varied from $P_{MV}^{load} = 0$ MW to $P_{MV}^{load} = 15$ MW. In simulation scenario 6 to 9 the natural load is being reduced to $P_{MV}^{load} = 1$ MW and $Q_{MV}^{load} = 1$ Mvar, while the active power output of the distributed generation is varied again from $P_{MV}^{load} = 0$ MW to $P_{MV}^{load} = 15$ MW. For example simulation scenario 6 represents a situation of a very low natural load demand and a very high distributed generation production. On the other hand simulation scenario 5 represents a very high natural load situation and a low distributed generation production. The different simulation scenarios shall represent different situations of the power system, e.g. the load is changing during the day and during the week, and the distributed generation production is pending on the weather, e.g. wind power plants are pending on the wind and photovoltaic cells on the sun.

The algorithm to create the characteristic of the load is explained in chapter 3.2. The centralized generation is kept stable and the voltage of the medium voltage grid is controlled by manipulating the tap status of the on-load tap changer transformer. The on-load tap changer transformer adds 1% of the nominal voltage per tap step and it has been set to 60 steps (±30). Normally an on-load tap changer transformer has 20 steps (±10), but in this thesis the tap steps have been extended to extract the static load characteristic. Varying the on-load tap changer transformer steps continuously from 30 to -30 varies the voltage on the medium voltage bus bar from $U_{MV} = 0.85$ p.u. to $U_{MV} = 1.45$ p.u.. The reactive power and the active power through the HV/MV transformer is used to calculate the $Q(U)$ characteristic of the load k_{SLC} (see equation 2.15), which is a very important parameter for the voltage stability. The synchronous condenser is deactivated for this simulation scenario.

The nominal active power of the natural load has been set to $P_{MV}^{load} = 10$ MW and the nominal reactive power of the natural load has been set to $Q_{MV}^{load} = 10$ Mvar. The minimal active power of the natural load has been set to $P_{MV}^{load} = 1$ MW and the minimal reactive power of the natural load has been set to $Q_{MV}^{load} = 1$ Mvar. The natural load is modelled using the constant impedance load model (see equations 2.23 and 2.24)

The nominal active power of the distributed generation has been set to $P_{DG}^{nominal} = 15$ MW. A detailed illustration of the $Q(U)$ controller of the distributed generation can be seen in chapter 2.2.6. According to equation 2.21 the reactive power varies from $Q_{DG} = -0.32868 \cdot P_{DG}$, if the voltage is above $U = 1.08$ p.u., to $Q_{DG} = 0.32868 \cdot P_{DG}$, if the voltage is below $U = 0.99$ p.u.. That means an active power output of $P_{DG} = 15$ MW results in a reactive power output between $Q_{DG} = \pm4.9302$ Mvar pending on the medium

voltage bus bar voltage. The reactive power output of the distributed generation is only depending on the voltage of the medium voltage bus bar at a certain and stable active power output. The static load characteristic has been calculated at different nominal power values of the natural load and different distributed generation production which can be seen in Table 3.1.

Table 3.1: Natural Load and Distributed Generation Production of the two bus network

Simulation Scenario	P_{MV}^{load} MW	Q_{MV}^{load} Mvar	P_{DG} MW
1	1.00	10.00	15.00
2	10.00	10.00	15.00
3	10.00	10.00	7.50
4	10.00	10.00	1.50
5	10.00	10.00	0.00
6	1.00	1.00	15.00
7	1.00	1.00	7.50
8	1.00	1.00	1.50
9	1.00	1.00	0.00

The voltage of the medium voltage bus bar, the active and reactive power of the HV/MV supplying transformer has been calculated with the data gotten from the power flow program.

Additionally the $Q(U)$ load behaviour of the load seen from different voltage levels has been analysed and compared. For this scenario the interesting voltage range is from $U_{MV} = 0.9$ p.u. to $U_{MV} = 1.1$ p.u., as there are the violation limits. If the voltage violates these limits then security actions would be started. That's the reason why the load behaviour in this range is interesting. In this case study the $Q(U)$ characteristic of the load seen from the high voltage bus bar (Q_{HV}^{lumped}) is compared with the $Q(U)$ characteristic of the load seen from the medium voltage bus bar (Q_{HV}^{lumped}). The difference is that the $Q(U)$ load characteristic seen from the high voltage bus bar is a superposition of the natural load behaviour, the $Q(U)$ controlled distributed generation and the characteristic of the on-load tap changer transformer. The transformer is set to be controlled automatically by the power flow program, to keep the medium voltage bus bar voltage between $U_{MV} = 1.02$ p.u. and $U_{MV} = 1.06$ p.u.. The $Q(U)$ characteristic of the load seen from the high voltage bus bar has been calculated according to the algorithm given in chapter 3.1.2. With this method the high voltage bus bar voltage has been varied from $U_{HV} = 0.9$ p.u. to $U_{HV} = 1.1$ p.u..

Simulation Results

Figures 3.6, 3.7, 3.8 give the $Q(U)$ behaviour of different simulation scenarios for a voltage range from $U = 0.9$ p.u. to $U = 1.1$ p.u.. Two curves have been plotted: The high voltage lumped load characteristic and the corresponding medium voltage lumped load characteristic. The main difference is that the high voltage lumped load includes the on-load tap changer transformer characteristic.

Figure 3.6 presents the simulation result of Scenario 5, where the natural load is set to it's nominal value ($P_{MV}^{load} = 10$ MW and $Q_{MV}^{load} = 10$ MW) and the distributed generation is deactivated. It can be seen that the static $Q(U)$ load characteristic seen from the medium voltage bus bar is almost linear with $k_{SLC} = 2.00$, which is because the natural load is modelled with a constant impedance model. The high voltage $Q(U)$ characteristic is nearly stiff as the on-load tap changer transformer keeps the medium voltage bus bar voltage very close to $U_{MV} = 1.03$ p.u. and that's why it is almost independent of the natural load characteristic as the voltage of the natural load is almost constant. The medium voltage bus bar voltage is controlled by the transformer and kept between $U_{MV} = 1.02$ p.u. and $U_{MV} = 1.06$ p.u..
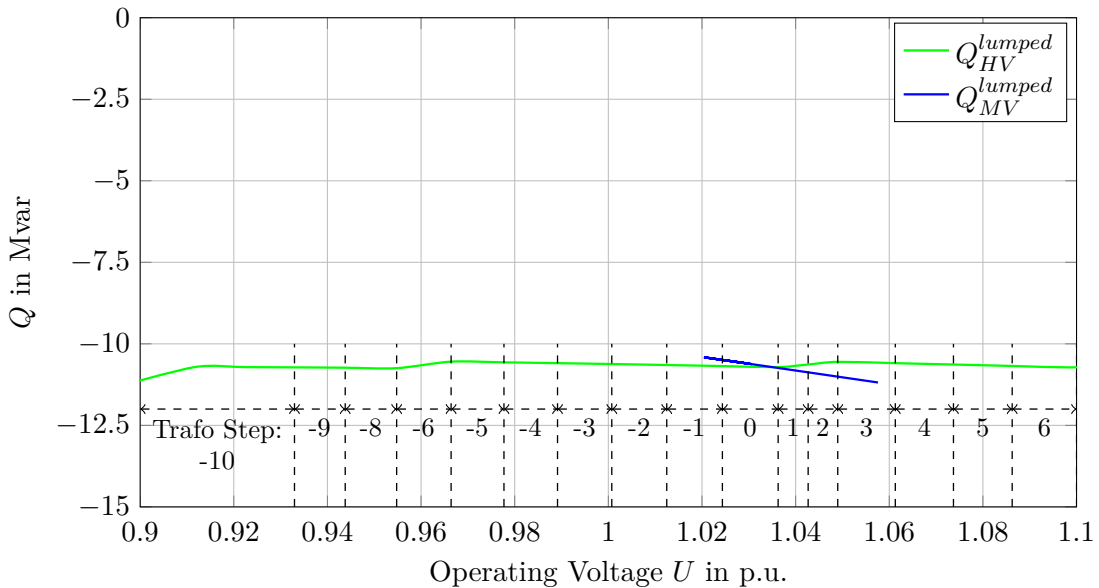
Figure 3.6: Load behaviour $P_{MV}^{load} = 10$ MW and $P_{DG} = 0$ MW, Simulation Scenario 5

Figure 3.7 gives the $Q(U)$ behaviour of the load in case of a very high distributed generation penetration ($P_{DG} = 15$ MW) where the natural load is set to it's nominal value ($P_{MV}^{load} = 10$ MW and $Q_{MV}^{load} = 10$ MW). The superposition of the natural load characteristic and the $Q(U)$ controller output of the distributed generation is very obvious and can be seen in the medium voltage $Q(U)$ load characteristic. But also the behaviour of the high voltage bus bar $Q(U)$ load characteristic is changing it's behaviour in presence of a distributed generation production and is not stiff any more. The reason for this is the on-load tap changer transformer.

The transformer steps have been added to figure 3.6, 3.7 and 3.8. Figure 3.7 shows that the medium voltage lumped load characteristic for a voltage range from $U_{MV} = 1.02$ p.u. to $U_{MV} = 1.06$ is reflected multiple times in the high voltage lumped load characteristic (Trafo Step: -7, -1, 3).
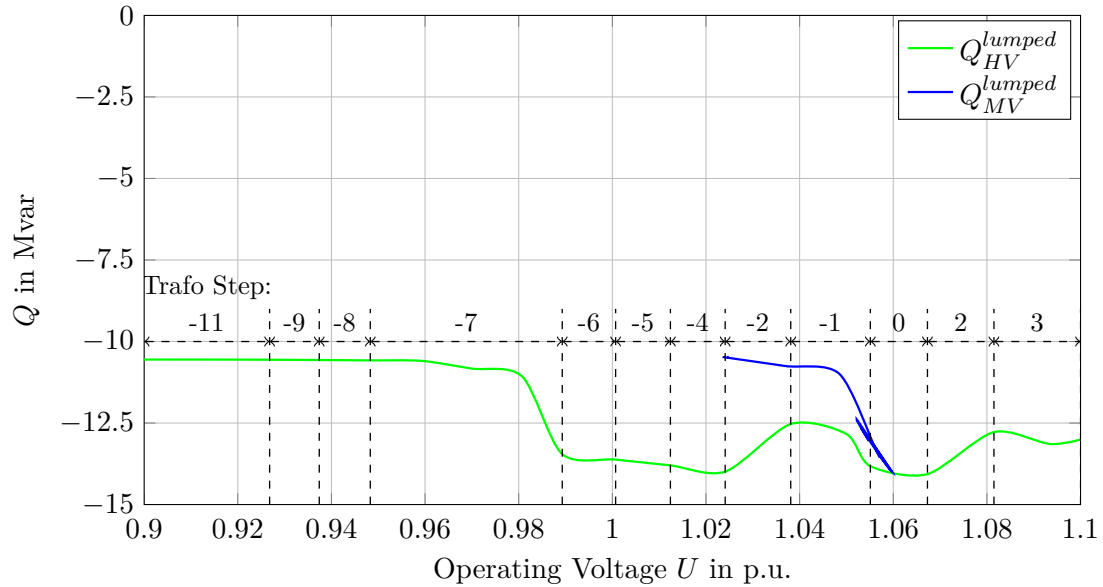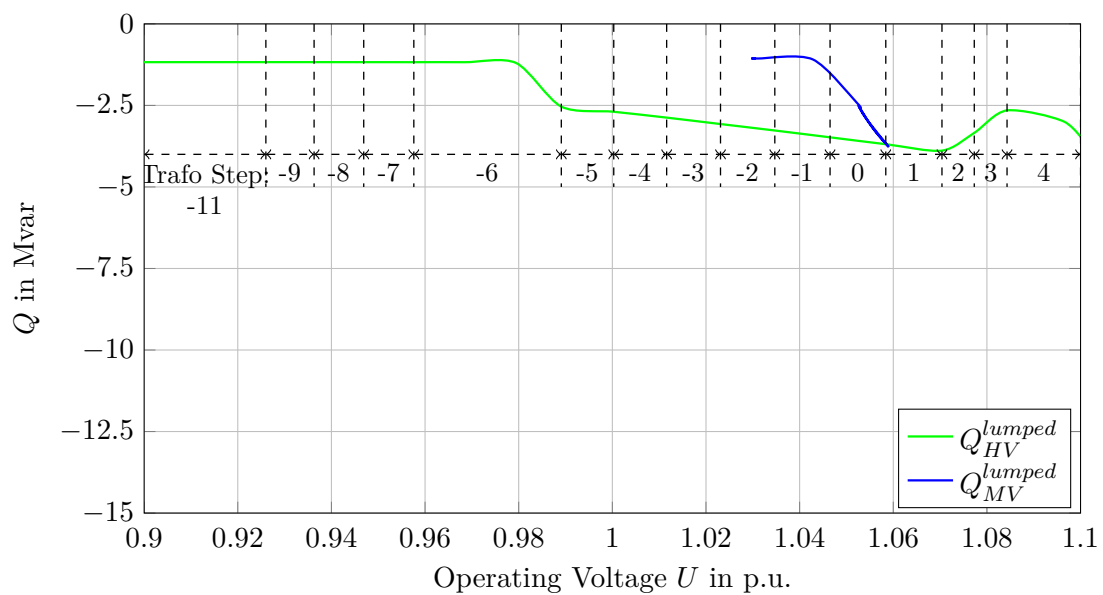

Figure 3.7: Load behaviour $P_{MV}^{load} = 10$ MW and $P_{DG} = 15$ MW, Simulation Scenario 2

Finally figure 3.8 presents the $Q(U)$ load behaviour in case of a very low load and a very high distributed generation situation ($P_{MV}^{load} = 1$ MW, $Q_{MV}^{load} = 1$ MW and $P_{DG} = 15$ MW - Simulation Scenario 6). It can be seen that the reactive power demand of the medium voltage grid is reduced and stays between $Q_{HV}^{lumped} = -1.25 Mvar$ and $Q_{HV}^{lumped} = -3.5 Mvar$.

Figure 3.8: Load behaviour $P_{MV}^{load} = 1$ MW and $P_{DG} = 15$ MW, Simulation Scenario 6

After that the $Q(U)$ behaviour of the load seen from the medium voltage bus bar is analysed in more detail and the static load characteristic is calculated as well. The used algorithm can be seen in figure 3.2. The medium voltage bus bar voltage is controlled via the tap steps of the on-load tap changer transformer. The tap status of the on-load tap changer transformer is varied continuously from 30 to -30 (maximum to minimum) and a power flow calculation has been done for each step. The centralized generation which feeds into the high voltage grid is kept stable. The simulation results can be seen in table 3.2.

Table 3.2: Simulation results: Voltage Sensitivity - 2 bus network

Simulation Scenario	P_{MV}^{lumped} MW	Q_{MV}^{lumped} Mvar	P_{MV}^{load} MW	Q_{MV}^{load} Mvar	P_{DG} MW	$k_{SLC,min}$	$k_{SLC,max}$
1	14.00	-6.18	-1.00	-10.00	15.00	1.43	22.82
2	5.00	-6.13	-10.00	-10.00	15.00	1.44	21.19
3	-2.50	-8.09	-10.00	-10.00	7.50	1.67	9.65
4	-8.50	-9.62	-10.00	-10.00	1.50	1.92	3.29
5	-10.00	-10.00	-10.00	-10.00	0.00	2.00	2.00
6	14.00	2.88	-1.00	-1.00	15.00	0.36	49.43
7	6.50	0.92	-1.00	-1.00	7.50	0.66	49.67
8	0.50	-0.61	-1.00	-1.00	1.50	1.44	19.89
9	-1.00	-1.00	-1.00	-1.00	0.00	2.00	2.00

Figure 3.9 shows the plotted simulation results for a maximal load situation (simulation scenario 2 to 5) while figure 3.10 shows the plotted simulation results for a minimal natural load situation (simulation scenario 6 to 9). The reactive power through the HV/MV transformer is shown as a function of the medium voltage bus bar voltage. The simulation results show that the extreme values of the static load characteristic k_{SLC} are 0.36 and 49.67 which are highly depending on the produced active power of the distributed generation and the reactive power of the natural load. If the distributed generation produces more active power, or the reactive power demand of the natural load is getting lower, then the diversification of the static load characteristic k_{SLC} is becoming higher. On the other hand the static load characteristic is almost independent from the active power demand of the load, if the reactive power demand is independent from the active power demand of the load. The static load characteristic is highly varying because of the characteristic of the $Q(U)$ controller of the distributed generation. The plots "Simulation 5" and "Simulation 9" (see figure 3.9 and 3.10) display the $Q(U)$ load characteristic without decentralized generation by different load situations. The static load characteristic in this simulation scenario is $k_{SLC} = 2$, which is because the natural load is modelled with a constant impedance load model. The green curve shown in figure 3.9 and figure 3.10 (simulation scenario 2 and 6) include a high amount of distributed generation which makes the $Q(U)$ load behaviour very mutable.

On the other hand in case of a high amount of distributed generation a reactive power flow from the medium voltage grid to the high voltage grid has been detected (Simulation Scenario 6 and 7, $P_{DG} = 15$ MW and $P_{DG} = 7.5$ MW in figure 3.10). In this case the reactive power flow is from medium voltage to high voltage, which means the high voltage grid must absorb this additionally produced reactive power. Simulation scenario 4 and 8 ($P_{DG} = 0$ MW curve in figure 3.9 and 3.10) show the medium voltage lumped load characteristic in case of a very low distributed generation $P_{DG} = 1.5$ MW at two different natural load levels (maximal and minimal load). Finally the plots Simulation 3 and 7 ($P_{DG} = 7.5$ MW curve in figure 3.9 and 3.10) display the $Q(U)$ load characteristic with a decentralized generation of $P_{DG} = 7.5$ MW by different load situations.
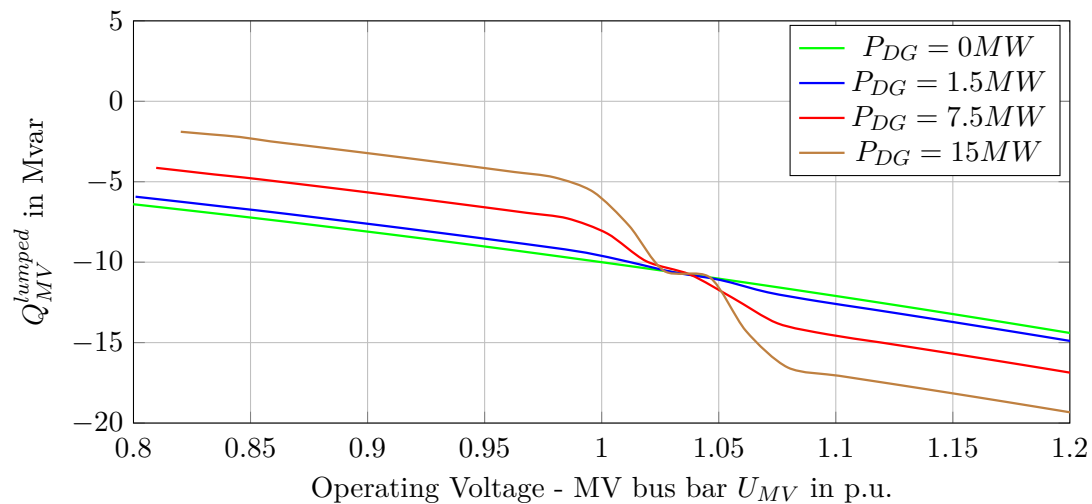
Figure 3.9: MV lumped load behaviour for a maximal load of $P_{MV}^{load} = 10$ MW
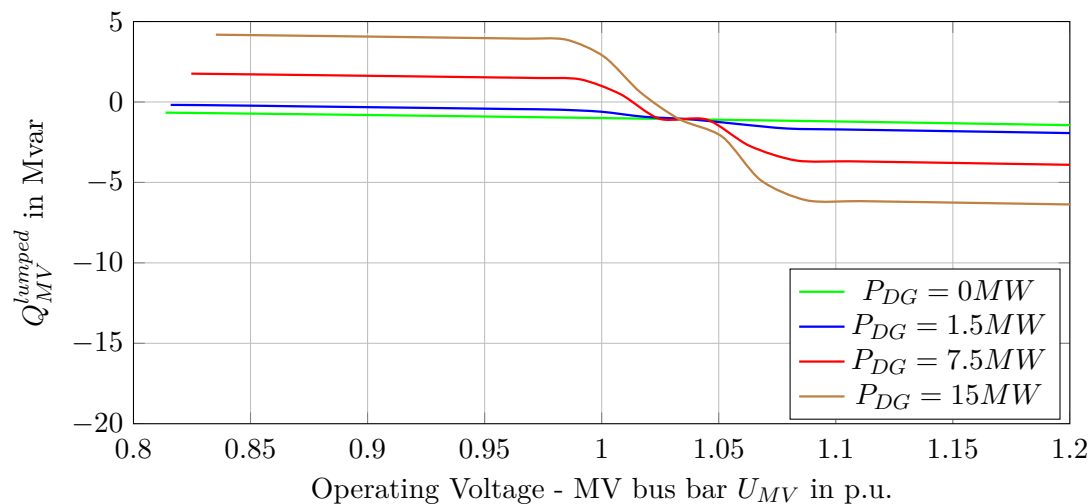
Figure 3.10: MV lumped load behaviour for a minimal load of $P_{MV}^{load} = 1$ MW

Figure 3.11 shows how the static load characteristic is changing with varying distributed generation, as well as the change of the active power by varying distributed generation. The calculated values are given also in tabular form, table 3.3. For this simulation scenario the voltage of the MV bus bar has been kept stable at $U_{MV} = 1$ p.u.. The figure 3.11 shows the dependency of the static load characteristic and the active power transfer from the medium voltage grid to the high voltage grid in case of a changing distributed generation, which means a change of the weather. As a result of the weather the static load characteristic is changing dramatically. In case of a cloudy weather, the distributed generation production is low and if the weather is sunny there is a high amount of distributed generation production. Additionally the active power through the HV/MV transformer is changing if the weather is changing. Figure 3.11 plots the static load characteristic over the active power through the HV/MV transformer for a minimal and a maximal load situation.
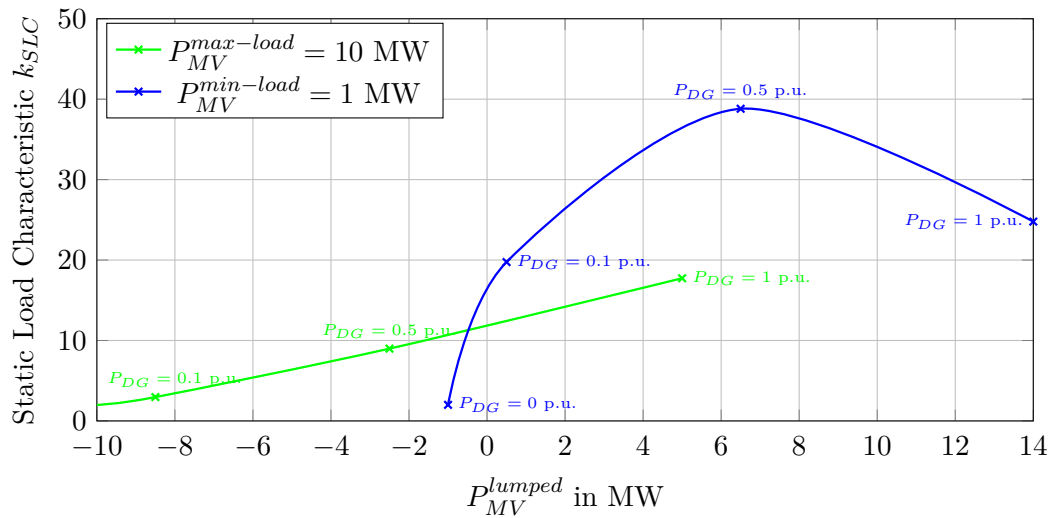
Figure 3.11: k_{SLC} over P_{MV}^{lumped} at $U_{MV} = 1$ p.u.

Table 3.3: k_{SLC} and P_{MV}^{lumped} at varying distributed generation

Maximal Load ($P_{MV}^{load} = 10$ MW)		Minimal Load ($P_{MV}^{load} = 1$ MW)		
P_{MV}^{lumped} MW	k_{SLC}	P_{MV}^{lumped} MW	k_{SLC}	P_{DG} MW
-10.00	2.00	-1.00	2.00	0.00
-8.50	2.96	0.50	19.75	1.50
-2.50	8.99	6.50	38.81	7.50
5.00	17.74	14.00	24.78	15.00

3.2.2 Voltage Stability and Power System Characteristic

Scenario Definition

The voltage stability has been analysed using Q-U curves which are described in chapter 2.2.7. The influences of the $Q(U)$ controlled distributed generation on the static load characteristic has been shown in chapter 3.2.1. Q-U curves provide a measure of the absolute stability and the stability margin. A fictitious and adjustable reactive power source is needed to control the voltage of the high voltage bus bar. Therefore a synchronous condenser is added to the power network which can be seen in figure 3.5. Three curves are created with the power flow program. The first curve is the reactive power of the synchronous condenser. The second curve represents the power system characteristic, which measures the ability of the network to supply the network with reactive power in the vicinity of the bus. And the third curve is the high voltage lumped load characteristic. The synchronous condenser is needed to keep the voltage of the high voltage bus bar at a certain amount. For more clarity of the figures the synchronous condenser characteristic isn't plotted. Several simulations, with different distributed generation and different natural load situations have been performed. The natural load in simulation scenario 1 to 4 is kept at the nominal value of $P_{MV}^{load} = 10$ MW and $Q_{MV}^{load} = 10$ Mvar, while the active power output of the distributed generation is varied from $P_{DG} = 15$ MW to $P_{DG} = 0$ MW. Simulation scenario 8 is calculated with a low natural load of $P_{MV}^{load} = 1$ MW and $Q_{MV}^{load} = 1$ Mvar and a high distributed generation of $P_{DG} = 15$ MW. Finally, simulation scenario 7 and 9 have a very high natural load of $P_{MV}^{load} = 100$ MW and $Q_{MV}^{load} = 100$ Mvar while the distributed generation is varied.

The voltage of the high voltage bus bar has been changed continuously from $U_{HV} = 0.5$ p.u. to $U_{HV} = 1.4$ p.u. using the fictitious synchronous condenser, for each simulation scenario. The HV/MV on-load tap changer transformer is set to control the medium voltage bus bar automatically. The target voltage range of the transformer controller is set from $U_{MV} = 1.02$ p.u. to $U_{MV} = 1.06$ p.u.. An overview of each simulation scenario is given in table 3.4.

Simulation Results

The system characteristic is normally parabolic. At some point, the generators stop decreasing their reactive power value. In this case the system characteristic reaches the top of the curve. This point represents the maximum increase in the reactive power of the load at this bus, also called the reactive power margin of the system. Any higher and a voltage collapse would occur [10]. Close to this point the power flow program has problems to reach convergence, which is the reason why the left side of the, normally parabolic, curve is missing, where the power system is unstable. The reactive power margin (stability margin) of the power system is calculated as the difference of the bottom

of the synchronous condenser characteristic curve and the $Q(U)$ load characteristic curve. The reactive power margin of each simulation scenario can be seen in table 3.4. A low reactive power margin of a power system means, the power system works near a voltage collapse situation. If the reactive power margin is negative, the power system is not in an operational situation. The reactive power margin is a very effective way, to compare how close the system is to a voltage collapse in different simulation scenarios. Additionally the synchronous condenser characteristic is moved to the left side in case of a high natural load and a low distributed generation production.

Table 3.4: Simulation Scenario - Voltage Stability - Two Bus Network

Simulation Scenario	P_{MV}^{load} MW	Q_{MV}^{load} Mvar	P_{DG} MW	Stability Margin Mvar
1	10.00	10.00	0.00	165.44
2	10.00	10.00	1.50	178.76
3	10.00	10.00	7.50	194.03
4	10.00	10.00	15.00	200.32
5	100.00	10.00	1.50	162.62
6	1.00	10.00	15.00	202.66
7	100.00	100.00	15.00	115.43
8	1.00	1.00	15.00	216.07
9	100.00	100.00	1.50	99.28

Figure 3.12 shows the Q-U curve for the two bus system without distributed generation while the natural load is set to the nominal values ($P_{MV}^{load} = 10$ MW and $Q_{MV}^{load} = 10$ Mvar). The reactive power margin of simulation scenario 1 is 165.44 Mvar which is the difference between the high voltage lumped load curve (P_{HV}^{lumped}) and the synchronous condenser characteristic at the lowest point of the curve. For this specific natural load situation and distributed generation production the power system can be considered as voltage stable (according to the equilibrium point analysis presented in chapter 3.3.3) for a high voltage bus bar voltage range of $U_{HV} = 0.7$ p.u. to $U_{HV} = 1.3$ p.u..
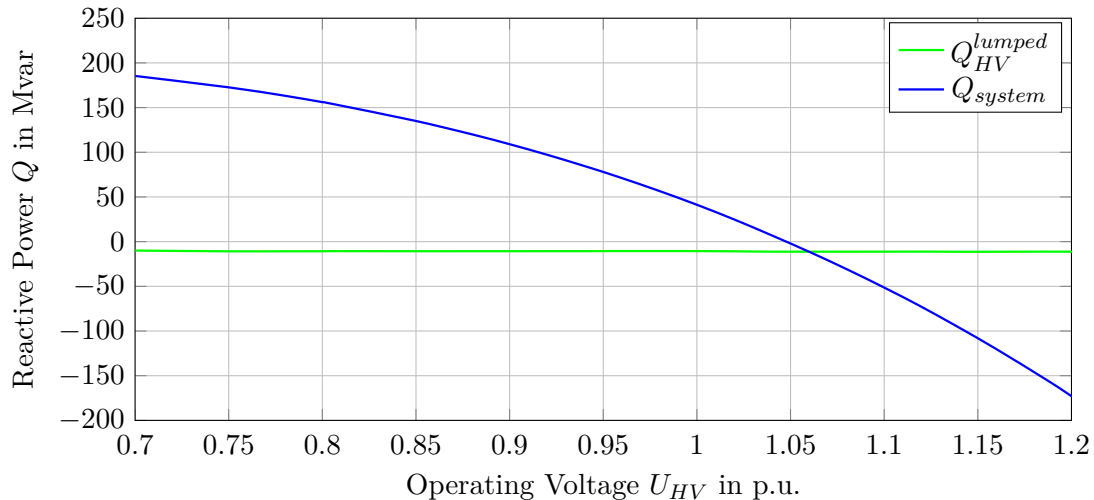
Figure 3.12: Q-U curve, $P_{MV}^{load} = 10$ MW and $P_{DG} = 0$ MW; Scenario 1

Figure 3.13 presents the Q-U curve with a high amount of distributed generation ($P_{DG} = 15$ MW) and the natural load is set to the nominal values ($P_{MV}^{load} = 10$ MW and $Q_{MV}^{load} = 10$ Mvar). The reactive power margin of Simulation Scenario 4 is 200.32 Mvar. According to the Q-U curve stability analysis method the power system becomes more stable in case of a high distributed generation as the stability margin is becoming higher. It can be seen that the reactive power margin is highly pending on the distributed generation production, and as a result of that, it is pending on the weather, as the weather influences the distributed generation production directly. The influence of the local controlled distributed generation can be seen in the high voltage lumped load curve (Q_{HV}^{lumped}) as the reactive power is decreasing from $Q_{HV}^{lumped} = -2.57$ Mvar to $Q_{HV}^{lumped} = -13.25$ Mvar by increasing the high voltage bus bar voltage from $U_{HV} = 0.6$ p.u. to $U_{HV} = 0.85$ p.u..
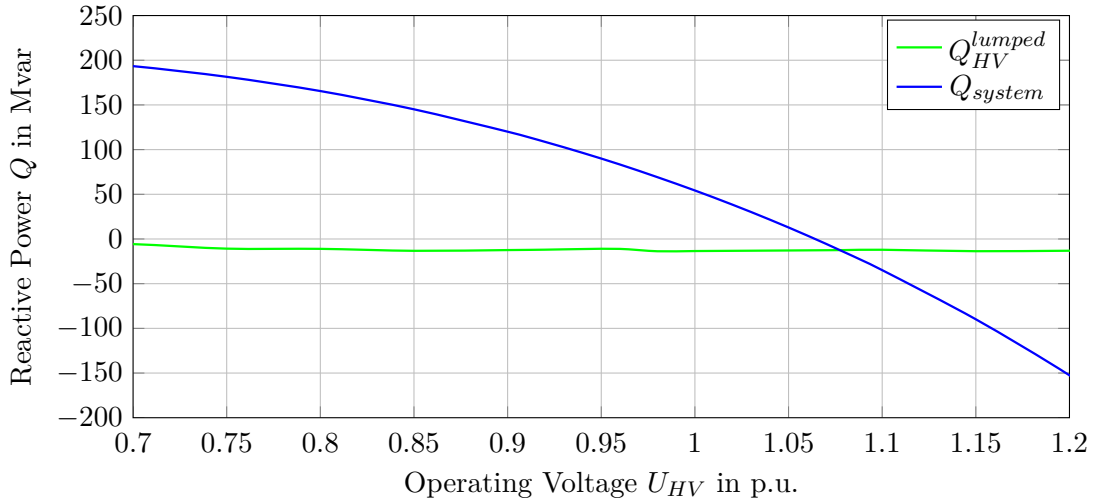
Figure 3.13: Q-U curve, $P_{MV}^{load} = 10$ MW and $P_{DG} = 15$ MW; Scenario 4

The Q-U curve for a very high natural load situation ($P_{MV}^{load} = 100$ MW and $Q_{MV}^{load} = 100$ MW) and a distributed generation production of $P_{DG} = 15$ MW is given in figure 3.14. The stability margin for this natural load situation and distributed generation production is significantly lower than in simulation scenario 1 and 4 (115.43 Mvar). According to the Q-U curve method the critical situation, in terms of voltage stability, is the situation of a very high load and a low distributed generation production, which is presented in figure 3.14.
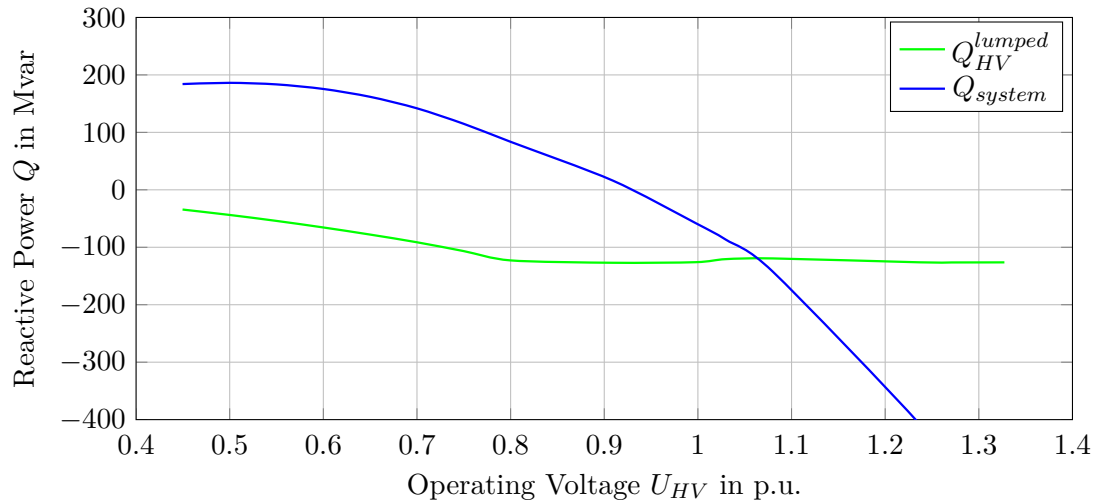
Figure 3.14: Q-U curve, $P_{MV}^{load} = 100$ MW and $P_{DG} = 15$ MW; Scenario 7

The natural load has been set to a very low value ($P_{MV}^{load} = 1$ MW and $Q_{MV}^{load} = 1$ Mvar) and the distributed generation production has been set to the nominal value ($P_{DG} = 15$ MW) for simulation scenario 8 which is presented in figure 3.15. This simulation scenario has the highest stability margin of 216.07 Mvar which means the power system is farthest from a voltage collapse.
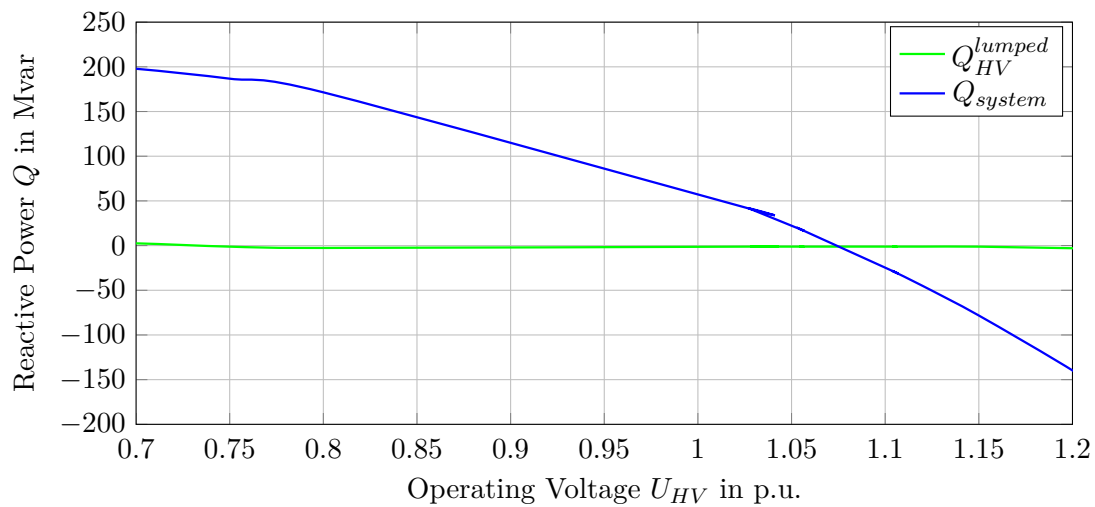
Figure 3.15: Q-U curve, $P_{MV}^{load} = 1$ MW and $P_{DG} = 15$ MW; Scenario 8

Figure 3.16 plots the stability margin over an increasing distributed generation production for a nominal natural load situation and a minimal load situation. The stability margin has been calculated using the $Q(U)$ curve method, as the difference of the bottom of the synchronous condenser characteristic curve and the $Q(U)$ load characteristic line. It can be seen that by increasing distributed generation production, the power system is becoming more stable, as the stability margin is increasing. (see table 3.4). An explanation of this behaviour is, that the analysed power system is very simplified and the centralized generator, is located closely to the medium voltage grid. The centralized generator can vary it's reactive power output and compensate the changing $Q(U)$ behaviour of the lumped load. It has been shown, that the power system is becoming even more stable (according to the stability margin analysis) if the distributed generation production is increasing but only if the high voltage grid is able to supply the medium voltage grid with reactive power (in both directions).
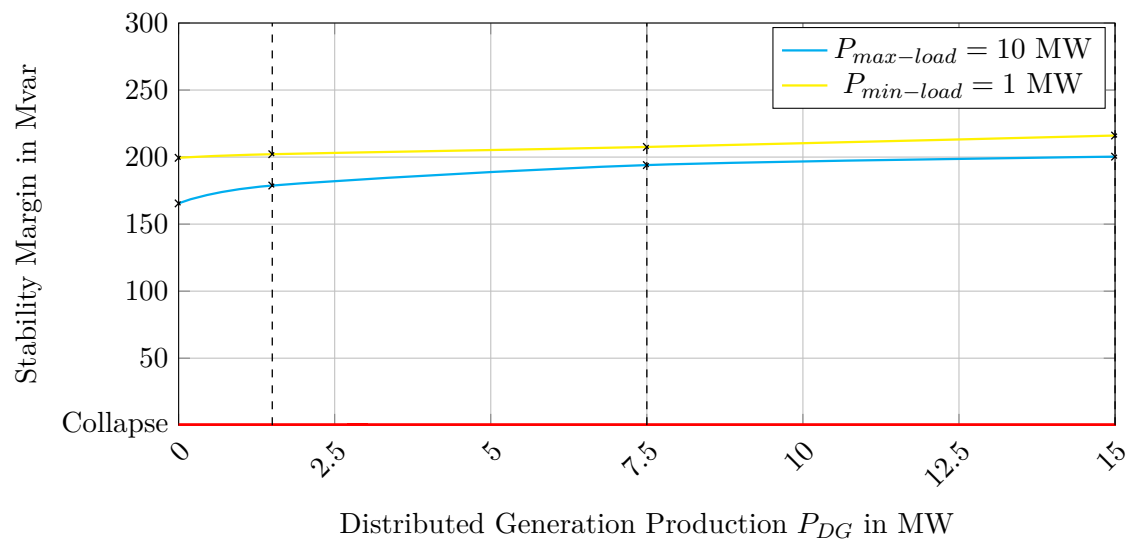
Figure 3.16: Stability Margin of the two-bus network

3.3 IEEE Test Network Simulations

In this chapter a case study in a IEEE 30 bus test network is presented. The system has been chosen to demonstrate the voltage stability and the voltage sensitivity in a complex power network which includes a high amount of distributed generation. The $Q(U)$ load characteristic and the system characteristic, of a complex power network, including a transmission grid, three distribution grids, several medium voltage and high voltage loads, several distributed generators and two centralized generators, is being analysed. Figure 3.17 shows the general layout of the analysed IEEE network. The original IEEE network has been modified in order to analyse the system characteristic. That's why 3 fictitious generator have been added to the system. Figure 3.18 gives the modified IEEE power network and shows how it has been implemented to PSS Sincal. The network consists of the following components and elements.

- 132kV transmission grid.

- Three 33kV distribution grids.

- Two generators which feed into the transmission grid.

- Three on-load tap changer transformer which connect the transmission grid and the distribution grids.

- Transmission lines which connect the generators, the on-load tap changer transformers and the high voltage loads.

- Six high voltage loads, which are modelled with a constant impedance model and have a total power consumption of $P = 178.70$ MW and $Q = 75.40$ Mvar.

- The distribution grid "Hancock" which consists of 6 natural loads (total nominal consumption of $P_{MV}^{load} = 40.70$ MW and $Q_{MV}^{load} = 20.80$ Mvar) and 5 distributed generators (total nominal production: $P_{DG} = 69$ MW).

- The distribution grid "Roanoke" which consists of 6 natural loads (total nominal consumption of $P_{MV}^{load} = 47.50$ MW and $Q_{MV}^{load} = 24.90$ Mvar) and 6 distributed generators (total nominal production: $P_{DG} = 75$ MW).

- The distribution grid "Cloverdale" which consists of 3 natural loads (total nominal consumption of $P_{MV}^{load} = 16.50$ MW and $Q_{MV}^{load} = 5.10$ Mvar) and 4 distributed generators (total nominal production: $P_{DG} = 50$ MW).

- The 15 distribution generators are controlled by $Q(U)$ controllers.

- Two real synchronous condenser which are connected to the transmission grid and which generate reactive power to control the voltage of a high voltage bus bar.

- Three fictitious synchronous condenser (1 per high voltage bus bar) which are needed to control the high voltage bus bar voltage. Basically the synchronous condenser is an adjustable reactive power source without reactive power generation limits. The synchronous condenser is deactivated for the voltage sensitivity analysis.
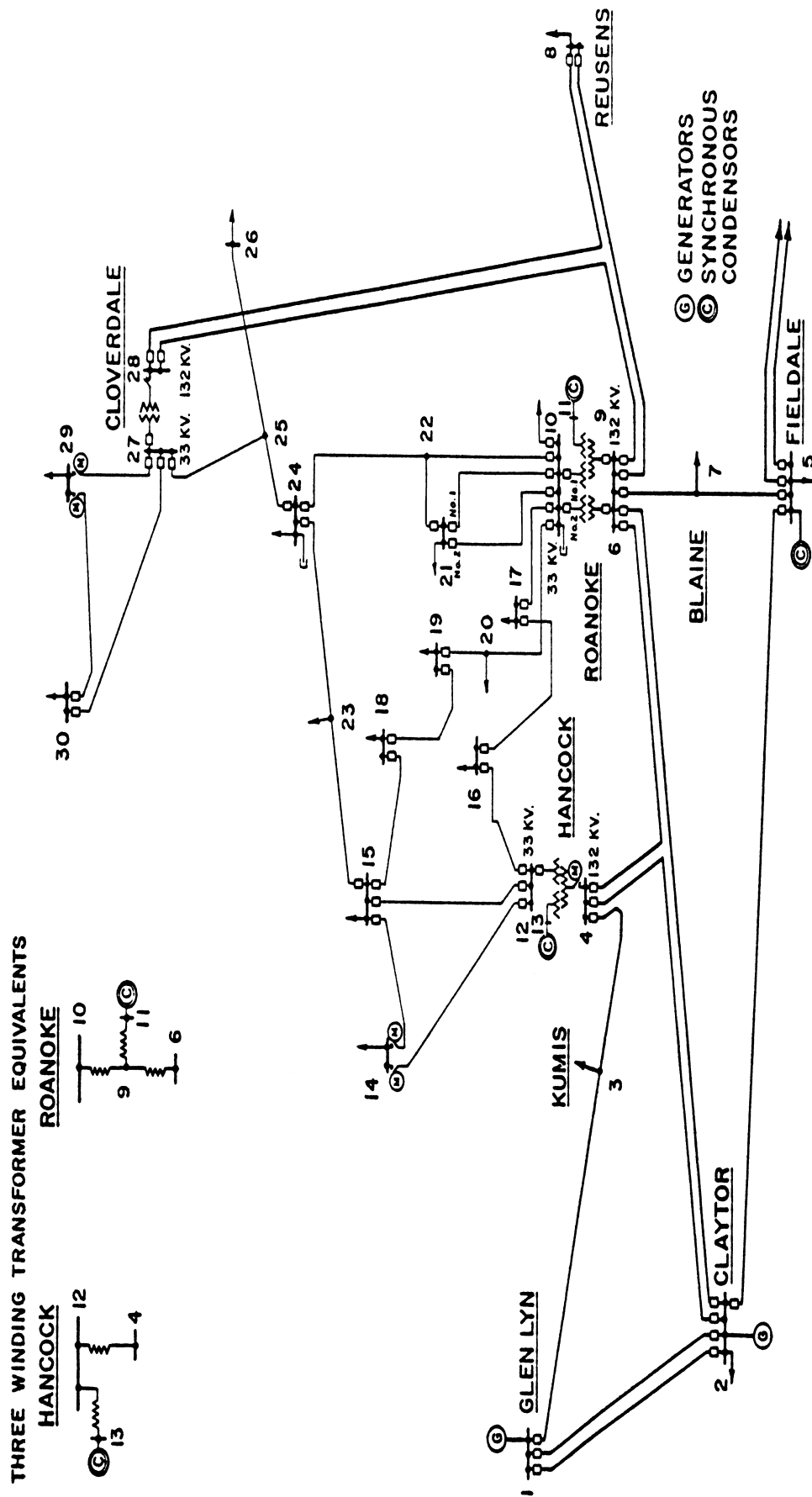
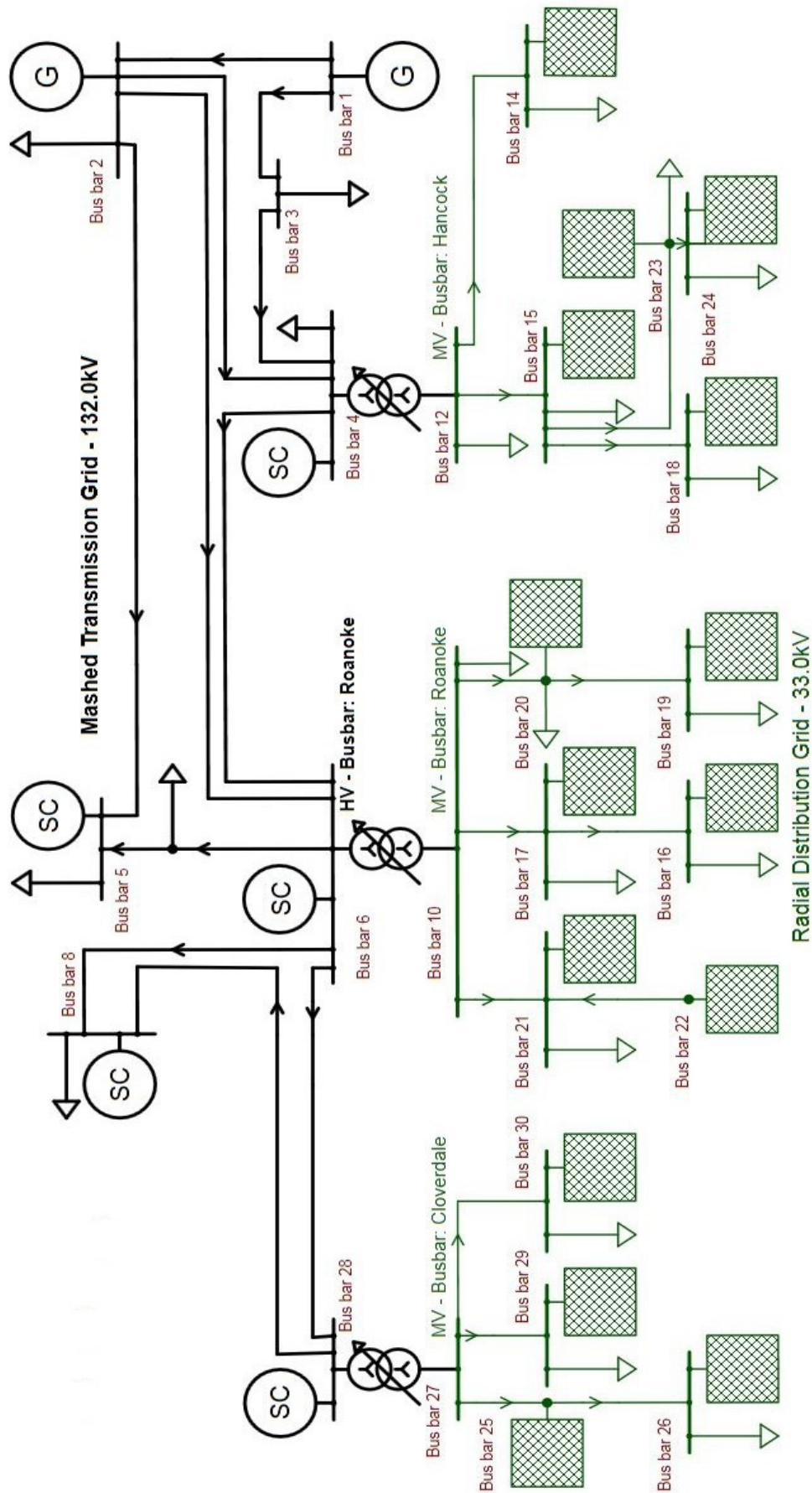Figure 3.17: One line diagram of the IEEE 30 Bus test case

Figure 3.18: Modified layout of the IEEE 30 Bus test case

The IEEE test network consists of three HV/MV supplying transformers which connect three medium voltage grids ("Hancock", "Roanoke", "Cloverdale") to the high voltage grid. The medium voltage grids consist of different natural loads and different distributed generation penetration. The nominal natural load and the nominal distributed generation of the distribution grids can be seen in table 3.5.

Table 3.5: Natural load and distributed generation production of the IEEE network

	Hancock				Roanoke				Cloverdale		
Bus	P_{MV}^{load}	Q_{MV}^{load}	P_{DG}	Bus	P_{MV}^{load}	Q_{MV}^{load}	P_{DG}	Bus	P_{MV}^{load}	Q_{MV}^{load}	P_{DG}
Bar	MW	Mvar	MW	Bar	MW	Mvar	MW	Bar	MW	Mvar	MW
12	11.20	7.50		10	5.80	2.00		25			10.00
14	6.20	1.60	18.00	16	3.50	1.80	5.00	26	3.50	2.30	10.00
15	8.20	2.50	15.00	17	9.00	5.80	15.00	29	2.40	0.90	10.00
18	3.20	0.90	9.00	19	9.50	3.40	15.00	30	10.60	1.90	20.00
23	3.20	1.60	12.00	20	2.20	0.70	10.00				
24	8.70	6.70	15.00	21	17.50	11.20	20.00				
				22			10.00				
	40.70	20.80	69.00		47.50	24.90	75.00		16.50	5.10	50.00

3.3.1 *Q(U)* Load Behaviour of different grid levels

Simulation Scenario

The appropriate load modelling is of primary importance in voltage stability studies, which have been so often called load stability studies. The $Q(U)$ characteristic of the load seen from the high voltage bus bar and the corresponding $Q(U)$ characteristic of different grid levels is shown in this chapter. Additionally the $Q(U)$ behaviour seen from the medium voltage grid and a voltage level at the end of the feeder has been analysed for a voltage range from $U = 0.9$ p.u. to $U = 1.1$ p.u.. The load in different medium voltage grid levels is changing it's behaviour due to the increasing amount of distributed generation. The IEEE network shown in figure 3.18 is used to demonstrate the distributed generation impact on the $Q(U)$ characteristic of the load. The $Q(U)$ characteristic of the natural load and the output of the $Q(U)$ controller of the distributed generators overlap. With distributed generation the load seen from the medium voltage bus bar can't be modelled with one of the described load models presented in chapter 2.2.3. The following load levels of the distribution grid "Roanoke" have been selected for this study (see figure 3.19):

- 1: Medium voltage load level Roanoke (Bus bar 16): The $Q(U)$ characteristic of the load seen from a bus bar which is not close to the medium voltage bus bar is a composition of the natural load characteristic (modelled with the constant impedance load model) and the reactive power output of the $Q(U)$ controlled distributed generators.

- 2: Medium voltage lumped load in Roanoke (Bus bar 10): The $Q(U)$ characteristic of the load seen from the medium voltage bus bar "Roanoke" is a composition of the characteristic (modelled with the constant impedance load model) of all natural loads, the reactive power output of the $Q(U)$ controller of the distributed generators and the characteristics of the medium voltage lines.

- 3: High voltage lumped load in Roanoke (Bus bar 6): The $Q(U)$ characteristic of the load seen from the high voltage bus bar "Roanoke" is a composition of the characteristic (modelled with the constant impedance load model) of all natural loads, the reactive power output of the $Q(U)$ controller of the distributed generators, the characteristic of the on-load tap changer transformer and the characteristics of the medium voltage lines.
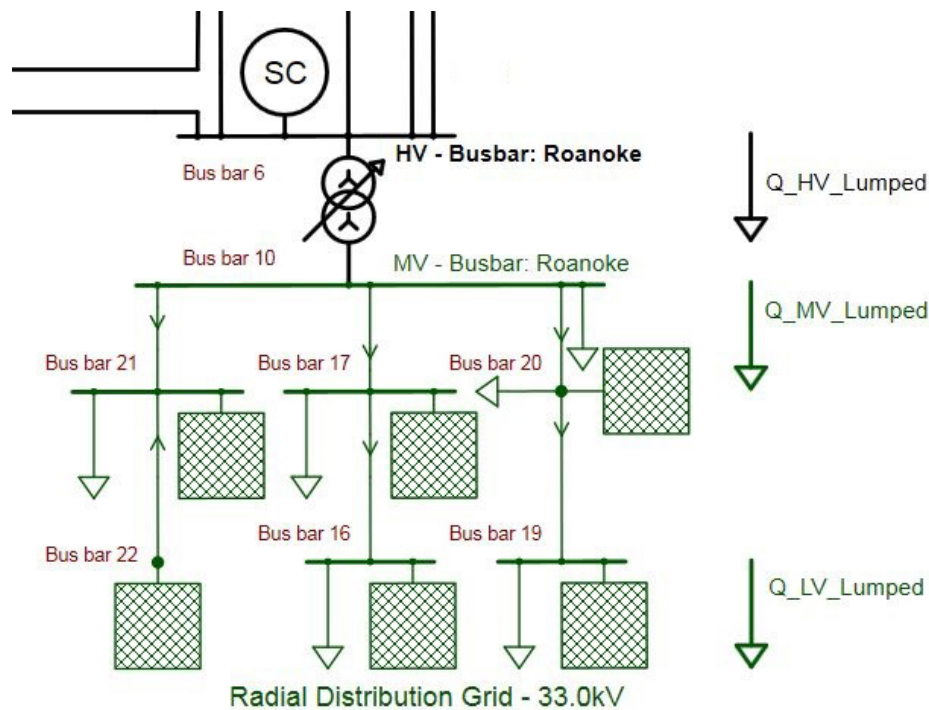
Figure 3.19: Extract of IEEE network which shows the load position for different investigation levels

The algorithm to create the $Q(U)$ load behaviour seen from the medium voltage bus bar (Q_{MV}^{lumped}) and the load levels below is given in chapter 3.1.1. The high voltage lumped load characteristic has been created according to the algorithm presented in chapter 3.1.2. The interesting voltage range is from $U = 0.9$ p.u. to $U = 1.1$ p.u. in this simulation case as these are the violation limits. If the voltage violates these limits then security actions would be started. The different settings of the natural load and distributed generation production of the different simulation scenarios can be seen in table 3.7. The load behaviour of the distribution grids supplied from "Hancock" and

"Cloverdale" are being analysed in chapter 3.3.2 but different natural load and distributed generation situations are being considered in this study, as they may affect the static load behaviour of the analysed distribution grid "Roanoke".

Table 3.6: Normalized values of the natural load and distributed generation production

Unit	Hancock			Roanoke			Cloverdale		
	P_{MV}^{load}	Q_{MV}^{load}	P_{DG}	P_{MV}^{load}	Q_{MV}^{load}	P_{DG}	P_{MV}^{load}	Q_{MV}^{load}	P_{DG}
MW or Mvar	40.70	20.80	69.00	47.50	24.90	75.00	16.50	5.10	50.00
p.u.	1.00	1.00	1.00	1.00	1.00	1.00	1.00	1.00	1.00

All values of the medium voltage lumped loads as well as the distributed generation values which can be seen in table 3.7 are normalized to the nominal values which are given in table 3.5. Table 3.6 gives the nominal values of the natural load and the distributed generation of all three distribution grids.

Table 3.7: Medium voltage lumped load and DG production of the different simulation scenarios

	Hancock			Roanoke			Cloverdale		
Simulation	P_{MV}^{load}	Q_{MV}^{load}	P_{DG}	P_{MV}^{load}	Q_{MV}^{load}	P_{DG}	P_{MV}^{load}	Q_{MV}^{load}	P_{DG}
Scenario	p.u.	p.u.	p.u.	p.u.	p.u.	p.u.	p.u.	p.u.	p.u.
1	1.0	1.0	0.0	1.0	1.0	0.0	1.0	1.0	0.0
2	1.0	1.0	0.5	1.0	1.0	0.5	1.0	1.0	0.5
3	1.0	1.0	1.0	1.0	1.0	1.0	1.0	1.0	1.0

Simulation Results

Firstly the high voltage lumped load characteristic has been analysed using the algorithm described in chapter 3.1.2. The high voltage lumped load characteristic and the corresponding medium voltage lumped load characteristic and the $Q(U)$ characteristic seen from a medium voltage load level (Bus bar 16) has been calculated. The high voltage bus bar voltage has been varied from $U_{HV} = 0.9$ p.u. to $U_{HV} = 1.1$ p.u.. The HV/MV supplying transformer keeps the medium voltage bus bar voltage between $U_{MV} = 1.02$ p.u. and $U_{MV} = 1.06$ p.u., which can be seen in figures 3.20, 3.21, 3.22. Figure 3.20 gives the $Q(U)$ load behaviour of the high voltage lumped load and the corresponding characteristic of the other two grid levels (see figure 3.19) for a nominal natural load situation ($P_{MV}^{load} = 1$ p.u., $P_{MV}^{load} = 1$ p.u.) and without distributed generation. The active power flow of about $P_{HV}^{lumped} = 50$ MW is from the high voltage grid to the medium voltage grid. The reactive power flow of about $Q_{HV}^{lumped} \approx 18$ Mvar has the same direction.
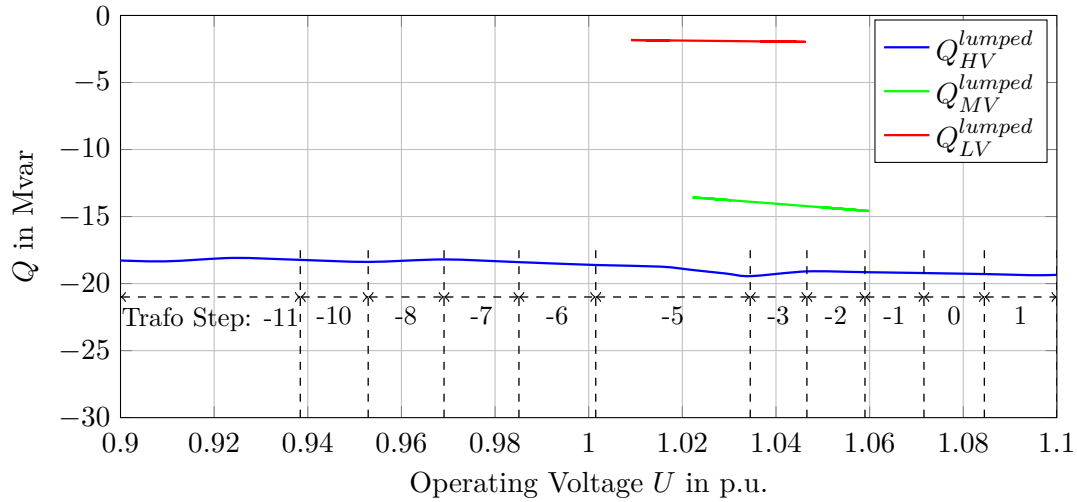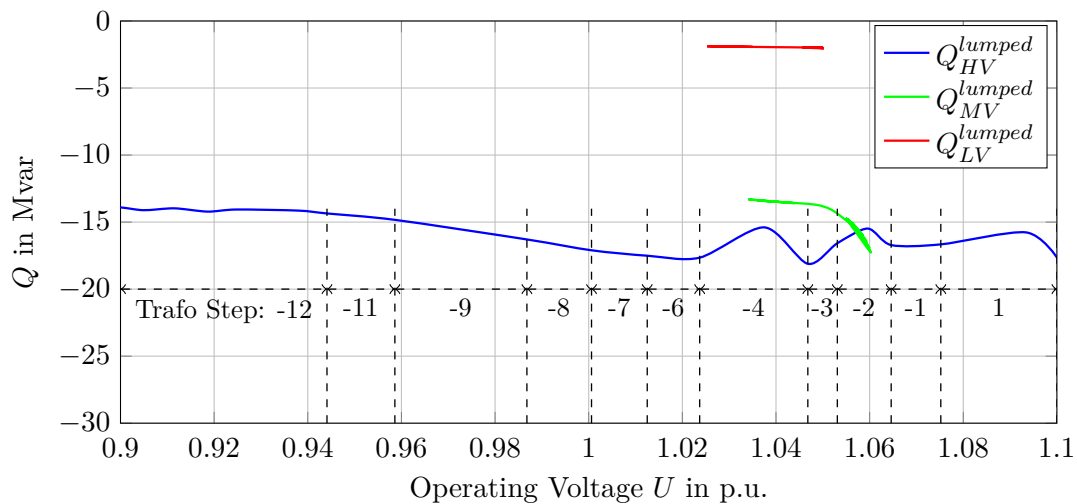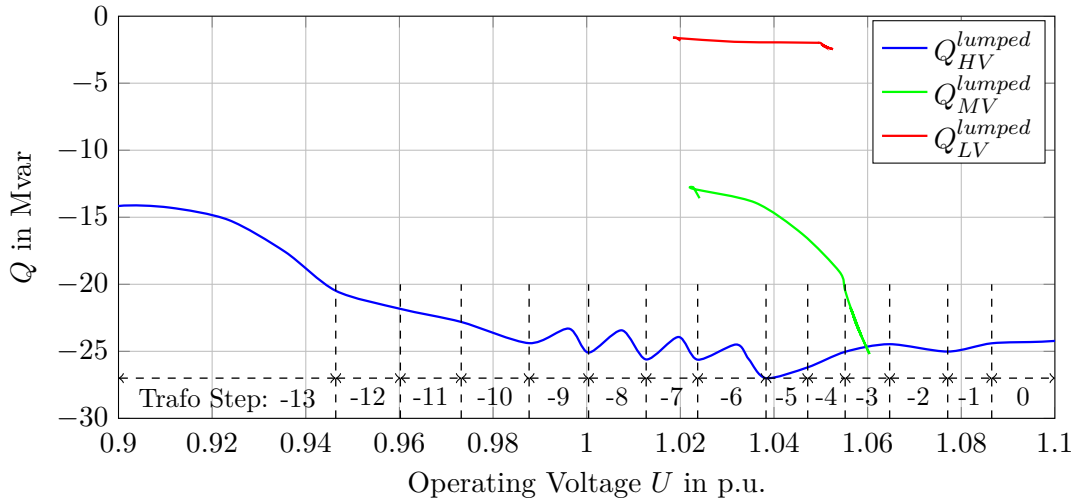
Figure 3.20: $Q(U)$ load behaviour of three different grid levels for $P_{MV}^{load} = 1$ p.u., $Q_{MV}^{load} = 1$ p.u., $P_{DG} = 0$ p.u.; Scenario 1

On the other hand figure 3.21 gives the $Q(U)$ load behaviour of different grid levels for a nominal natural load situation ($P_{MV}^{lumped} = 1$ p.u., $Q_{MV}^{lumped} = 1$ p.u.) and a distributed generation production of $P_{DG} = 0.5$ p.u.. The influence of the local $Q(U)$ controller can be seen in the medium voltage lumped load characteristic (Q_{MV}^{lumped}). The HV/MV supplying transformer keeps the medium voltage bus bar voltage between $U_{MV} = 1.02$ p.u. and $U_{MV} = 1.06$ p.u.. The active power flow of about $P_{HV}^{lumped} = 15$ MW and the reactive power flow is from the high voltage grid to the medium voltage grid. The transformer steps have been added to figure 3.20, 3.21, 3.22 . The medium voltage lumped load characteristic for a voltage range from $U_{MV} = 1.02$ p.u. to $U_{MV} = 1.06$ p.u. is reflected multiple times in the high voltage lumped load characteristic which can be seen in 3.21 (Trafo Steps: $-4, -2, 1$) and figure 3.21 (Trafo Steps: $-9, -8, -7, -6$).

Figure 3.21: $Q(U)$ load behaviour of three different grid levels for $P_{MV}^{load} = 1$ p.u., $Q_{MV}^{load} = 1$ p.u., $P_{DG} = 0.5$ p.u.; Scenario 2

Finally figure 3.22 presents the characteristic of the load seen from the high voltage grid for a natural load situation ($P_{MV}^{lumped} = 1$ p.u., $Q_{MV}^{lumped} = 1$ p.u.) and a very high amount of distributed generation production ($P_{DG} = 1$ p.u.). The active power flow of about $P_{HV}^{lumped} = 22$ MW has changed it's direction and is from the medium voltage grid to the high voltage grid. The reason is the high amount of distributed generation production. But the reactive power flow is still from the high voltage grid to the medium voltage grid. Also the high voltage lumped load $Q(U)$ characteristic is changing due to the $Q(U)$ controlled distributed generation penetration, and can't be considered as stiff any more. The reactive power demand varies from -14 Mvar to -27 Mvar. Also the medium voltage lumped load characteristic is changing dramatically. Even if the medium voltage bus bar voltage is kept between $U_{MV} = 1.02$ p.u. and $U_{MV} = 1.06$ p.u. from the HV/MV supplying transformer the reactive power demand varies from -12 Mvar and -25 Mvar.

Figure 3.22: $Q(U)$ load behaviour of three different grid levels for $P_{MV}^{load} = 1$ p.u., $Q_{MV}^{load} = 1$ p.u., $P_{DG} = 1$ p.u.; Scenario 3

Figure 3.23 presents the $Q(U)$ load characteristics seen from a medium voltage load level (bus bar 16) for different distributed generation production situations. The influence of the $Q(U)$ controller is noticeable, but the changes in the reactive power demand are little. The reason for that is the relatively small amount of distributed generation production ($P_{DG}^{busbar16} = 5$ MW) installed at bus bar 16. The reactive power demand changes from $Q_{LV}^{lumped} = 0.2$ Mvar to $Q_{LV}^{lumped} = -3.8$ Mvar for a distributed generation production of $P_{DG} = 1.0$ p.u.. The $Q(U)$ load behaviour has been created by using the algorithm described in chapter 3.1.1.
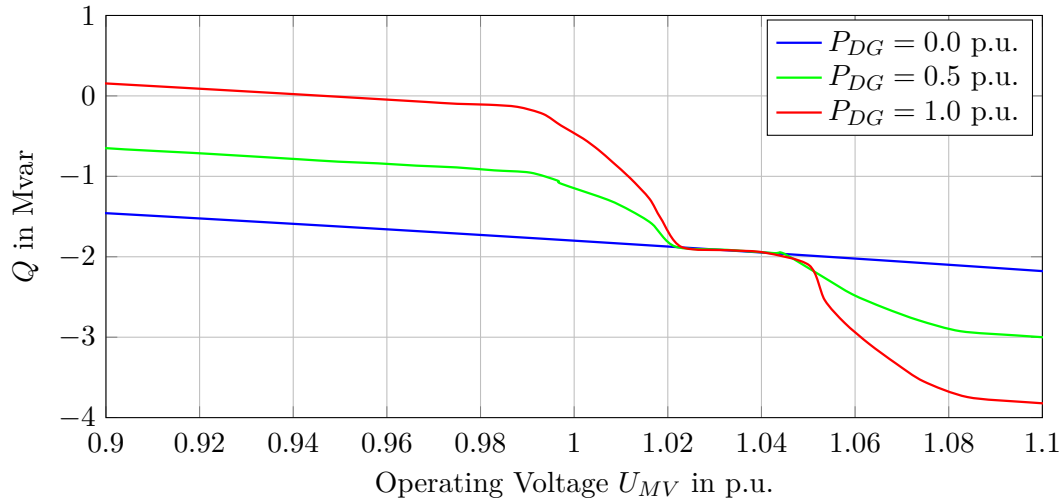
Figure 3.23: $Q(U)$ load behaviour for a MV load level (bus bar 16 - Q_{LV}^{lumped})

The $Q(U)$ load characteristic seen from the medium voltage bus bar for different distributed generation penetration is given in figure 3.24. It can be seen that the reactive power flow changes it's direction by increasing the distributed generation production. If the medium voltage bus bar voltage is below $U_{MV} = 1.0$ p.u. and the distributed generation production is above $P_{DG} = 0.5$ p.u. then reactive power is transferred from the medium voltage grid to the high voltage grid. On the other hand if the medium voltage bus bar is above $U_{MV} = 1.04$ p.u. the reactive power demand of the medium voltage grid is increasing rapidly up to a reactive power transfer of $Q_{MV}^{lumped} = 40$ Mvar from the high voltage grid to the medium voltage grid.
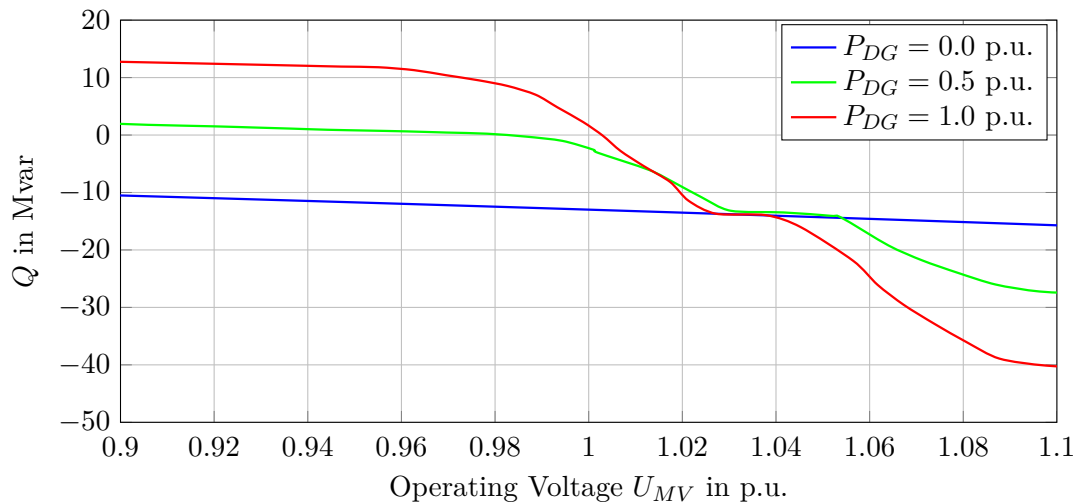
Figure 3.24: $Q(U)$ load behaviour seen from the MV bus bar (bus bar 10 - Q_{MV}^{lumped})

Finally the $Q(U)$ load behaviour seen from the high voltage bus bar is presented in 3.25. The algorithm described in chapter 3.1.2 has been used to create the high voltage lumped load characteristic.
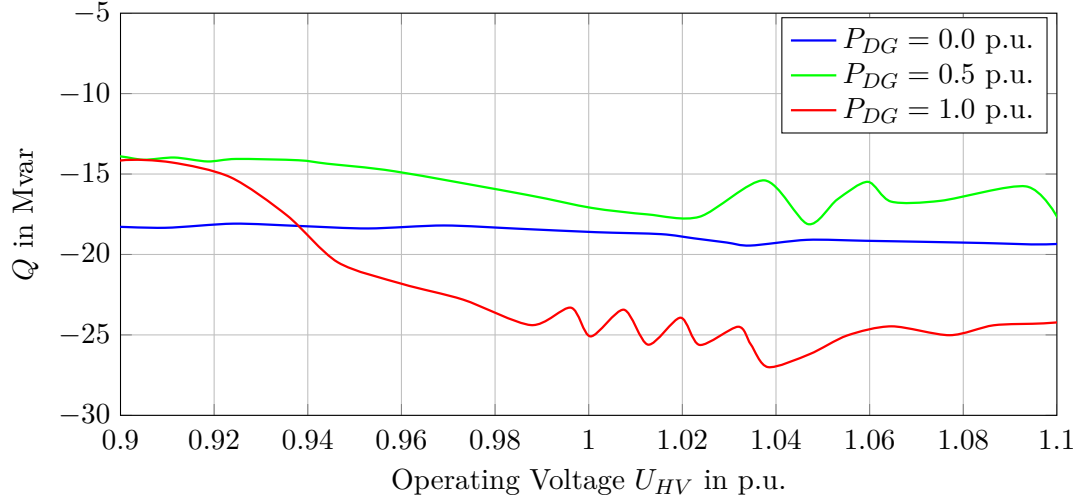
Figure 3.25: $Q(U)$ load behaviour seen from the HV bus bar (bus bar 6 - Q_{HV}^{lumped})

3.3.2 *Q(U)* Load Behaviour of different Medium Voltage Grids

Scenario Definition

The $Q(U)$ controlled distributed generation is located in the medium and low voltage network. Distributed generators have been added to the IEEE 30 bus test network which is shown in Figure 3.18 to analyse the static load characteristic and voltage stability. Different simulation scenarios have been performed where the active power of the distributed generation and the active, as well as the reactive power of the natural load have been varied. The nominal active and reactive power of the natural load, as well as the active power output of the distributed generation can be seen in table 3.5. The natural load is modelled using the constant impedance load model, which is explained in chapter 2.2.8.

A detailed illustration of the $Q(U)$ controller of the distributed generation can be seen in chapter 2.2.6. According to equation 2.21 the reactive power output of the $Q(U)$ controller of the distributed generation is depending on the bus voltage and the active power output of the distributed generation.

The static load characteristic (k_{SLC}) has been analysed by using the on-load tap changer transformer, which adds 1% of the nominal voltage per tap step. The on-load tap changer transformer has 60 steps (±30) and varying the on-load tap changer transformer steps continuously from 30 to -30 varies the voltage on the medium voltage bus bar from minimum to maximum. Only one medium voltage grid bus bar is controlled per

voltage sensitivity simulation scenario. The on-load tap changer transformer steps of the other two distribution grids is controlled automatically to keep the voltage of the medium voltage bus bar between 1.02 p.u. and 1.06 p.u. (see figure 3.1). The reactive power through the HV/MV supplying transformer, of the analysed distribution grid, which represents the medium voltage lumped load (see chapter 2.2.9), is used to calculate the static load characteristic k_{SLC}, according to equation 2.15. The fictitious synchronous condensers are deactivated for this test scenario and the used algorithm is described in chapter 3.1.1. The results from this simulation scenario can be used to create new load models using PSS Netomac. These macros are programmed to control the lumped loads, which allows the simulation of a bigger, more complex power network. Furthermore the distribution network can be reduced by a macro controlled lumped load. The advantage of this procedure is, that the network is extremely reduced but has the same $Q(U)$ and $P(U)$ behaviour as the original network.

Different simulation scenarios have been performed to create the $Q(U)$ load characteristic of the different medium voltage grids. The natural load and the distributed generation production has been varied for each simulation scenario which can be seen in table 3.8. The power demand of the natural load and the active power output of the distributed generators have been normalized to the nominal value presented in table 3.5. The natural load has been set to it's nominal value in simulation scenario 1 to 4 and a varying distributed generation has been added only to the distribution grid "Hancock". The distributed generation which feeds into the distribution grids "Roanoke" and "Cloverdale" has been deactivated in these simulation scenarios. Simulation Scenario 5 to 7 has been calculated with the nominal natural load values, but a varying distributed generation in all three distribution grids. Finally the natural load has been reduced to $P_{MV}^{lumped} = 0.5$ p.u. and $Q_{MV}^{lumped} = 0.5$ p.u. for simulation scenario 8 to 11. The distributed generation production has been varied again from $P_{DG} = 0$ p.u. to $P_{DG} = 1$ p.u..

Table 3.8: Natural Load and DG Production of the different Simulation Scenarios

Sim.	Hancock			Roanoke			Cloverdale		
	P_{MV}^{load}	Q_{MV}^{load}	P_{DG}	P_{MV}^{load}	Q_{MV}^{load}	P_{DG}	P_{MV}^{load}	Q_{MV}^{load}	P_{DG}
	p.u.	p.u.	p.u.	p.u.	p.u.	p.u.	p.u.	p.u.	p.u.
1	1.0	1.0	0.0	1.0	1.0	0.0	1.0	1.0	0.0
2	1.0	1.0	0.1	1.0	1.0	0.0	1.0	1.0	0.0
3	1.0	1.0	0.5	1.0	1.0	0.0	1.0	1.0	0.0
4	1.0	1.0	1.0	1.0	1.0	0.0	1.0	1.0	0.0
5	1.0	1.0	0.1	1.0	1.0	0.1	1.0	1.0	0.1
6	1.0	1.0	0.5	1.0	1.0	0.5	1.0	1.0	0.5
7	1.0	1.0	1.0	1.0	1.0	1.0	1.0	1.0	1.0
8	0.5	0.5	0.0	0.5	0.5	0.0	0.5	0.5	0.0
9	0.5	0.5	0.1	0.5	0.5	0.1	0.5	0.5	0.1
10	0.5	0.5	0.5	0.5	0.5	0.5	0.5	0.5	0.5
11	0.5	0.5	1.0	0.5	0.5	1.0	0.5	0.5	1.0

Simulation Results

Distribution grid: "Hancock": Firstly the static load characteristic of the medium voltage grid "Hancock" has been analysed. Table 3.9 displays the most important simulation results, like the extreme values of the static load characteristic (k_{SLC}) and the power through the HV/MV transformer, which represents the medium voltage lumped load of the distribution grid "Hancock". The natural load and the distributed generation production have been varied for the different simulation scenarios. The simulation results shows that the extreme values of the static load characteristic (k_{SLC}) are becoming higher by increasing the distributed generation penetration. The highest, as well as the lowest value of the static load characteristic (k_{SLC}) has been calculated in simulation scenario 11, where the natural load has been reduced to the half of the nominal value, and the distributed generation production has been set to the nominal value.

Table 3.9: Static Load Characteristic - Simulation Results - Hancock

Sim. Scen.	P_{MV}^{lumped} MW	Q_{MV}^{lumped} Mvar	P_{MV}^{load} MW	Q_{MV}^{load} Mvar	P_{DG} MW	$k_{SLC,min}$	$k_{SLC,max}$
1	−39.40	−6.20	−40.70	−20.80	0.00	2.00	2.00
2	−32.70	−3.70	−40.70	−20.80	6.90	1.60	10.74
3	−6.40	2.40	−40.70	−20.80	34.50	0.80	33.29
4	26.30	−2.70	−40.70	−20.80	69.00	0.20	45.67
5	−32.70	−3.70	−40.70	−20.80	6.90	1.70	10.99
6	−6.40	2.50	−40.70	−20.80	34.50	0.60	39.57
7	26.30	−2.60	−40.70	−20.80	69.00	0.20	43.79
8	−20.20	4.50	−20.35	−10.40	0.00	2.00	2.00
9	−13.40	6.60	−20.35	−10.40	6.90	0.70	11.44
10	−39.40	−6.20	−20.35	−10.40	34.50	0.50	63.10
11	45.90	2.70	−20.35	−10.40	69.00	0.10	86.26

Simulation Scenario 1 to Simulation Scenario 4 has been calculated with a natural load of $P_{MV}^{load} = 1.0$ p.u. and $Q_{MV}^{load} = 1.0$ p.u. and a varying distributed generation which feeds in the distribution grid "Hancock". The distributed generation in "Roanoke" and "Cloverdale" has been deactivated in these scenarios. The simulation results, which can be seen in Figure 3.26, show that the static load characteristic is highly depending on the active power output of the distributed generation. Without distributed generation the static load characteristic is constant ($k_{SLC} = 2$), which is because the natural load is modelled with a constant impedance load model. In case of a $Q(U)$ controlled distributed generation penetration the static load characteristic of the specific distribution grid is highly influenced and varies from $k_{SLC} = 0.10$ to $k_{SLC} = 86.26$. Table 3.9 shows that the higher the distributed generation production the higher the static load characteristic margin. Another effect is that an uncontrolled reactive power flow occurs if the distributed generation production exceeds a certain amount.

Figure 3.26 shows a reactive power flow from the medium voltage grid to the high voltage grid in case of a distributed generation above $P_{DG} = 0.1$ p.u. if the medium voltage bus bar voltage is below $U_{MV} = 1.0$ p.u.. On the other hand if the medium voltage bus bar voltage is above $U_{MV} = 1.05$ p.u. a high amount of reactive power needs to be transferred from the high voltage grid to the medium voltage grid.
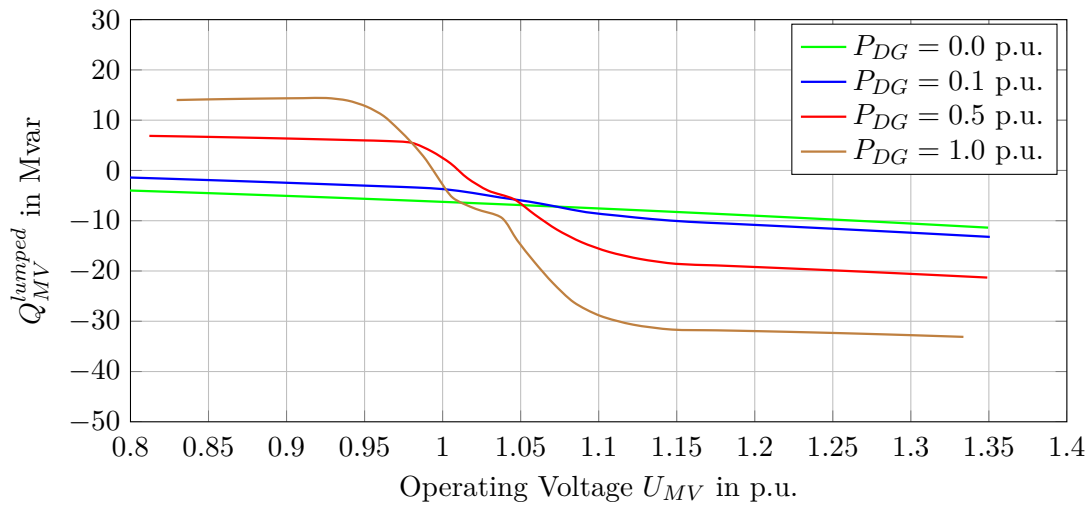
Figure 3.26: $Q(U)$ load behaviour, Hancock, DG production only in Hancock, $P_{MV}^{load} = 1.0$ p.u.; Scenario 1 - 4

Figure 3.27 presents the simulation results for scenario 5, 6 and 7. The natural load has been set to the nominal value and the distributed generation has been varied. Simulation scenarios 5, 6 and 7 have been performed with a distributed generation penetration in all medium voltage grids, where the distributed generation penetration is reduced to "Hancock" in simulation scenarios 2, 3 and 4 (presented in figure 3.26).
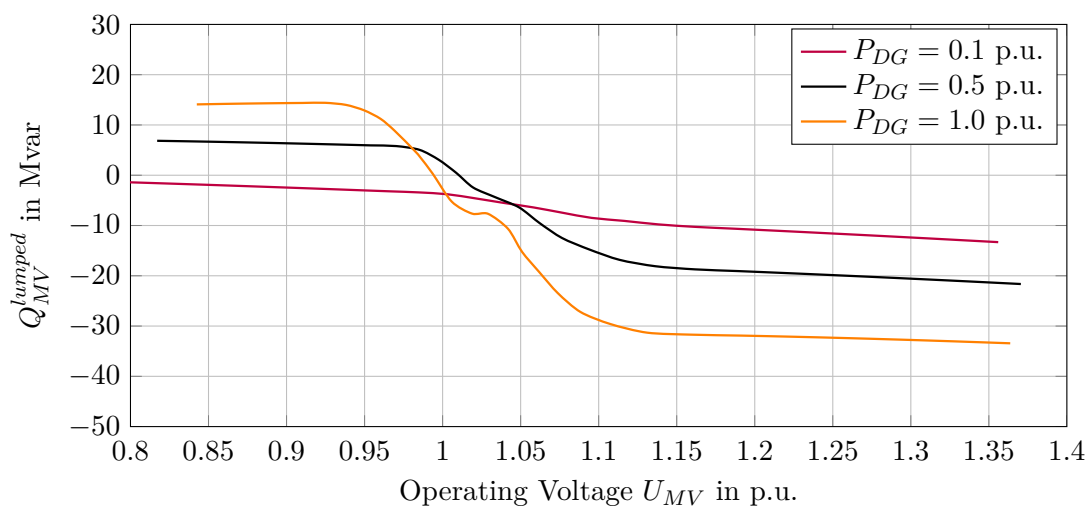
Figure 3.27: $Q(U)$ load behaviour, Hancock, DG production everywhere, $P_{MV}^{load} = 1.0$ p.u.; Scenario 5 - 7

Simulation scenarios 8, 9, 10 and 11 have been calculated with a reduced natural load of $P_{MV}^{load} = 0.5$ p.u. and $Q_{MV}^{load} = 0.5$ p.u. and a varying distributed generation which feed into all three distribution grids. The medium voltage lumped load characteristic for the medium voltage grid Hancock is given in figure 3.28. The reactive power transfer from the medium voltage grid to the high voltage grid varies from $Q_{MV,max}^{lumped} = 20$ Mvar to $Q_{MV,min}^{lumped} = -20$ Mvar.
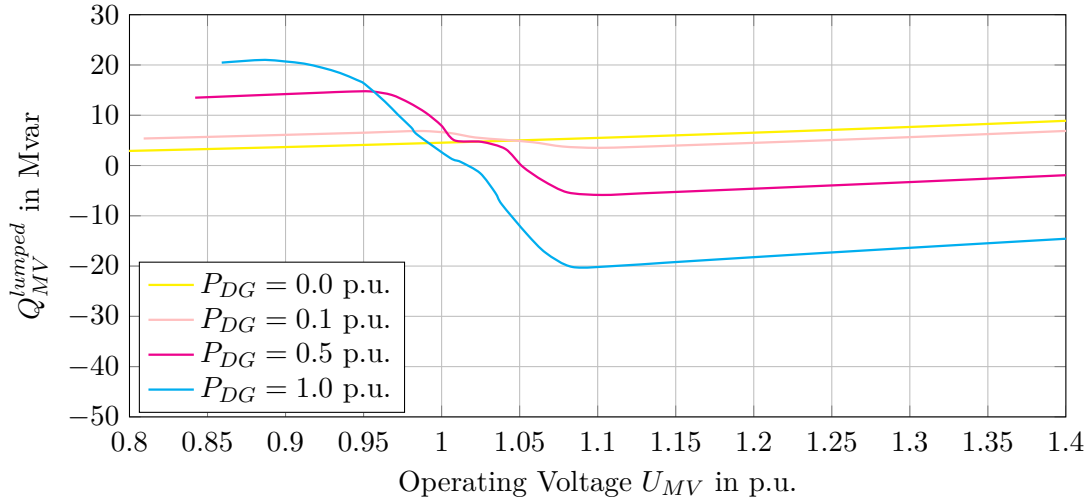
Figure 3.28: $Q(U)$ load behaviour, Hancock, DG production everywhere, $P_{MV}^{load} = 0.5$ p.u.; Scenario 8 - 11

Distribution grid: "Roanoke": Secondly the static load characteristic of the medium voltage grid "Roanoke" has been analysed in detail. The most important simulation results are displayed in table 3.10. The static load characteristic of simulation scenario 1 to 4 is constant ($k_{SLC} = 2.0$ p.u.) as the distributed generation which feeds into "Roanoke" has been deactivated. The extreme values of the static load characteristic (k_{SLC}) differs the most in simulation scenario 11 ($k_{SLC,min} = 0.10$ and $k_{SLC,max} = 73.71$) which shows that the voltage sensitivity is depending on the $Q(U)$ controller of the distributed generation and on the natural load.

Table 3.10: Static Load Characteristic - Simulation Results - Roanoke

Sim. Scen.	P_{MV}^{lumped} MW	Q_{MV}^{lumped} Mvar	P_{MV}^{load} MW	Q_{MV}^{load} Mvar	P_{DG} MW	$k_{SLC,min}$	$k_{SLC,max}$
1	-46.80	-13.00	-47.50	-24.90	0.00	2.00	2.00
2	-46.80	-13.00	-47.50	-24.90	0.00	2.00	2.00
3	-46.80	-13.00	-47.50	-24.90	0.00	2.00	2.00
4	-46.80	-13.00	-47.50	-24.90	0.00	2.00	2.00
5	-39.40	-10.54	-47.50	-24.90	7.50	1.80	7.85
6	-9.90	-2.60	-47.50	-24.90	37.50	1.10	53.51
7	26.70	1.00	-47.50	-24.90	75.00	0.70	76.41
8	-23.70	-0.25	-23.75	-12.45	0.00	2.00	2.00
9	-16.20	1.90	-23.75	-12.45	7.50	0.10	14.05
10	13.40	7.70	-23.75	-12.45	37.50	0.10	61.29
11	50.10	9.10	-23.75	-12.45	75.00	0.10	73.71

Figure 3.29 presents the simulation results of the medium voltage grid "Roanoke" for a nominal natural load situation ($P_{MV}^{load} = 1.0$ p.u. $= 47.5$ MW and $Q_{MV}^{load} = 1.0$ p.u. $= 12.45$ Mvar) and varying distributed generation production. Again, the reactive power flow changes it's direction if the distributed generation production is above $P_{DG} = 0.5$ p.u. $= 37.5$ MW. A reactive power transfer of $Q_{MV}^{lumped} = 40$ Mvar from the high voltage to the medium voltage grid is needed to keep the medium voltage bus bar voltage above $U_{MV} = 1.1$ p.u. in case of a high distributed generation production ($P_{DG} = 1.0$ p.u.).
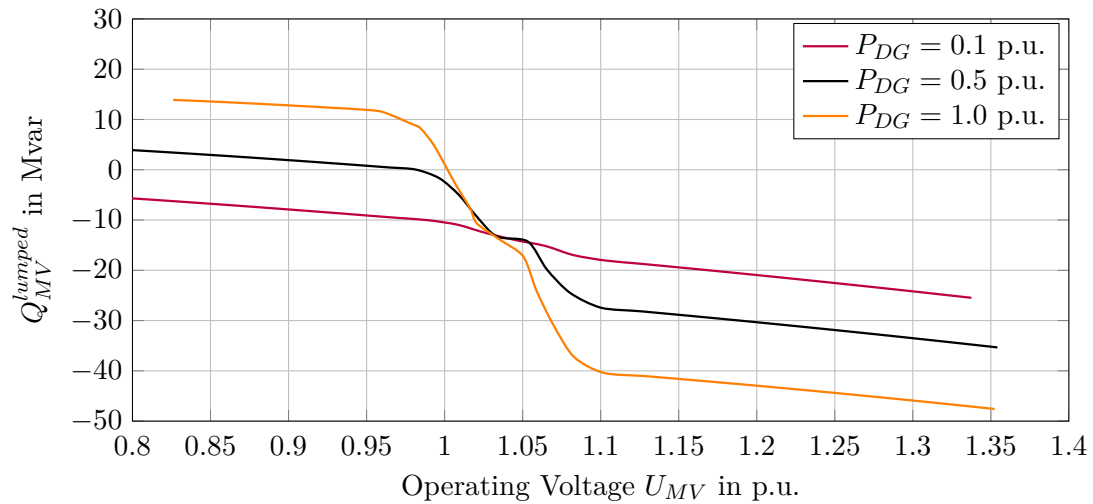
Figure 3.29: $Q(U)$ load behaviour, Roanoke, DG production everywhere, $P_{MV}^{load} = 1.0$ p.u.; Scenario 5 - 7

The medium voltage lumped load characteristic of the medium voltage grid "Roanoke" is presented in figure 3.30. Therefore the natural load has been halved and the distributed generation production has been varied. The reactive power demand of the medium voltage lumped load is reduced, compared to the nominal load situation shown in figure 3.29.
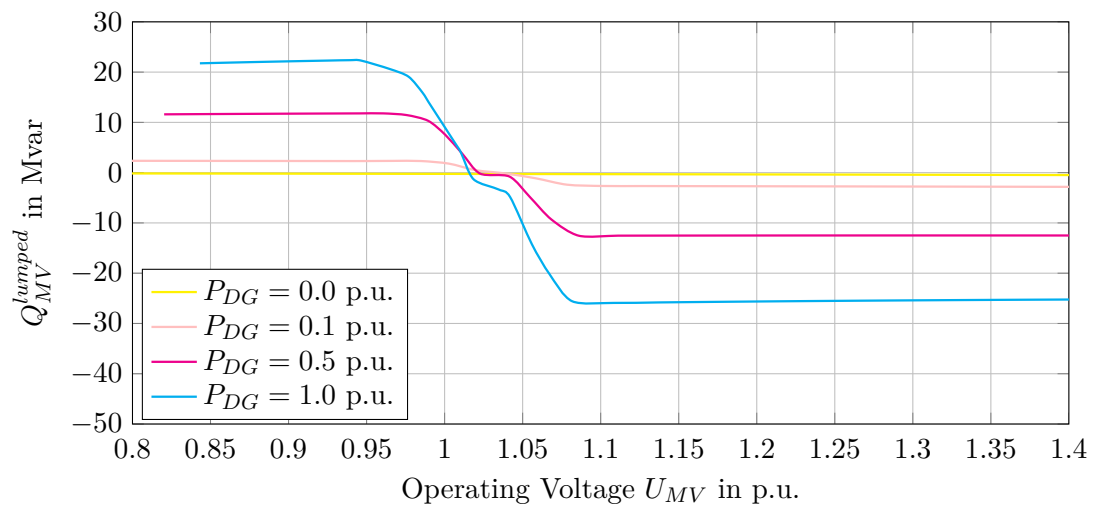
Figure 3.30: $Q(U)$ load behaviour, Roanoke, DG production everywhere, $P_{MV}^{load} = 0.5$ p.u.; Scenario 8 - 11

Distribution grid: "Cloverdale": Finally the simulation results of the third medium voltage grid "Cloverdale" are presented in table 3.11. Again, the static load characteristic of simulation scenario 1 to 4 is constant ($k_{SLC} = 2.0$ p.u.) as the distributed generation which feeds into "Cloverdale" has been deactivated. The extreme values of the static load characteristic (k_{SLC}) are further apart if the distributed generation production is increased.

Table 3.11: Static Load Characteristic - Simulation Results - Cloverdale

Sim. Scen.	P_{MV}^{lumped} MW	Q_{MV}^{lumped} Mvar	P_{MV}^{load} MW	Q_{MV}^{load} Mvar	P_{DG} MW	$k_{SLC,min}$	$k_{SLC,max}$
1	−16.10	7.30	−16.50	−5.10	0.00	2.00	2.00
2	−16.10	7.30	−16.50	−5.10	0.00	2.00	2.00
3	−16.10	7.30	−16.50	−5.10	0.00	2.00	2.00
4	−16.10	7.30	−16.50	−5.10	0.00	2.00	2.00
5	−11.30	9.00	−16.50	−5.10	5.00	0.30	3.20
6	8.00	11.70	−16.50	−5.10	25.00	0.75	39.91
7	31.80	7.70	−16.50	−5.10	50.00	0.40	42.07
8	−23.70	−0.20	−8.25	−2.55	0.00	2.00	2.00
9	−3.40	11.60	−8.25	−2.55	5.00	0.30	2.80
10	16.20	11.60	−8.25	−2.55	25.00	0.90	26.25
11	39.80	8.20	−8.25	−2.55	50.00	0.50	39.68

Figure 3.31 gives the $Q(U)$ load behaviour of the medium voltage grid "Cloverdale" at different distributed generation production situations. The natural load has been set to it's nominal value of $P_{MV}^{load} = 1.0$ p.u. and $Q_{MV}^{load} = 1.0$ p.u.. It's interesting that the reactive power flow is from medium voltage grid to the high voltage grid even if the distributed generation production is deactivated or low. This is a difference to the distribution grids "Hancock" and "Roanoke". A reason for this behaviour is the relatively low amount of reactive power demand of natural load ($Q_{MV}^{lumped} = 5.1$ Mvar).
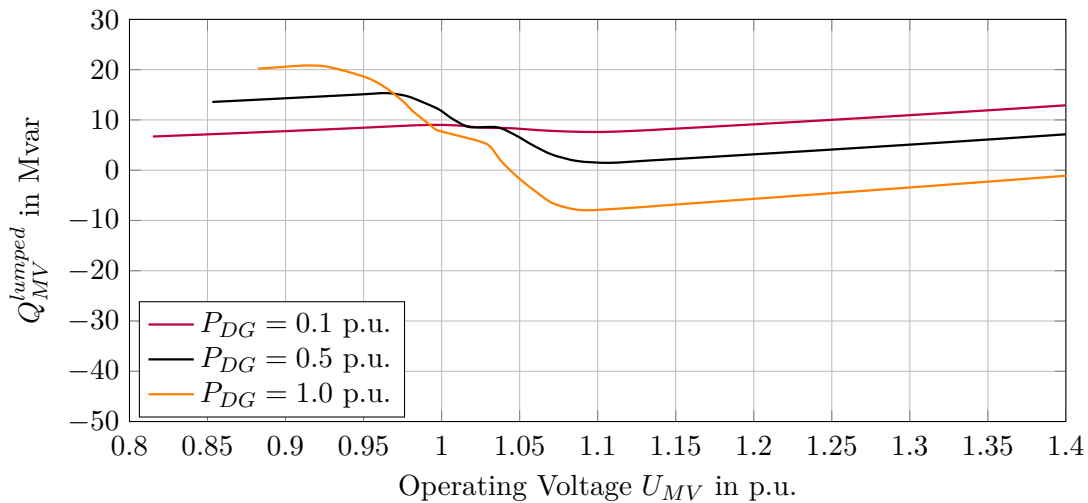
Figure 3.31: $Q(U)$ load behaviour, Cloverdale, DG production everywhere, $P_{MV}^{load} = 1.0$ p.u.; Scenario 5 - 7

Simulation scenarios 8, 9, 10 and 11 have been calculated with a reduced natural load of $P_{MV}^{load} = 0.5$ p.u. and $Q_{MV}^{load} = 0.5$ p.u. and a varying distributed generation which feed into all three distribution grids. The medium voltage lumped load characteristic for the medium voltage grid Cloverdale is given in figure 3.28.
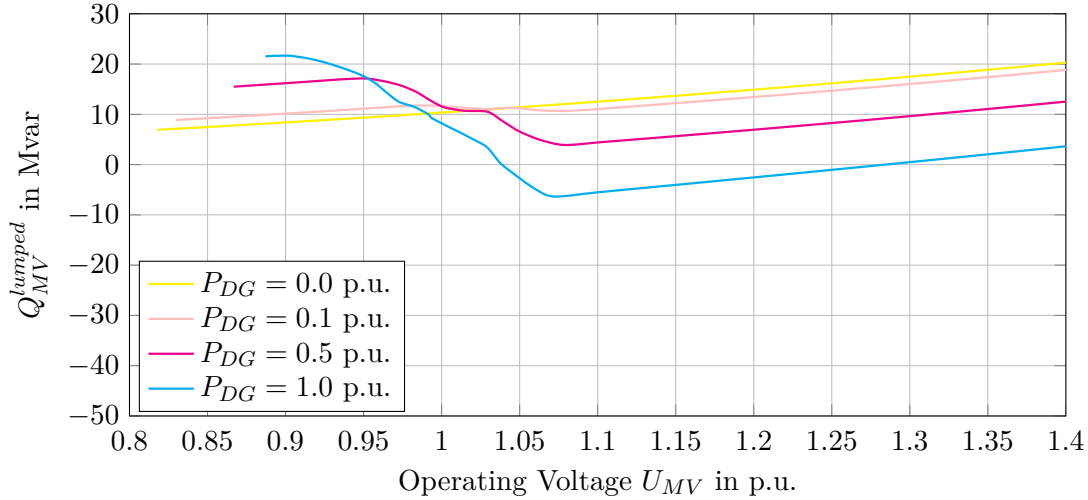
Figure 3.32: $Q(U)$ load behaviour, Cloverdale, DG production everywhere, $P_{MV}^{load} = 0.5$ p.u.; Scenario 8 - 11

The changes of the static load characteristic (k_{SLC}) by varying distributed generation in all three distribution grids can be seen in figure 3.33. Table 3.12 gives the simulation results in tabular form. The active power through the HV/MV supplying transformer which represents the medium voltage lumped load (P_{MV}^{lumped}) is depending on the distributed generation. The static load characteristic has been taken for a medium voltage bus bar voltage of $U_{MV} = 1$ p.u.. The distribution grid "Cloverdale" has been chosen to be displayed in figure 3.33 and table 3.12 but the plots for the two other distribution grids look quite similar. The distributed generation production is highly pending on the weather and as a result of that the static load characteristic is changing with the weather. Most of the distributed generation production comes from photovoltaic cells which results in a low distributed generation production in case of a cloudy weather and a high amount of distributed generation if the weather is sunny. Additionally the active power through the HV/MV supplying transformer is changing with the weather.

Table 3.12: k_{SLC} and P_{MV}^{lumped} at varying distributed generation, Cloverdale

Maximal Load ($P_{MV}^{load} = 1$ p.u.)		Minimal Load ($P_{MV}^{load} = 0.5$ p..u.)		
P_{MV}^{lumped} MW	k_{SLC}	P_{MV}^{lumped} MW	k_{SLC}	P_{DG} MW
-16.15	2.00	-8.29	2.00	0.00
-11.29	0.95	-3.37	1.12	0.10
8.00	15.06	16.15	9.25	0.50
31.80	14.24	39.77	21.28	1.00
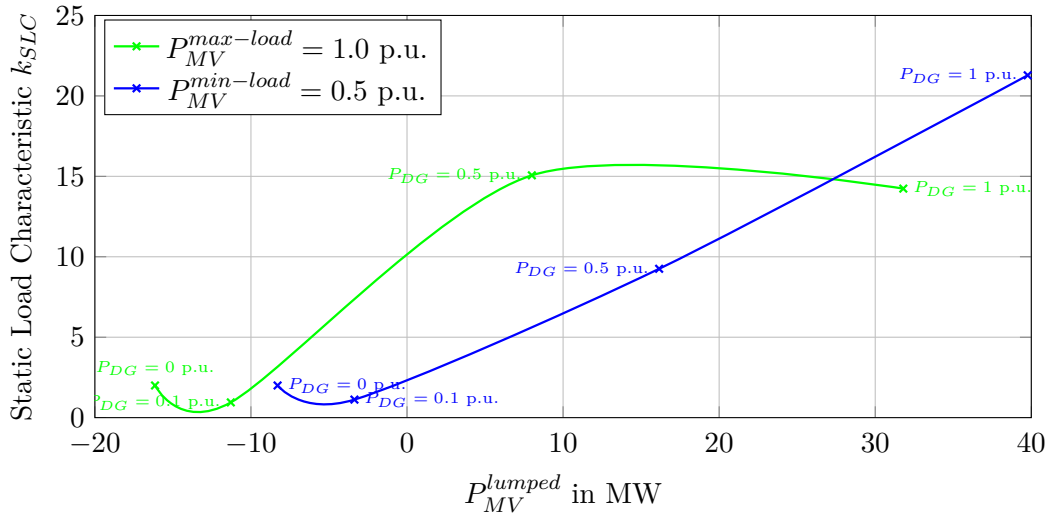
Figure 3.33: k_{SLC} over P_{MV}^{lumped} at $U_{MV} = 1$ p.u., Cloverdale

3.3.3 Voltage Stability and Power System Characteristic

Scenario Definition

The voltage stability has been analysed using the Q-U curve method which is described in chapter 2.2.7. The influences of the $Q(U)$ controlled distributed generation on the voltage sensitivity and the $Q(U)$ load characteristic has been shown in chapter 3.3.2. Q-U curves are used to measure the absolute stability as well as the stability margin. A fictitious and adjustable reactive power source is needed to control the voltage of the high voltage bus bar and has been added to the power network which can be seen in figure 3.18. A Q-U curve has been created for each of the three distribution grids (Hancock, Roanoke, Coverdale) for each simulation scenario (see table 3.13). Three curves are created with the power flow program according to the algorithm described in chapter 3.1.2. For more clarity of the figures the synchronous condenser characteristic isn't plotted, except figure 3.42 which gives a graphical explanation of the stability margin calculation and the equilibrium point stability analysis. According to the equilibrium point stability analysis method [12] the power system is stable if the system characteristic and the high voltage $Q(U)$ load characteristic intersect in a stable operating point. The Q-U curve method allows a measurement of the stability margin. It is calculated as the difference of the bottom of the synchronous condenser characteristic curve and the load characteristic line. A low reactive power margin of a power system means, the power system works near a voltage collapse situation. If the reactive power margin is negative, the power system is not in a operational situation. The reactive power margin is a very effective way, to compare how close the system is to a voltage collapse in different simulation scenarios [14]. Several simulations, with different distributed generation and different natural load situations have been performed. Using the fictitious synchronous condenser

the voltage has been changed continuously from $U_{HV} = 0.4$ p.u. to $U_{HV} = 1.4$ p.u., for each simulation scenario. The on-load tap changer HV/MV supplying transformer has been set to change the tap status automatically to keep the medium voltage bus bar voltage between $U_{MV} = 1.02$ p.u. and $U_{MV} = 1.06$ p.u.. An overview of the simulation scenarios can be seen in table 3.13.

Table 3.13: Simulation Scenario - Voltage Stability - IEEE network

| Sim. Scen. | Hancock | | | Roanoke | | | Cloverdale | | |
	P_{HV}^{load} MW	Q_{HV}^{load} Mvar	P_{DG} MW	P_{HV}^{load} MW	Q_{HV}^{load} Mvar	P_{DG} MW	P_{HV}^{load} MW	Q_{HV}^{load} Mvar	P_{DG} MW
1	1.00	1.00	0.00	1.00	1.00	0.00	1.00	1.00	0.00
2	1.00	1.00	0.10	1.00	1.00	0.10	1.00	1.00	0.10
3	1.00	1.00	0.50	1.00	1.00	0.50	1.00	1.00	0.50
4	1.00	1.00	1.00	1.00	1.00	1.00	1.00	1.00	1.00
5	0.50	0.50	0.10	0.50	0.50	0.10	0.50	0.50	0.10
6	0.50	0.50	1.00	0.50	0.50	1.00	0.50	0.50	1.00
7	10.00	10.00	0.10	10.00	10.00	0.10	10.00	10.00	0.10

Simulation Results

The reactive power margin (stability margin) of the different simulation scenarios and different medium voltage grids can be seen in table 3.14. The natural load has been set to the nominal value in simulation scenario 1 to 4 and the distributed generation production has been varied from $P_{DG} = 0$ p.u. to $P_{DG} = 1$ p.u.. Simulation scenario 5 and 6 has been calculated by using a reduced natural load of $P_{MV}^{load} = 0.5$ p.u. and $Q_{MV}^{load} = 0.5$ p.u. and the distributed generation has been varied again. Finally the natural load has been set to a very high value of $P_{MV}^{load} = 10$ p.u. and $Q_{MV}^{load} = 10$ p.u. in simulation scenario 7 and the distributed generation production has been set to a very low value of $P_{DG} = 0.1$ p.u.. The algorithm to create the simulation results is given in chapter 3.1.2.

The synchronous condenser characteristic is normally parabolic. At some point, the generators stop decreasing their reactive power value. In this case the synchronous condenser characteristic reaches the bottom of the curve and the system characteristic reaches the top of it's curve. This point represents the maximum increase in the reactive power of the load at this bus, also called the reactive power margin of the system. Any higher and a voltage collapse would occur. Shortly after this point the power flow program, has problems to reach convergence, which is the reason why most of the left side of the, normally parabolic, curve is missing, where the power system is unstable. A graphical illustration is given in figure 3.42.

Table 3.14: Stability Margin - IEEE network

Simulation	Hancock	Roanoke	Cloverdale
Scenario	Mvar	Mvar	Mvar
1	327.59	301.06	192.80
2	333.21	313.15	205.44
3	386.08	365.78	230.52
4	399.92	382.50	236.84
5	373.58	351.61	225.82
6	405.87	387.10	239.38
7	299.00	281.45	169.17

Figure 3.34 shows the Q-U curve of the distribution grid "Cloverdale" in case of a nominal natural load situation and without distributed generation. The stability margin has been calculated as 192.80 Mvar and the high voltage lumped load characteristic is almost stiff with a voltage sensitivity of $k_{SLC} = 2.00$.
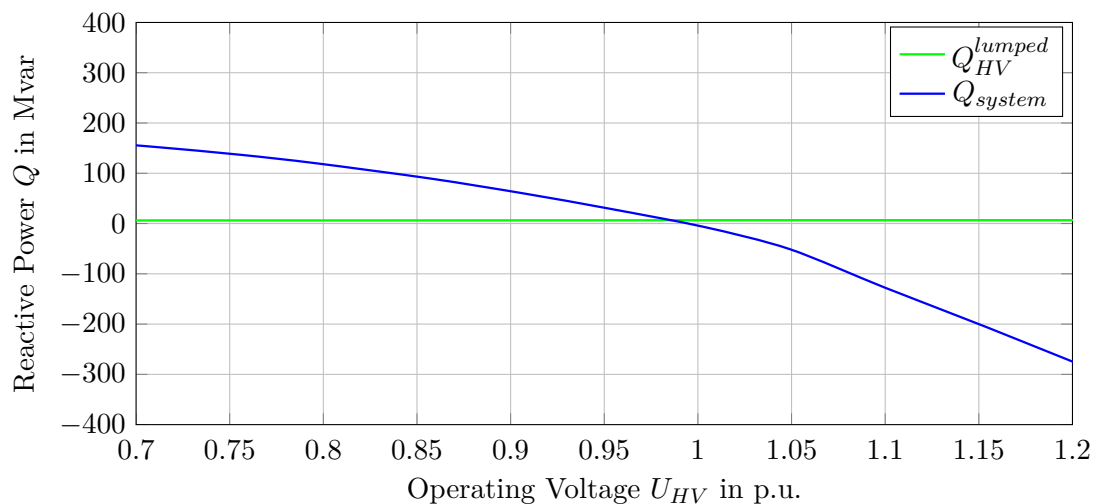
Figure 3.34: Q-U curve, Cloverdale, $P_{MV}^{load} = 1.0$ p.u., $P_{DG} = 0.0$ p.u.; Scen. 1

The results of simulation scenario 2, where the natural load has been set to it's nominal value and the distributed generation production has been set to $P_{DG} = 0.1$ p.u. is given in 3.35. The distribution grid "Hancock" is presented and the stability margin of this scenario is 333.21 Mvar.
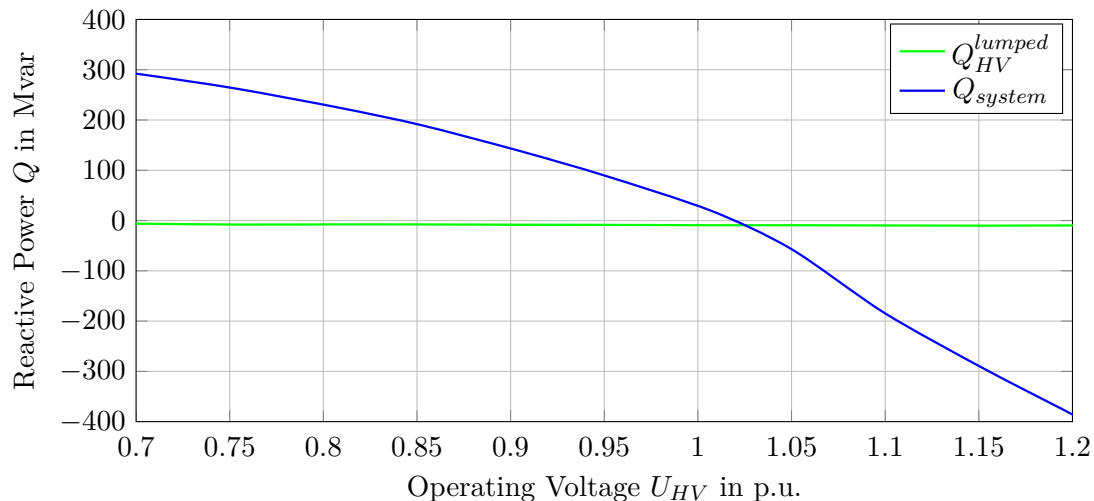
Figure 3.35: Q-U curve, Hancock, $P_{MV}^{load} = 1.0$ p.u., $P_{DG} = 0.1$ p.u.; Scen. 2

Simulation scenario 3 has been performed for a nominal natural load situation and the distributed generation production has been halved. Figure 3.36 gives the system characteristic as well as the high voltage lumped load characteristic of the distribution grid "Cloverdale".
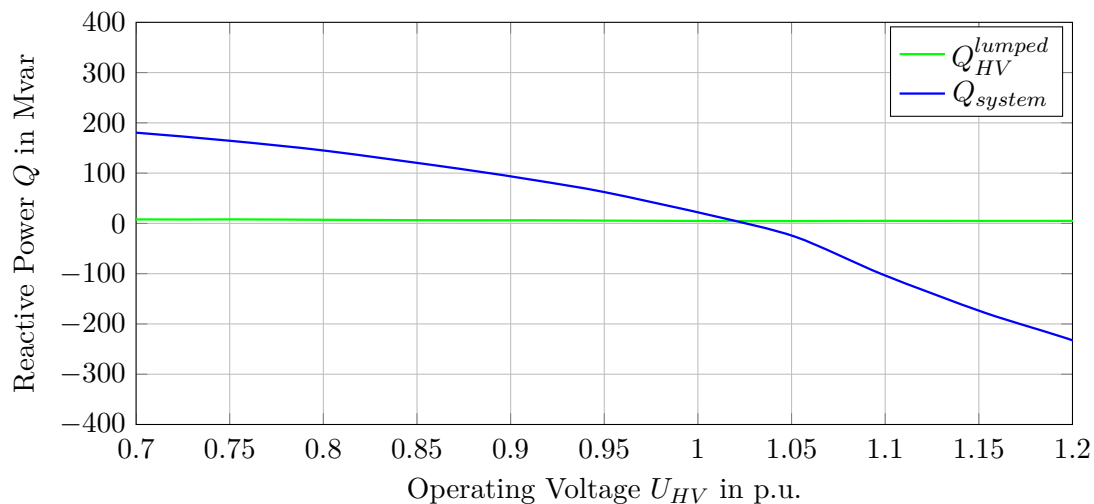
Figure 3.36: Q-U curve, Cloverdale, $P_{MV}^{load} = 1.0$ p.u., $P_{DG} = 0.5$ p.u.; Scen. 3

Figure 3.37 gives the Q-U curve of "Hancock" in case of a high distributed generation situation of $P_{DG} = 1$ p.u. and a nominal natural load. It can be seen that the system characteristic has been slightly shifted to the right side and the $Q(U)$ load characteristic is decreasing and varying because of the high amount of $Q(U)$ controlled distributed generation.
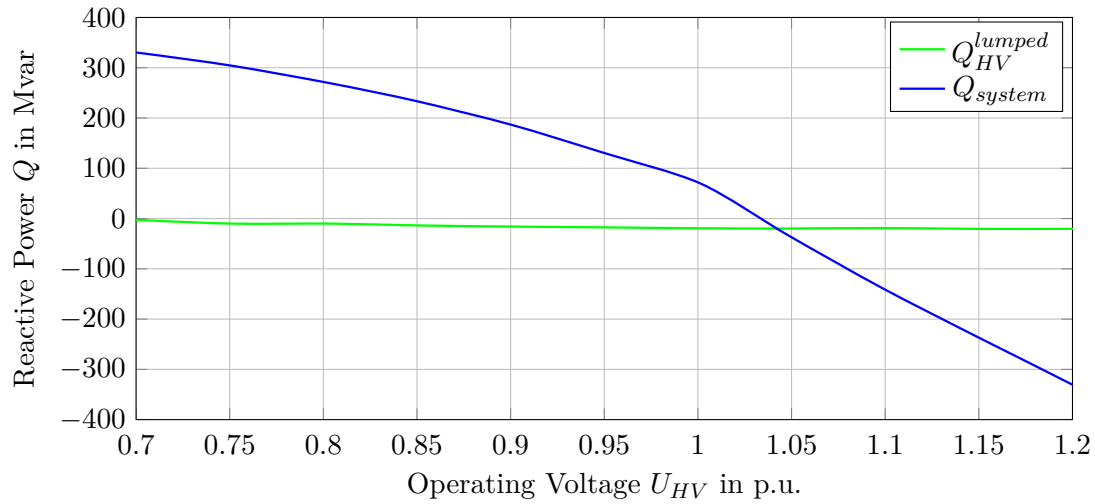
Figure 3.37: Q-U curve, Hancock, $P_{MV}^{load} = 1.0$ p.u., $P_{DG} = 1.0$ p.u.; Scen. 4

Simulation scenario 5 has been performed with a reduced natural load of $P_{MV}^{load} = 0.5$ p.u. and $Q_{MV}^{load} = 0.5$ p.u. and a distributed generation penetration of $P_{DG} = 0.1$ p.u.. The system characteristic reaches it's maximum ($Q_{system,max} = 350$ Mvar) at a high voltage bus bar voltage of $U_{HV} = 0.5$ p.u.. It represents the reactive power which is needed to be supplied from the system to reach a high voltage bus bar voltage of $U_{HV} = 0.5$ p.u.. Simulation scenario 2 is performed with a nominal natural load and the same distributed generation penetration. Therefore the maximum of the system characteristic is reached at $Q_{system,max} = 320$ Mvar.
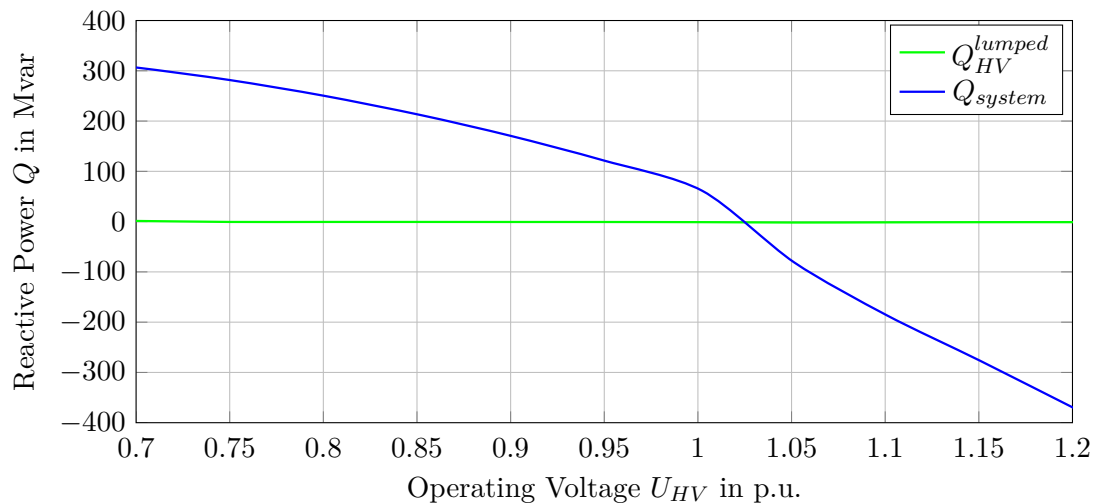
Figure 3.38: Q-U curve, Roanoke, $P_{MV}^{load} = 0.5$ p.u., $P_{DG} = 0.1$ p.u.; Scen. 5

Figure 3.39 gives the Q-U curve of "Hancock" in case of a high distributed generation situation of $P_{DG} = 1$ p.u. and a reduced natural load ($P_{MV}^{load} = 0.5$ p.u. and $Q_{MV}^{load} = 0.5$ p.u.).
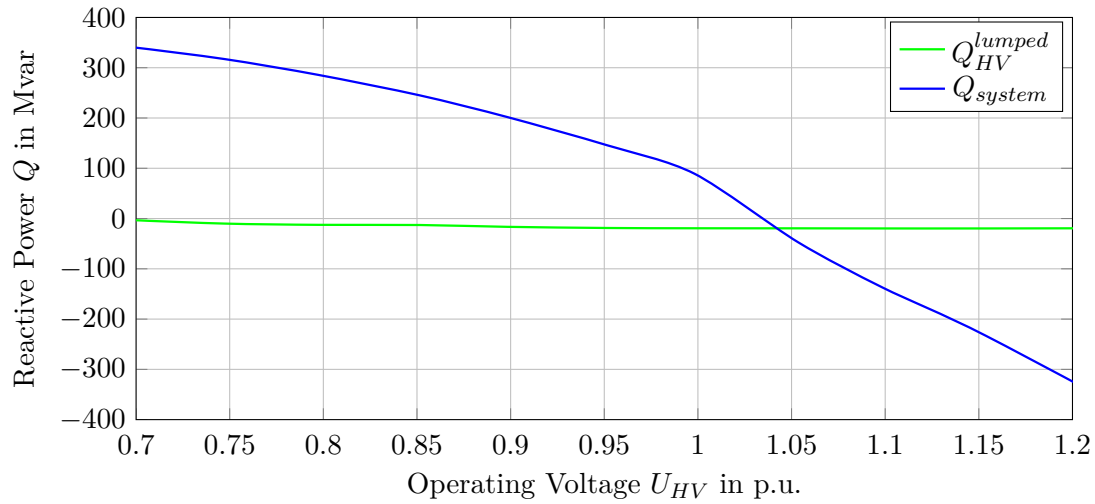
Figure 3.39: Q-U curve, Hancock, $P_{MV}^{load} = 0.5$ p.u., $P_{DG} = 1.0$ p.u.; Scen. 6

Finally simulation Scenario 7 gives the lowest stability margin value (169.17 Mvar). The scenario represents a situation of a very high load and simultaneously a very low distributed generation production. The $Q(U)$ curve of the distribution grid "Cloverdale" is presented in figure 3.40.
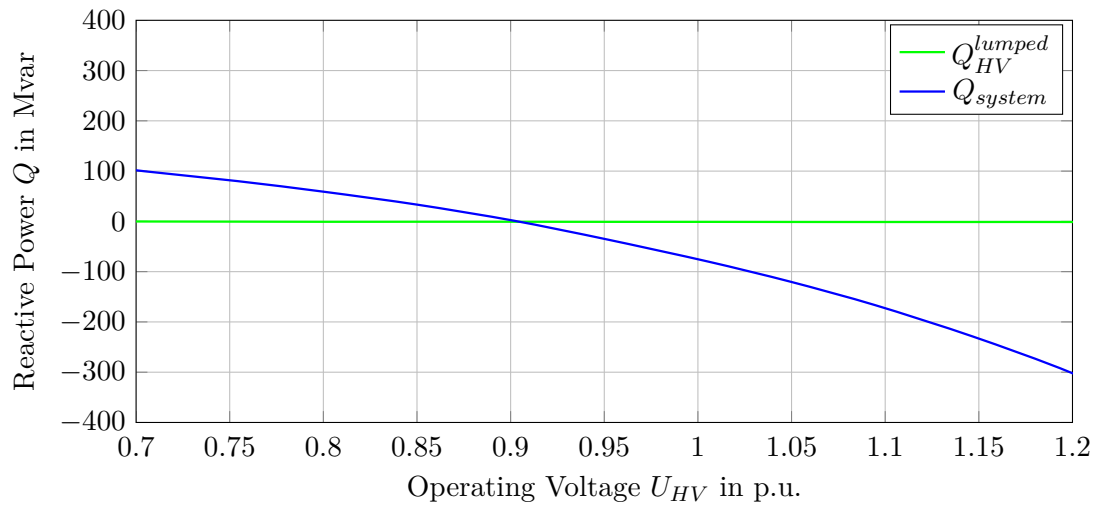
Figure 3.40: Q-U curve, Cloverdale, $P_{MV}^{load} = 10$ p.u., $P_{DG} = 0.1$ p.u.; Scen. 7

The highest stability margin 405.87 has been calculated with the simulation data of scenario 6 in the distribution grid "Hancock". The natural load has been set to a low value ($P_{MV}^{load} = 0.5$ p.u. and $Q_{MV}^{load} = 0.5$ p.u.) and the distribution generation has been set to the nominal value ($P_{DG} = 1.0$ p.u.) in this simulation scenario. The lowest stability margin 169.17 has been found in simulation scenario 7 in the distribution grid "Cloverdale". The natural load has been set to a very high value ($P_{MV}^{load} = 10$ p.u. and $Q_{MV}^{load} = 10$ p.u.) and the distribution generation has been reduced to $P_{DG} = 0.1$ in this

simulation scenario. Generally can be said that the distribution grid "Cloverdale" has the lowest stability margin of all three distribution grids which is because the distribution grid is farthest away from the two centralized generators (see figure 3.18). This reduces the ability of the high voltage grid to supply the medium voltage grid with the needed reactive power. According to the Q-U curve analysis can be said that the power system is closest to a voltage collapse in simulation scenario 7, at a very high natural load situation and a very low distributed generation production.

Figure 3.41 plots the stability margin of all three distribution grids versus an increasing distributed generation production for a nominal natural load situation. It can be seen that by increasing the distributed generation production, the power system is becoming more stable, as the stability margin is increasing. (see table 3.14). An explanation of this behaviour is, that the IEEE power system is a simplification of a real power network. The centralized generators, are located closely to the medium voltage grid, which increases the ability of the generators to supply the distribution grids with reactive power. Additionally the centralized generators are modelled with very high reactive power generation limits, according to the IEEE generator data, which enables the generators to provide the needed reactive power. That means the centralized generators can vary their reactive power output and compensate the changing $Q(U)$ behaviour of the high voltage lumped load. It has been shown, that the power system is becoming even more stable (according to the stability margin analysis) if the distributed generation production is increasing but only if the high voltage grid is able to supply the medium voltage grid with reactive power (in both directions). It is questionable if a test network like the IEEE power network or the two bus network are usable for a Q-U curve voltage stability analysis.
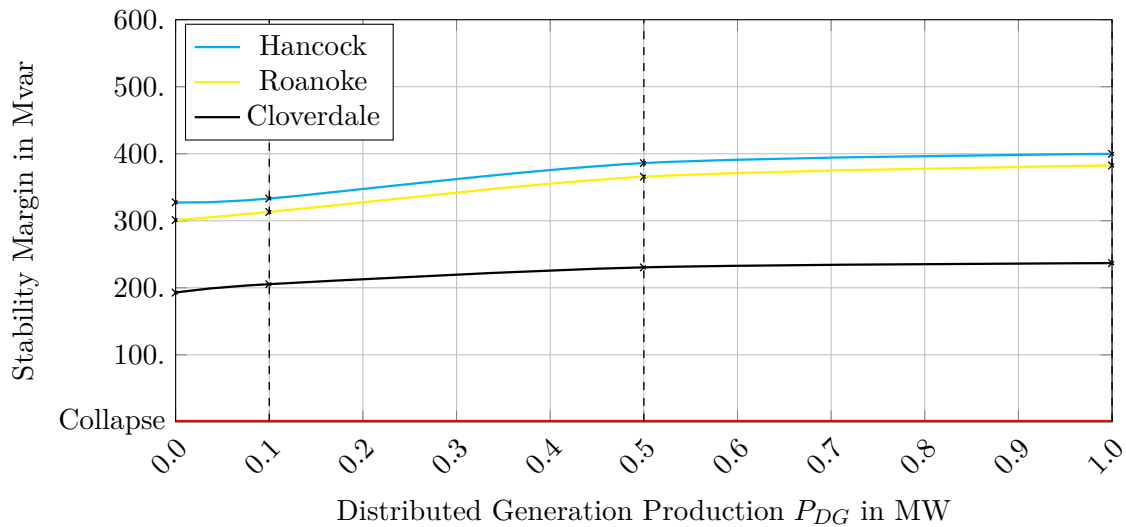
Figure 3.41: Stability Margin for $P_{load} = 1.0$ p.u.

Equilibrium Point Analysis

The stability of the power system has been analysed by calculating the stability margin as well as analysing the equilibrium point using the small-disturbance method. At equilibrium the reactive power demand (Q_{HV}^{lumped}) meets the supply (Q_{system}) which means $Q_{system} = Q_{HV}^{lumped}$ and is satisfied by the equilibrium point U_{HV}^s. According to the small-disturbance method an excess of reactive power produces an increase in the voltage while a deficit of reactive power results in a voltage decrease. The equilibrium point *s* is marked in figure 3.42. Assuming a small negative voltage disturbance ΔU_{HV}, will result in the supplied reactive power (Q_{system}) becoming greater than the demand (Q_{HV}^{lumped}). This will tend to increase the voltage and therefore force the voltage to return to point s. On the other hand if the voltage is increased by a disturbance, the resulting deficit in reactive power produces a voltage decrease and the voltage returns to point s. According to this analysis equilibrium point s is stable. A graphical illustration of this phenomenon is given in figure 3.42 [12].

Additionally the Q(U) characteristic of the synchronous condenser (Q_{SC}) has been plotted in figure 3.42 to demonstrate the calculation of the stability margin. It is calculated as the difference of the bottom of the synchronous condenser characteristic and the high voltage $Q(U)$ load characteristic. If the stability margin is negative the power system is not in a operational situation and must be considered as voltage unstable.
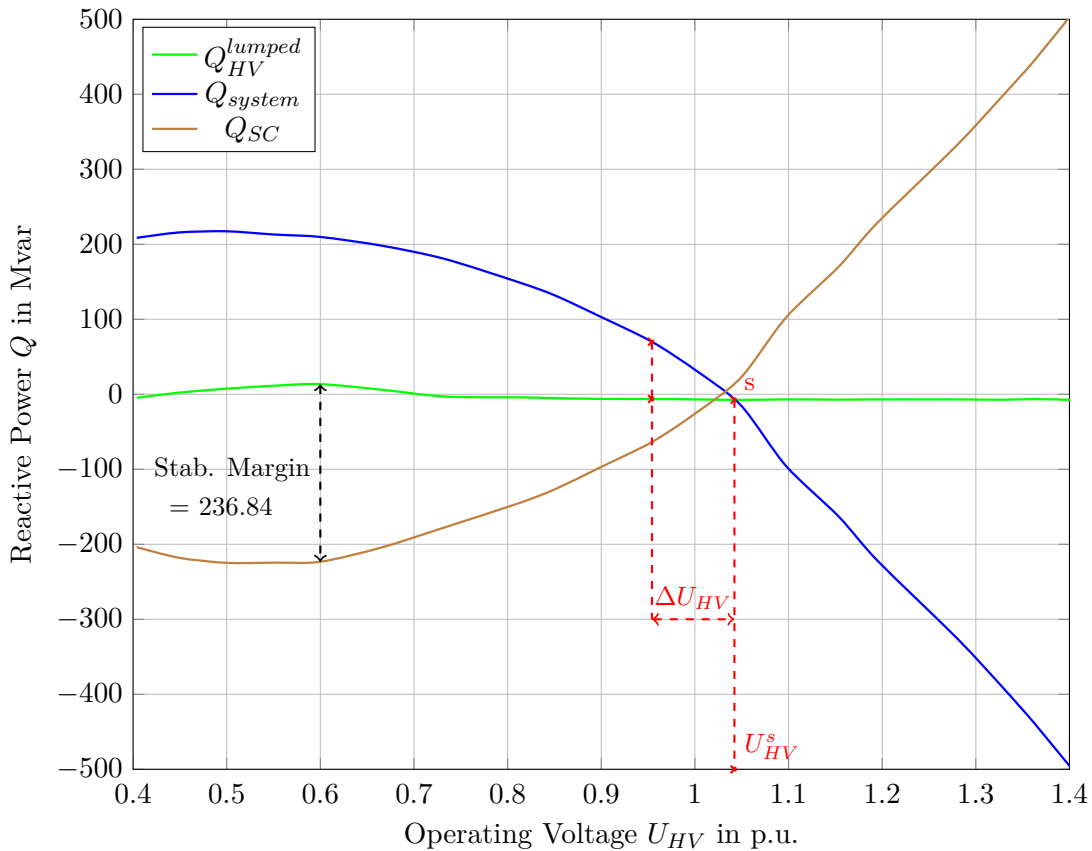
Figure 3.42: Q-U curve, Cloverdale, $P_{MV}^{load} = 1.0$ p.u., $P_{DG} = 1.0$ p.u.; Scen. 4

3.4 Real Network Simulations

It is not allowed to publish this chapter due to privacy and security policies. Therefore page 67 to 87 is not available in this version.

4 Conclusion

4.1 Static Load Characteristic

This thesis has shown that the $Q(U)$ load behaviour is becoming non-linear by increasing the amount of distributed generation production. The high voltage lumped load characteristic (Q_{MV}^{lumped}) is changing dramatically and can't be considered as stiff any more. The on-load tap changer installed on the HV/MV supplying transformer reduces the influence of the $Q(U)$ controller on the high voltage lumped load characteristic (Q_{MV}^{lumped}) but it is still becoming more non-linear.

Additionally the reactive power flow direction is changing, pending on the bus bar voltage, in presence of $Q(U)$ controlled distributed generation production. A reactive power flow from the medium voltage grid to the high voltage grid has been detected if the medium voltage bus bar voltage is above a certain amount. If the bus bar voltage is below a certain amount the reactive power flow direction is changing and the reactive power demand of the medium voltage grid is increasing, which must be supplied from the high voltage grid. Very interesting phenomenons have been detected in case of a very high distributed generation production, e.g. if the active power production of the distributed generators exceeds the active power demand of the medium voltage grid. Obviously there is a active power transfer from the medium voltage grid to the high voltage grid, but besides that the reactive power demand of the medium voltage grid is increasing rapidly (see chapter 3.4.1), which leads to the situation where active power is transferred from the medium voltage grid to the high voltage grid and reactive power is transferred in the other direction. An explanation of this issue is that due to the high amount of distributed generation and the low load the voltage over the feeder is increasing. This leads to the situation that the $Q(U)$ controllers decide to consume reactive power in order to reduce the voltage, which must be supplied from the high voltage grid.

The $Q(U)$ sensitivity of the load, the static load characteristic (k_{SLC}), is changing with varying distributed generation. The static load characteristic is nearly constant ($k_{SLC} \approx 2$) if the distributed generation production is deactivated. It has been shown that the static load characteristic is not constant if the distributed generation production is increased and the extreme values are further apart. The distributed generation production is highly pending on the weather as most of it comes from photovoltaic cells or wind

power plants, which means the static load characteristic is pending on the weather, as well as the power transfer through the HV/MV supplying transformer.

4.2 Voltage Stability and Power System Characteristic

The stability margin analysis of the two bus network and the IEEE test network has shown that by increasing the distributed generation production, the power system is becoming more stable, as the stability margin is increasing. The centralized generators, are located closely to the distribution grids in the two analysed test power networks and can directly compensate the changing $Q(U)$ behaviour of the medium voltage lumped load. The power system is becoming even more stable according to the stability margin analysis if the $Q(U)$ controlled distributed generation production is increasing but only if the high voltage grid is able to supply the medium voltage grid with reactive power (reactive/capacitive). The two bus network and the IEEE 30 bus network are closest to a voltage collapse situation in case of a very high medium voltage load and a low distributed generation production.

The real power network is becoming more stable if the distributed generation production is increased up to a certain amount. The stability margin decreases if the active power production of the distributed generation production exceeds the active power demand of the load. According to the Q-U curve method the real power system is coming close to a voltage collapse situation if the active power produced from distributed generators is twice higher than the active power demand of the medium voltage load. This leads to a situation where active power is transferred from the medium voltage grid to the high voltage grid and at the same time a high amount of reactive power must be transferred in the opposite direction.

4.3 Further Work

Terms like Smart Grid Evolution or Energiewende are closely connected to stability issues as it will become more complex to operate a power system. Therefore additionally voltage stability investigations are necessary:

- Load Modelling: The load has been modelled in this thesis using the constant impedance load model. According to the literature [15, 16] the acquainted load models are limited in some areas. In addition these models are satisfactory only in certain voltage areas (e.g. $U = 0.9$ p.u. to $U = 1.1$ p.u.). The correct and accurate modelling of the load is of great importance. The voltage stability study could be expanded by using other load models or mixing load models.

- Supplying Transformer Modelling: The HV/MV supplying transformer has been set to regulate the medium voltage bus bar voltage automatically for the voltage stability analysis in this thesis. The transformer step has been calculated to keep the voltage between $U_{MV} = 1.2$ p.u. to $U_{MV} = 1.6$ p.u.. It has been found that this voltage range is too high in some scenarios. In order to obtain a complete picture of the voltage stability of the power system a Q-U curve analysis could be performed for each transformer step and each simulation scenario.

- Expansion of the Model Areas: The real network which has been analysed in this thesis was limited to one model region, means to one distribution subsystem and the high voltage grid. The other 28 distribution grids have been limited to a lumped load and/or an injection. An extension of the simulation area, means to represent all distribution grids completely, would increase the accuracy of the study.

- Full Representation of the Low Voltage Grid: The low voltage grids have been reduced to a lumped load and/or an injection in this thesis. They could be simulated completely in further studies.

- Dynamic Analysis: A dynamic voltage stability study which analyses the transient behaviour of the power system over a period of time will complete the picture in terms of voltage stability. But there are several open issues. The reliability in dynamic load models is too low, particularly as the dynamic load behaviour seems to be one of the major reasons for voltage collapse in power systems [18]. It is therefore necessary to improve the modelling of the load dynamics considered from the transmission level. Additionally dynamic modelling of generators is of great importance. Also the dynamic interdependency of centralized generators and distributed generators needs to be investigated.

5 Bibliography

[1] A.F. Zobaa, J.S. McConnach, *"International Response to Climate Change: An Overview"*, IEEE, 2006.

[2] White House, *"The President's Clean Power Plan", 2015*, *"https://www.whitehouse.gov/climate-change#section-clean-power-plan"*, (Accessed: 01-August-2015).

[3] European Commission, *"The EU Climate and Energy Package", 2013*, *"http://ec.europa.eu/clima/policies/package/index_en.htm"*, (Accessed: 01-August-2015).

[4] A. Ilo, W. Gawlik, W. Schaffer, R. Eichler, *"Uncontrolled Reactive Power Flow due to Local Control of Distributed Generators"*, CIRED, 23rd International Conference on Electricity Distribution, no. Paper 0512, 2015

[5] P. Lund, *"The Danish Cell Project - Part 1: Background and General Approach"*, IEEE, Power Engineering Society General Meeting, 2007.

[6] S. Cherian, V. Knazkins, *"The Danish Cell Project - Part 2: Verification of Control Approach via Modelling and Laboratory Tests"*, IEEE, Power Engineering Society General Meeting, 2007.

[7] C. Vournas, T. Van Cutsem, *"Voltage Stability of Electric Power Systems"*, Springer, 2007, ISBN: 78-0387755359.

[8] W. Gawlik, *"Energieübertragung und Hochspannungstechnik"*, Skriptum - TU Wien, ESEA, 2014.

[9] N.I. Voropai, D.N. Efimov, *"Analysis of Blackout Development Mechanisms in Electric Power Systems"*, IEEE, 2008.

[10] L.L. Grigsby, *"Power System Stability and Control, Third Edition"*, CRC Press, 2012, ISBN-13: 978-1439883204.

[11] P. Kundur, J. Paserba, V. Ajjarapu, G. Andersson, A. Bose, C. Canizares, N. Hatziargyriou, D. Hill, A. Stankovic, C. Taylor, T. Van Cutsem, V. Vittal, *"Definition and Classification of Power System Stability"*, IEEE \CIGRE Joint Task Force on Stability Terms and Definitions, Vol. 19, pp. 1387-1400, 2004.

[12] J. Machowski, J. W. Bialek, J. R. Bumby, *"Power System Dynamics: Stability and Control"*, John Wiley and Sons Ltd., 2008, ISBN: 978-0-470-72558-0.

[13] B. Wille-Haussmann, W. Biener, P.-S. Ganner, *"Applied Approach for Reactive Power Control with Medium Voltage Distributed Units"*, CIRED, 22nd International Conference on Electricity Distribution, Paper 1222, 2013.

[14] H.K. Clark, *"Voltage Stability Analysis requires accurate Q-V curves"*, Power Technologies INC., Vol. issue no. 61, 1990.

[15] IEEE Task Force on Load Representation for Dynamic Performance, *"Load Representation for Dynamic Performance Analysis"*, IEEE Transactions on Power Systems, Vol. 8, No. 2, 1993.

[16] Y. Li, H.-D. Chiang, B.-K. Choi, Y.-T. Chen, D.-H. Huang, M.G. Lauby, *"Representative Static Load Models for Transient Stability Analysis: Development and Examination"*, IET Gener. Transm. Distrib., Vol. 1, No. 3, 2007.

[17] A. Hinz, *"Der regelbare Ortsnetztransformator im Verteilungsnetz", 2012, "http://www.fge.rwth-aachen.de/fileadmin/Uploads/PDF/FGE Kolloquium 2012-2013/FGE Kolloquiumsvortrag Hinz.pdf"*, (Accessed: 07-July-2015).

[18] S. Johansson, F. Sjögren, *"Voltage collapse in power systems"*, Chalmers University of Technology, Dissertation, 1995.

List of Figures

List of Tables

Eidesstattliche Erklärung

Hiermit erkläre ich, dass die vorliegende Arbeit gemäßdem Code of Conduct - Regeln zur Sicherung guter wissenschaftlicher Praxis (in der aktuellen Fassung des jeweiligen Mitteilungsblattes der TU Wien), insbesondere ohne unzulässige Hilfe Dritter und ohne Benutzung anderer als der angegebenen Hilfsmittel, angefertigt wurde. Die aus anderen Quellen direkt oder indirekt übernommenen Daten und Konzepte sind unter Angabe der Quelle gekennzeichnet.
Die Arbeit wurde bisher weder im In- noch im Ausland in gleicher oder in ähnlicher Form in anderen Prüfungsverfahren vorgelegt.

Wien, im Oktober 2015

—————————————————

Christian Schirmer, BSc